University of Southampton Research Repository

University of Southampton

FACULTY OF NATURAL AND ENVIRONMENTAL SCIENCES

School of Ocean and Earth Science

Megabenthic ecology of abyssal polymetallic nodule fields

by Erik Simon-Lledó

ORCID ID: 0000-0001-9667-2917

Thesis for the degree of Doctor of Philosophy

October 2018

UNIVERSITY OF SOUTHAMPTON

ABSTRACT

FACULTY OF NATURAL AND ENVIRONMENTAL SCIENCES

Ocean and Earth Sciences

Thesis for the degree of Doctor of Philosophy

Megabenthic ecology of abyssal polymetallic nodule fields

by Erik Simon-Lledó

Abyssal polymetallic nodule fields constitute an unusual deep-sea habitat. The mix of soft sediment and the hard substratum provided by nodules increases the complexity of these environments, and is thought to promote the occurrence of some of the most biologically diverse seafloor assemblages in the abyss. This unusual and diverse habitat is potentially subject to imminent large-scale human impacts in the form of seafloor mining. Mining disturbances are likely to extend over extremely large seafloor areas and have a clear potential to drive major changes in the resident fauna. Predicting the nature of such changes remains difficult; the ecology of this remote and vast habitat is poorly understood. The large seafloor areal coverage that can be investigated using photographic surveys presents an opportunity to numerically quantify variation in megafaunal communities inhabiting these abyssal plain environments. In this thesis, the fundamental drivers of megabenthic community variations in abyssal polymetallic nodule fields are explored based on extensive acoustic and imagery data collected using autonomous underwater vehicles. First, baseline ecological patterns of megafaunal distribution are investigated at different factor-operating scales, i.e. different environmental factors, in the proposed conservation zone 'Area of Particular Environmental Interest 6' of the Clarion Clipperton Zone (NE Pacific; water depth: 3950-4250 m). Broad-scale (tens of kilometres) variations in seafloor geomorphology appear to control megabenthic standing stock, while fine-scale (tens of meters) variations in nodule occurrence appear more important in the regulation of diversity and community composition. Both of these factors seem to play a key role in the functional structuring of megafauna assemblages across a nodule field. Second, long term effects of disturbance on megafaunal distribution patterns are investigated in the Peru Basin (E Pacific; 3800-4300 m water depth), 26 years after simulated mining impacts were induced during the "DISturbance and reCOLonization" experiment. Distinct ecological patterns are found across different seafloor disturbance levels; i.e. suspension feeder standing stock remains strongly reduced in directly disturbed seafloor areas, suggesting that the megabenthos of the DISCOL area has not yet recovered from simulated mining impacts. The findings of this thesis provide evidence of the habitat heterogeneity of polymetallic nodule field ecosystems, which appears promoted by both geomorphological and nodule occurrence variations across space. The nodule field is likely better considered as a mosaic habitat where nodules act as keystone structures, modulating a continuous community variation across a gradient of this resource. Consequently, successful conservation actions will likely require the preservation of areas comprising the full range of nodule cover and not just the low cover areas that are least attractive to mining.

Table of Contents

Table of Tables

Table of Figures

Academic Thesis: Declaration of Authorship

I, Erik Simon-Lledó, declare that this thesis, with title "Megabenthic ecology of abyssal polymetallic nodule fields" and the work presented in it is my own and has been generated by me as the result of my own original research.

I confirm that:

1. This work was done wholly or mainly while in candidature for a research degree at this University;

2. Where any part of this thesis has previously been submitted for a degree or any other qualification at this University or any other institution, this has been clearly stated;

3. Where I have consulted the published work of others, this is always clearly attributed;

4. Where I have quoted from the work of others, the source is always given. With the exception of such quotations, this thesis is entirely my own work;

5. I have acknowledged all main sources of help;

6. Where the thesis is based on work done by myself jointly with others, I have made clear exactly what was done by others and what I have contributed myself;

7. Parts of this work have been submitted to relevant journals, as described in section 1.2.2.

Signature: ESL

Date: 10/10/2018

Acknowledgements

First and foremost, I would like to thank Dan for being my main supervisor and mentor all these years. I have learnt an incredible amount from you, both professionally, and personally. Thank you for your unlimited patience, and for encouraging me to do better and think bigger. Veerle, thank you for everything you have taught me, your knowledge and hard work have been a great source of inspiration for me. Brian, thank you very much for teaching me how to be a thorough researcher, and thanks Jen for setting me up when I had no idea what I was doing, your help made a real difference. I really admire the passion and dedication you all put on the study and exploration of the deep ocean; it was a pleasure to have had the opportunity to work with you all.

Thank you to all the fellow DEEPSEAS group students, postdocs and researchers who shared this experience with me over the years. I am especially grateful to Henry, Tammy, Kat, Jen, Simone, Marla, Andy (Gates), and Andy (Gooday), whose help and knowledge has improved my research skills over the course of these years, and to Noelie whose incredibly hard work contributed to this thesis. Thank you Timm and Kevin for your excellent work and help, both at the Sea and after.

I would also like to thank Phil for being supportive and helpful as my panel chair, as well as Martin for providing highly valuable points of view during scientific discussions, I learned a lot from you and your inputs were always really appreciated over the course of these years.

To my office friends, Rose, Kat, and Steph, thanks for going through this experience together. All would have been much harder without you.

I would like to thank my family for their unconditional support over these years, and my partner Natalia for being always there; it would have been impossible without you.

Definitions and Abbreviations

1/D	Inverse form of Simpson diversity index
APEI	Area of Particular Environmental Interest
AUV	autonomous underwater vehicle
C:N	carbon : nitrogen (ratio)
$CaCO_3$	Calcium carbonate
CCD	carbon compensation depth
CCPM	complete coverage photo-mosaic
CCZ	Clarion Clipperton Fracture Zone
C_{org}	organic carbon
CV	coefficient of variation
Exp *H’*	Exponential form of Shannon diversity index (idem: exp H')
g fwwt	grams of fresh wet weight
ind	faunal specimens
IQR	inter-quartile range
ISA	International Seabed Authority
IRZ	impact reference zone
MDS-d1	dimension 1 (x) of nMDS analysis
NA	nodule-attached fauna
NFL	nodule-free-living fauna
nMDS	non-metric multi-dimensional scaling
POC	particulate organic carbon
PRZ	preservation reference zone
r_S	Spearman’s rank correlation coefficient
r_P	Pearson’s correlation coefficient
ROV	Remotely Operated Vehicle
S	species richness
TN	total nitrogen
TOC	total organic carbon
wt	wet weight

1. Chapter 1. Introduction

1.1. Background

1.1.1. The nature of abyssal (plain) environments

Abyssal environments (3000-6000 m water depth) represent more than 80% of the global ocean seafloor (Harris et al. 2014) and provide important ecosystem services, including biological and mineral resources (Glover and Smith 2003, Ramirez-Llodra et al. 2011). Technological advances have gradually made deep-sea resources become important targets for exploitation, enabling their harvesting trough activities such as fishing (Clark et al. 2010a, Victorero et al. 2018b), or the planned mining of minerals (Wedding et al. 2015) in hydrothermal vents (Van Dover 2014), seamounts (Boschen et al. 2015), or abyssal plains (Vanreusel et al. 2016). High species diversity in abyssal ecosystems potentially results from a strong specialisation of its inhabiting fauna to the 'hostile' (i.e. ultra-low food and high pressure) conditions of this environment (Gage and Tyler 1992, Ebbe et al. 2010) and suggests an important role of abyssal habitats as reservoirs of biodiversity and as sources of unique ecosystem functions (Snelgrove 1999, Smith et al. 2008a, Danovaro et al. 2014). However, despite representing the vast majority of the abyssal seafloor, abyssal plains are the least explored ecosystems of the ocean, with less than 1% of their area having been explored (Ramirez-Llodra et al. 2010). Consequently, spatial and temporal patterns of biodiversity and community structure in these environments are still poorly understood, which constrains the generation of comprehensive regulatory frameworks to manage the impacts of planned resource exploitation.

Bordered by trenches, subdivided by ridges and interspersed by seamounts, abyssal plains extend almost continuously between continental margins, representing the single largest contiguous feature of our planet (Ramirez-Llodra et al. 2010). Abyssal plain seafloors are generally covered by very fine pelagic sediments (fine sands to clays) (Weaver and Thomson 1987) and are typically characterised by low temperatures ranging from -0.5 to 3 °C, well oxygenated waters, and a lack of primary production (Hannides and Smith 2003, Smith et al. 2008a). Bottom-water currents in abyssal environments are generally weak and hence there is normally little sediment erosion effects (Smith and Demopoulos 2003), although intense intermittent currents (i.e. benthic storms) can generate high concentrations of suspended sediment and grooved mud beds in some regions (Hollister and McCave 1984). Many of the habitat structures found in abyssal plain sediments are biogenic, such as burrows, mounds and tracks of megabenthos, or the tests of xenophyophores (giant foraminifera) (Bett et al. 1995, Hannides and Smith 2003, Kamenskaya et al. 2013). Hard substrata can be found in the shape of polymetallic nodules (Veillette et al. 2007b), iceberg drop-stones (Meyer et al. 2016), or clinker (Ramirez-Llodra et al. 2011), and these commonly support distinct faunal assemblages from those in sediments.

Energy limitation is possibly the most important ecological feature of abyssal ecosystems (Ruhl and Smith 2004, Smith et al. 2008a). The main food resource in these environments is the particulate organic carbon (POC) generated in the photosynthetically active euphotic zone, found thousands of meters above (Rex et al. 2006, Ruhl et al. 2008). Primary production in the euphotic zone can vary spatially (Yool et al. 2007), i.e. distance to continental margins (Smith and Demopoulos 2003, Veillette et al. 2007b), or temporarily as a result of climate-driven variations occurring at both seasonal (Deuser and Ross 1980, Billett et al. 1983) and inter-annual scales (Ruhl et al. 2008, Smith et al. 2009). Yet, carbon flux decreases with increasing depth as organic particles get consumed during their sinking along the water column (Lampitt and Antia 1997), and hence only 1 to 5% of the surface production normally reaches the abyssal seafloor (Buesseler et al. 2007). Consequently, abyssal plain areas are generally oligotrophic and their faunal communities are highly sensitive to changes in POC fluxes (Billett et al. 2010). Hence, many structural aspects of these ecosystems can be strongly regulated by factors ultimately in control of the rate and nature of nutrient inputs to the seafloor (Smith et al. 2008a, Danovaro et al. 2014) such as depth, morphology of the terrain (geomorphology) or bottom current speeds.

Regional to global analyses have shown that standing stocks of the larger sized fauna, megafauna and macrofauna, decrease dramatically with water depth (and hence POC flux) (Thiel 1975, Rowe et al. 1991, Rex et al. 2006). Diminishing food supply may prevent growth to larger body sizes (McClain et al. 2005), although inefficiency in energy transfer to higher trophic levels (Smith et al. 2008a) coupled with a decreased relative oxygen consumption (Danovaro et al. 2014) may also explain this zonation. Bathyal ecosystems (200-3000 m water depth) are possibly more suitable for the development and radiation of macro- and megafaunal taxa, which has even led to the suggestion that abyssal populations may be partly regulated by immigration from bathyal sources (Rex et al. 2005), yet biogeographical dynamics are still poorly understood to confirm this hypothesis (McClain and Hardy 2010). The higher dominance of smaller fauna, meiofauna and bacteria, supports metabolic theory of ecology (McClain et al. 2012), and suggests fundamentally different ecosystem functions between abyssal and bathyal habitats (Smith et al. 2008a). However, even if the community biomass and the carbon consumption is dominated by bacteria (Sweetman et al 2019), megafauna typically incorporate more phyto-detritus carbon per unit biomass than macrofauna and meiofauna in abyssal ecosystems (Lauerman et al. 1997, Bett et al. 2001, Stratmann et al. 2018b), which suggests that these might play important functional roles in these habitats.

At the large scale, seafloor geomorphology can modulate ocean flows, but also inhibit or enhance the mixing and transport of waters (and hence POC flux) from different regions (Gille et al. 2004, Harris et al. 2014). At the local to regional scale, topographic variations can modulate abyssal current dynamics (Bell 1975, Polzin et al. 1997) in direct control of key environmental drivers of benthic fauna distribution, such as soft sediment composition (Levin and Thomas 1988b, Snelgrove and Butman 1995, Vanreusel et al. 2010) and the supply of food particles and larvae (Flach and Thomsen 1998, Hughes and Gage 2004). The complex interactions between these factors usually lead to variations in diversity associated with habitat heterogeneity (Levin et al. 2001). For instance, topographically-enhanced bottom currents can increase the food supply for suspension feeders and remove fine sediments causing winnowing, while topographically-attenuated flows can generate more sheltered soft-sediment habitats more suited for deposit feeder life-habits (Genin et al. 1986, Jumars et al. 1990, Dorschel et al. 2014). Hence, Habitat heterogeneity resulting from geomorphological variations has commonly been investigated at a local scale in seamounts (Clark et al. 2010b, Boschen et al. 2015), canyons (De Leo et al. 2010, McClain and Barry 2010), ridges (Morris et al. 2012), and channels (Jones et al. 2007). However, few studies have assessed the effects of geomorphology in the structuring of benthic communities within abyssal plain environments (Durden et al. 2015, Stefanoudis et al. 2016, Leitner et al. 2017).

The open ocean seafloor was long considered to be a homogeneous environment (Menzies 1965), with relatively monotonous slopes and mild depressions (Heezen and Laughton 1963, Sanders and Hessler 1969). Nonetheless, despite their name, abyssal plains can host a relatively large degree of terrain heterogeneity in the shape of flat plains, hills and valleys (Harris et al. 2014, Olive et al. 2015). Durden et al. 2015 stress that this heterogeneity may increase megafauna beta and gamma-diversity at the landscape scale, suggesting that interpretations of habitat complexity based on plains alone may underestimate abyssal biodiversity at the global scale. In the last decades, the progress of seafloor acoustic mapping techniques (Morris et al. 2014, Wynn et al. 2014) has led to more accurate characterisation of seafloor terrain variables (Brown et al. 2011), enabling more targeted geophysical (Gazis et al. 2018) and biological sampling (Foster et al. 2014). Novel deep-sea habitat mapping techniques (Huvenne et al. 2011, Robert et al. 2015) coupled with image-based ecological surveying (Jones et al. 2009, Jones and Brewer 2012, Durden et al. 2016c) may have hence the key to unveil the real complexity of remote abyssal habitats (see section 1.1.4).

The presence of hard substratum is thought to be a key factor in structuring heterogeneous deep-sea habitats (Buhl-Mortensen et al. 2010, Bell et al. 2016). For example, modest variations in the availability and the composition of hard surfaces can influence the larval settlement processes of the seafloor fauna (Van Dover et al. 1988, Roberts et al. 2006). Substratum selectivity is commonly exhibited by many deep-sea species, including soft corals (Sun et al. 2011), sponges (Lim et al. 2017), and foraminifera (Gooday et al. 2015). The presence and extent of hard substratum is therefore expected to exert a significant control on the composition of deep-sea benthic assemblages (Levin et al. 2001, Smith and Demopoulos 2003). Seafloor environments in the abyss with extensive hard substratum range in nature from landscape-scale features such as seamounts (Clark et al. 2010b) and canyons (De Leo et al. 2010), to widely dispersed pebbles, cobbles, and boulders referred to as iceberg drop-stones (Meyer et al. 2016), and the similar human artefact habitat produced by steamship clinker (Ramirez-Llodra et al. 2011). While individual polymetallic nodules are generally small, 1-20 cm in diameter, nodule fields, a specific type of abyssal plain ecosystem, can extend over extremely large areas, i.e. many hundreds of km^2, as occurs in the Clarion Clipperton Zone (CCZ) of the central Pacific Ocean (Kuhn et al. 2017).

1.1.2. Polymetallic nodule fields in the central Pacific abyss: the CCZ

The Clarion Clipperton Fracture Zone (CCZ) northeast Pacific basin is delimited by two WSW-ENE trending fracture zones, with eastern and western limits defined by the Mathematician Ridge and the Line Islands respectively (Macdonald et al. 1996, Barckhausen et al. 2013). There is a close link between topography and tectonics in the central Pacific abyss: volcanic seamount distribution appears to be controlled by fracture zones, smoother topographical profiles are found between fractures, and there is a gradual increase in water depth from east (3500 m) to west (5000 m) owing to the sinking of older and cooler oceanic crust towards the west (Pushcharovsky 2006, Barckhausen et al. 2013). Slight variations in spreading rate appear to have shaped the central Pacific abyssal plain seafloor as a juxtaposition of bathymetric highs and lows with a characteristic spacing of 1 to 10 km, elongated perpendicular to fracture zones (Klitgord and Mammerickx 1982, Olive et al. 2015). These horst and graben structures shape the CCZ seafloor as a succession of crenulated ridges, low profile valleys, and flat zones (Macdonald et al. 1996), and are also characteristic of most abyssal landscapes worldwide (Harris et al., 2014). Very low influx of terrigenous sedimentation maintain the horst and graben almost unobscured by blanketing of sediments at the CCZ, as opposed other abyssal plains closer to continental sediments (Smith and Demopoulos 2003).

The CCZ basin floor is covered by extensive polymetallic nodule fields and occasionally exposed basalts (Margolis and Burns 1976, Glasby et al. 1982), which add to the habitat heterogeneity constituting a unique deep-sea habitat (Radziejewska 2014a). Seafloor nodule cover can be extremely patchy and change drastically over tens of meters (Peukert et al. 2018). Genesis, abundance, and size of polymetallic nodules is thought to be controlled by bottom currents (Glasby et al. 1982, von Stackelberg and Beiersdorf 1991), as nodule growth may be regulated by sedimentation rates, which in turn, are controlled by small-scale variations in seafloor topography (Mewes et al. 2014). Surface sediment is mainly composed of Cenozoic pelagic clays and radiolarian oozes (ISA 2010), and the average carbonate compensation depth (CCD) is around 4500 m, although eastern CCZ sites have a much shallower CCD (~3500m) than western areas (~5000m) (Radziejewska 2014a). Bottom currents across the CCZ are generally weak (<10 cm sec^{-1}), but direction shifts and periods of intensified activity are not infrequent (Aleynik et al. 2017, Juan et al. 2018). The supply of sinking food particles to the CCZ seafloor is extremely low (Lutz et al. 2007), yet there appears to be a gradient increasing towards the more productive surface waters of the north east, based on biological findings (Glover et al. 2002, Smith et al. 2008b).

Polymetallic nodule fields represent an unusual type of abyssal plain habitat. The hard substratum resource provided by nodules combined with the background soft sediment seabed appears to increase habitat complexity, promoting the development of some of the most biologically diverse communities in the abyss (Amon et al. 2016, De Smet et al. 2017, Gooday et al. 2017, Pape et al. 2017). Morphospecies richness estimations from imagery data can rise above 200 taxa in local assessments (Amon et al. 2016) although genetic biodiversity is expected to be much higher (Glover et al. 2015). Nodules appear to support a specialised fauna that differs from that of nodule-free sediment areas (Thiel et al. 1993, Gooday et al. 2015). Nodule-dwelling meiofauna such as nematodes, tardigrades, harpacticoids, and foraminifera inhabit the crevices (Mullineaux 1987, Veillette et al. 2007b, Miljutina et al. 2010), while sessile macro- and megafauna such as polychaetes, sponges, cnidarians and xenophyophores are commonly found attached to nodule surfaces (Gooday et al. 2015, Amon et al. 2016). Consequently, nodule occurrence has been linked with variations in faunal standing stocks and distributions (Amon et al. 2016, Vanreusel et al. 2016). Epifauna, particularly suspension feeders, appear to have higher numerical densities in locations with higher nodule cover (Vanreusel et al. 2016, Tilot et al. 2018), while nodule-free areas host higher proportion of deposit feeders, such as holothurians (Radziejewska and Stoyanova 2000). However, the precise role of nodules and other local to regional environmental factors in the ecology of polymetallic nodule field communities is still poorly understood.

1.1.3. Polymetallic nodule mining

Nodules occur in commercially viable densities for potential exploitation in the central Indian Ocean basin, along the Cook Islands (equatorial Pacific), in the CCZ (NE Pacific), and in the Peru Basin (E Pacific) (Kuhn et al. 2017). Yet the composition and density (up to >30 kg m^{-2}) of nodule patches found in the CCZ attracted a particular mining interest in this area since the late 1960’s (Mero 1968, Amos et al. 1973, Ozturgut et al. 1978, Clark and Neutra 1983, Chung 1985). Deep-sea mining technologies have hence been progressing consistently since the late 1970’s (Chung 1985, Sharma 2011). At present time, the high global demand for minerals (Cu, Co) and rare earth elements combined with the progress in underwater technology appears to have balanced the potential profits with the high costs of abyssal nodule exploitation.

Sixteen polymetallic nodule mining exploration contract areas (150,000 km^2 each) were granted in the CCZ between 2001 and 2014 by the International Seabed Authority (ISA) (Wedding et al. 2015). The ISA, the institution responsible for the management of these resources (Lodge et al. 2014), also allocated a series of nine Areas of Particular Environmental Interest (APEIs) beyond contractor areas, where exploitation is prohibited (Smith et al. 2008b, ISA 2012), with the idea of preserving source populations of species for future recolonization of mining disrupted areas (Lodge et al. 2014). However, the majority of these APEIs remain unstudied; it is still largely unclear if their environmental conditions and faunas are similar to those of the mining claims (Glover et al. 2016a). Consequently, improved knowledge of the drivers structuring biological communities in the CCZ is urgently needed to test the presumed functionality and current spatial arrangement of the APEIs system, and to re-assess the regional environmental plan (ISA 2012).

The potential start of extractive activities within the CCZ has attracted considerable scientific and public awareness (Levin et al. 2016, Van Dover et al. 2017, Niner et al. 2018), as the magnitude of its inherent biological disturbance (Jones et al. 2017) could extend over extremely large seafloor areas (Aleynik et al. 2017), and full habitat recovery could take as long as nodules need to re-grow, i.e. millions of years. Despite the effects of mining impacts have been investigated for decades (Roels 1974, Ozturgut et al. 1981, Thiel and Schriever 1990), the ecology of these remote areas is still poorly understood. To date, it is largely unclear to what extent and timescale may these ecosystems recover from mining disturbance.

Exploitation of polymetallic nodule fields is expected to drastically change seafloor features (Morgan et al. 1999). Collector vehicles will remove the hard substratum provided by nodules, which is a basic resource for many sessile organisms and for small motile fauna inhabiting the crevices (Thiel et al. 1993, Veillette et al. 2007a, Vanreusel et al. 2016, Lim et al. 2017). Nodule-dwelling taxa can represent 50% of the of the megafaunal populations in polymetallic nodule fields (Amon et al. 2016), and hence nodule removal would represent a clear loss of habitat for the more specialised taxa (Gollner et al. 2017). In addition to nodule removal, the top ~10-15 cm of the surface sediment layer, containing much of the organic material and biomass, will be re-suspended into sediment plumes (Aleynik et al. 2017). Sediment plumes and their re-deposition can affect the feeding activities of suspension feeder fauna and limit the recolonization of disturbed areas by affecting larval dispersal, mortality and settlement success (Gollner et al. 2017). Moreover, physical and chemical alteration of surface sediments appears to be also long-lasting (>20 years), even in areas only affected by particle re-deposition (Paul et al. 2018).

The first polymetallic nodule test mining was undertaken in 1970 (Amos 1975), and similar small scale experiments followed over the years (Thiel and Schriever 1990, Harada and Fukushima 1997, Trueblood and Ozturgut 1997, Ingole et al. 2001, Radziejewska 2002, Miljutin et al. 2011). Jones et al. (2017) performed a meta-analysis of the effects of disturbance combining the results of all these experiments. The analysis showed that effects of simulated mining are severe immediately after disturbance, with an evident reduction in standing stock in all size classes, ranging from meio- to megafauna (Jones et al. 2017). Overall, mobile and small-sized fauna appear to be less sensitive at the long term compared to larger-sized fauna, as the former repopulate disturbed areas quicker (Jones et al. 2017), although there are clear examples of long term lack of recovery in particular meiofauna groups (Miljutin et al. 2011). Sessile fauna, typically suspension feeders like soft corals, remain virtually absent in directly disturbed seafloor, and very few faunal groups return to baseline or control conditions even after long periods (>20 years) (Vanreusel et al. 2016, Gollner et al. 2017, Jones et al. 2017). This variation in sensitivity amongst different size-classes and functional groups suggests a high potential impact of mining disturbance on polymetallic nodule field ecosystem functions. However, the ecology of this remote habitat is still poorly understood and therefore the real magnitude of commercial-scale mining disturbance remains highly difficult to predict.

1.2. Methodological considerations

1.2.1. The use of robots in deep-sea megabenthic ecology

Advances in underwater technology over the past ~15 years have opened up new perspectives in the ecological exploration of remote deep-sea habitats (Jones et al. 2009, Wynn et al. 2014, Huvenne et al. 2018). Progressively more sophisticated acoustical survey methodologies, e.g. multibeam and sidescan (Le Bas and Huvenne 2009), are being implemented in underwater robots to map variations in seafloor geophysical features (e.g. Brown et al. 2011, Harris and Baker 2012) across deep-sea landscapes (Grasmueck et al. 2006, Tempera et al. 2012, Clague et al. 2014, Peukert et al. 2018). In addition to these, progressively more sophisticated photographic and video survey methodologies, i.e. at higher resolutions (e.g. 4K video: Marouchos et al. 2018), are being used to map finer-scale environmental (Morris et al. 2016; Schoening et al. 2016) and biological (Jones et al. 2007, Jones et al. 2013) variations within deep-sea habitats. Acoustic mapping can provide large scale (i.e. hundreds of kilometers) information on geomorphological features at metre scale (or greater) resolutions, while imagery data can provide geological and biological data on a habitat scale of several square kilometres down to the millimetre scale (Durden et al. 2016c). The combination of these techniques, i.e. habitat mapping, has yield substantial advances in our understanding of deep-sea benthic ecosystems (Huvenne et al. 2011, Jones et al. 2013, Robert et al. 2014, Durden et al. 2015), usually upon the study of megafaunal distribution patterns using advanced marine robotics.

Megafauna are the largest animals (typically >1 cm length) inhabiting the deep seafloor and can hence be readily surveyed using imagery collected with underwater vehicles, either remotely operated (ROV) or autonomous (AUV) (Morris et al. 2014, Durden et al. 2016). ROV surveys are usually conducted upon live-video broadcasting (e.g. Martinez and Keener-Chavis 2006) that enables *in-situ* dive management (i.e. changes of course, camera zoom-in, etc.) or even the physical collection of specimens (e.g. Baker et al. 2012, Amon et al. 2016). In contrast, AUVs operate fully independently to conduct pre-programmed surveys that can last up to several days (Furlong et al. 2012), enabling the exploration of much larger (i.e. thousands of km^2 per dive) seafloor areas than with ROVs (Huvenne et al. 2018). AUVs can also be set to collect data at fixed altitudes, intervals, and speeds above the seabed (Morris et al., 2014). Thus, ROV-based image surveys are typically used for qualitative or small-scale investigations of benthic community change, for instance in structurally complex habitats like hydrothermal vents (Yoerger et al. 2000, Marsh et al. 2013), seamounts (Henry et al. 2014, Victorero et al. 2018a), or canyons (Orejas et al. 2009, McClain and Barry 2010, Fabri et al. 2017). In turn, AUV-based image surveys are more suited for comparably larger-scale quantitative assessments, for instance in open basins like abyssal plain areas (Durden et al., 2015; Vanreusel et al., 2016).

Image-based assessments have emerged in the past decade as a cost-effective approach to investigate the role of environmental factors in the structuring and distribution of remote megabenthic communities. Such studies can aim to describe baseline ecological patterns (Baker et al. 2012, Jones and Brewer 2012, Bell et al. 2016, Sautya et al. 2016) and/or investigate the effects of anthropogenic disturbance, to aid management and conservation activities (Bluhm 2001, Jones et al. 2012, Bo et al. 2014, Boschen et al. 2015, Vanreusel et al. 2016). In essence, most of these studies explore the roles of habitat heterogeneity in generating and maintaining biodiversity (Levin et al. 2001), which is also intended in the present work. In analytical terms, this aim can be achieved by statistically testing if variations in explanatory variables (e.g. seabed environmental factors) are non-randomly associated or covariate with variations in a set of response variables (e.g. biological parameters and community composition). Objective analysis of acoustic and photogrammetric data can be used to delineate specific areas of interest, i.e. survey strata or treatments, representing different ranges of a given environmental parameter (Jones et al. 2013, Morris et al. 2016) or anthropogenic impact (Kwasnitschka et al. 2016, Peukert et al. 2018). Part of this environmental mapping can be nowadays performed right after the data collection, i.e. while still on site during research expeditions (Greinert 2015, Jones 2015), opening up the possible use of environmentally stratified biological sampling.

1.2.2. Design and standardization of image surveys for megabenthic distribution analyses

The design of seabed photographic surveys requires accurate consideration of the biological parameters that can be inferred from image data, i.e. error ranges, and the potential sources of bias associated with the methodological approach used. Once this is clear, strict standardization protocols must to be conducted before and after the collection of benthic imagery to maximise the empirical value of the data obtained (Durden et al. 2016c; Fig. 1.1).

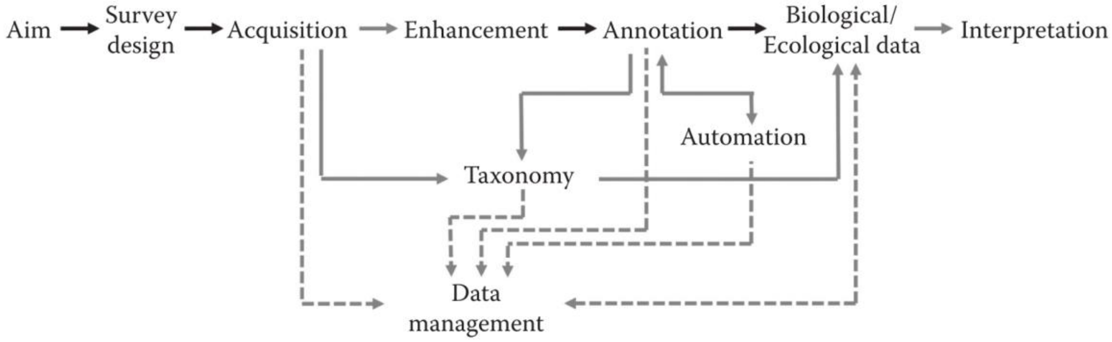

Figure 1.1. Steps in the use of marine imaging for biological assessment. Optional steps are shown in grey, and steps with data to be managed are shown with dashed connectors. Reproduced with permission of the authors (Durden et al. 2016c).

Stratified random sampling designs are amongst the most powerful data collection approaches that can be used for ecological pattern detection with relative ease (Ripley 1981, Krebs 1999). The idea of stratification is to collect independent samples (see next section) within different environmental strata or treatments to yield more precise parameter estimations, e.g. stratum means, than in systematic or simple random surveys (Green 1979, Andrew and Mapstone 1987). Stratification provides a way to optimise the sampling effort, i.e. to reduce the number of samples needed without reducing precision, while maximising the areal coverage (see e.g. Cochran 1977, Rao 2000). Minimum replication sizes can vary depending on the biological parameters targeted (Sokal and Rohlf 1995), but generic recommendations usually stablish a minimum of 2-3 replicates per unit or treatment (Krebs 1999). Objectively designed two-stage approaches usually allow analyses at multiple scales and minimise design-based bias in the spatial distribution of the replicate sampling units (Buckland et al. 2001, Strindberg and Buckland 2004). Greater precision is expected when strata are homogeneous within and heterogeneous among (Kenkel et al. 1989). In turn, completely randomized designs are best suited in the very particular case of known spatial homogeneity at large scale (Dutilleul 1993), which is precisely the null hypothesis against which investigations of habitat heterogeneity are formulated in deep-sea ecological research (e.g. Levin et al. 2001).

In the implementation of environmentally stratified sampling designs, photographic samples can be collected directly in the shape of line transects (i.e. Jones et al. 2009, Morris et al. 2014) or these can be generated *a posteriori* from the split of complete coverage photo-mosaics (CCPM) (Ludvigsen et al. 2007, Marcon et al. 2013) into smaller sub-units (tiles). CCPMs additionally provide a complete census, e.g. faunal presence/absence, that can serve the behavioural assessment of the patterns of taxa distributions (e.g. uniform, random, and clumped) at local scales (see e.g. Fortin and Dale 2005, Wiegand and Moloney 2013), for instance using point analyses (Ripley 1979, Baddeley et al. 2014). The application of CCPMs in deep-sea ecological research has so far been limited to small scale (tens of m^2) assessments, like studies of faunal zonation targeting hydrothermal vents (Podowski et al. 2010, Gerdes et al. 2019) or specific sections of wider habitats like seamounts and canyons, e.g. verticals walls (Robert et al. 2017) and coral mounds (Conti et al. 2019). Recent progress in the technology associated to marine image acquisition (e.g. improved camera resolutions and digital storing systems) enables the implementation of CCPMs to map very large (>1 km^2) seafloor areas at mm-resolution and in full colour (Prados et al. 2012, Bodenmann et al. 2013). These novel CCPMs approaches seem particularly well suited for the ecological study of deep-sea mining impacts, as mosaics can be used to visually map disturbance occurring at fine-scale, e.g. few-meter-wide nodule-collector tracks (Kwasnitschka et al. 2016), along sufficiently large areas to potentially conduct stratified random biological sampling (see Chapter 4). However, robust standardization protocols need to be conducted in both line transect or CCPM-based surveys to avoid pseudo-replication, i.e. extrapolation of results beyond the predefined sampling area (see e.g. Hurlbert 1984), and/or the inclusion of spatially-driven sampling biases.

Spatial autocorrelation (SA) is amongst the most important sources of bias in the interpretation of survey data derived from spatially-driven sampling designs (Legendre 1993). The concept of SA describes the dependence of the values of a given variable on the values of the same variable recorded at neighbouring locations, since observations that are structured in space are not independent (Fortin and Dale 2005, Getis 2008). SA prevails in virtually all remotely sensed georeferenced data (Griffith and Chun 2016), but tends to be overlooked in analyses targeting ecological aspects of faunal distribution (Dormann 2007, Kempenaers and Valcu 2010), particularly so in the design of AUV surveys (Foster et al 2014). SA-derived biases cannot be fully avoided but different approaches can be used in AUV surveys to minimise these, such as: i) the rigorous use of randomisation in as many steps within the survey and analysis as possible (Smith et al. 2017), for instance in the allocation of start positions in image transects (Strindberg and Buckland 2004, Buckland et al. 2015). ii) the collection of data across two spatial dimensions, for instance using a zig-zag transect allocation of survey transect (Foster et al. 2014). Both i) and ii) can also be implemented when using CCPMs, by applying a random selection of subunits, i.e. tiles, in the generation of samples. And iii) the use of sufficiently large physical sampling units with controlled outer boundaries (Legendre and Fortin 1989).

There is a range of different biological aspects that can be quantitatively assessed, using seabed photographic sampling, to investigate patterns in megabenthic community variation at the local scale. Standing stocks can be assessed using photogrammetric techniques. These range from the simple calculation of precise faunal densities, i.e. using biological count data and exact sample areal coverage derived from image analysis (Ruhl 2007, Jones et al. 2009), to the more complex calculation of proxy biomass per unit of sample, either based on faunal geometrical biovolume (Benoist et al. submitted) or length-weight ratios (Durden et al. 2016a, Stratmann et al. 2018a). Hill's (1973) values are a set of indices (H: 0, 1, and 2) that explore the different components of taxonomical diversity (Magurran 2004, Chao et al. 2014). Each of these indices reflects an increasing rate of appreciation of the relative abundances of different taxa (i.e. taxa evenness) in the calculation of diversity (Jost 2006). H0 indices (Species richness) only account for the presence/absence of taxa; H1 indices (e.g. Shannon-Weiner index) incorporate information on the relative abundance of different taxa, so adding some component of evenness; and H2 indices (e.g. Simpson's index) use a similar approach to H1, but amplifying the importance of the relative weight of taxa abundances to put more weight onto the evenness component of diversity (Hurlbert 1971, Magurran 2004, Jost 2006, 2010). H1 and H2 are hence considered heterogeneity diversity measures (Magurran 2004, p. 102). The Bray-Curtis (BC) dissimilarity measure (Clarke 1993) is one of the most commonly used multivariate approaches to quantify variations in assemblage composition (Legendre and Legendre 1998, Clarke et al. 2006). It calculates dissimilarity coefficients between different groups of samples based on faunal count data (Clarke 1993), the variation of which can be represented in different dimensions (Borg and Groenen 2003) and/or analysed in terms of statistical significance (Anderson 2001). As with Hill's values, the sensitivity of BC coefficients to the presence of rare taxa can be tuned using faunal count data transformations, i.e. from higher to lower appreciation of rare species occurrence:

presence/absence, double square root, log, square root, and no data transformation (see e.g. Legendre and Legendre 1998).

Image-based megabenthic assessments performed in abyssal areas usually target variations in density of the full community or particular faunal groups (Bluhm 2001, Ruhl 2007, 2008, Jones et al. 2014, Vanreusel et al. 2016). However, only a few studies have applied multi-component analyses of diversity (Durden et al. 2015, Amon et al. 2016), while others recommended their use but do not implement these (e.g. Tilot et al. 2018). The capacity of image-based research to contemplate multiple biological aspects (i.e. standing stock, all diversity components, and assemblage composition) appears directly related to the taxonomical resolution possible during faunal identification, which is inherently determined by the image quality, amongst other factors.

Image surveys tend to underestimate true taxonomical species richness (Glover et al., 2015) compared to sampling methodologies in which the organisms are physically collected and hence identified down to species level (e.g. coring in meio-, macrofauna sampling: De Smet et al. 2017, Pape et al. 2017). Megafauna species in most abyssal areas are poorly known (Jones et al. 2014, Tilot et al. 2018) and key body features for a full taxonomic identification are often not visible in images (e.g. oral disc in ophiuroids; O'Hara et al. 2018). Consequently, image-based megafauna studies typically require the development of local or regional catalogues describing the organisms found in the data collected, to standardise the identification process (e.g. Howell et al. 2010, Durden et al. 2015, Amon et al. 2016, Tilot et al. 2018). Such catalogues consist in photographic examples and descriptions of the visual features that support the morphological taxonomy of the putative species (i.e. morphospecies) encountered. Morphospecies catalogues are often published as field guides (e.g. Jones and Gates 2010, Gervais et al. 2012), scientific papers (Foell and Pawson 1986, Dahlgren et al. 2016, Amon et al. 2017) or in online repositories (e.g. www.dsg.mbari.org, www.ccfzatlas.com, www.discol.de/megafauna). The taxonomical resolution achieved in the classification of morphospecies normally depends on factors such as the image quality or the altitude of collection over the seafloor. For instance, using the *Autosub6000* AUV (McPhail 2009, Fig. 1.2) to collect imagery (2448 × 2048 pixels) at an altitude of 3 ± 1 m above the seabed of the Porcupine abyssal plain, Morris et al. (2016) were able to classify most of the morphospecies observed in images down to family or genus level. Despite this inherently lower taxonomical determination capacity, image-based surveys usually provide much accurate estimations of benthic taxa richness and numerical density than traditional trawling techniques (Bett et al. 2001, Morris et al. 2014, Ayma et al. 2016), with a minor impact.

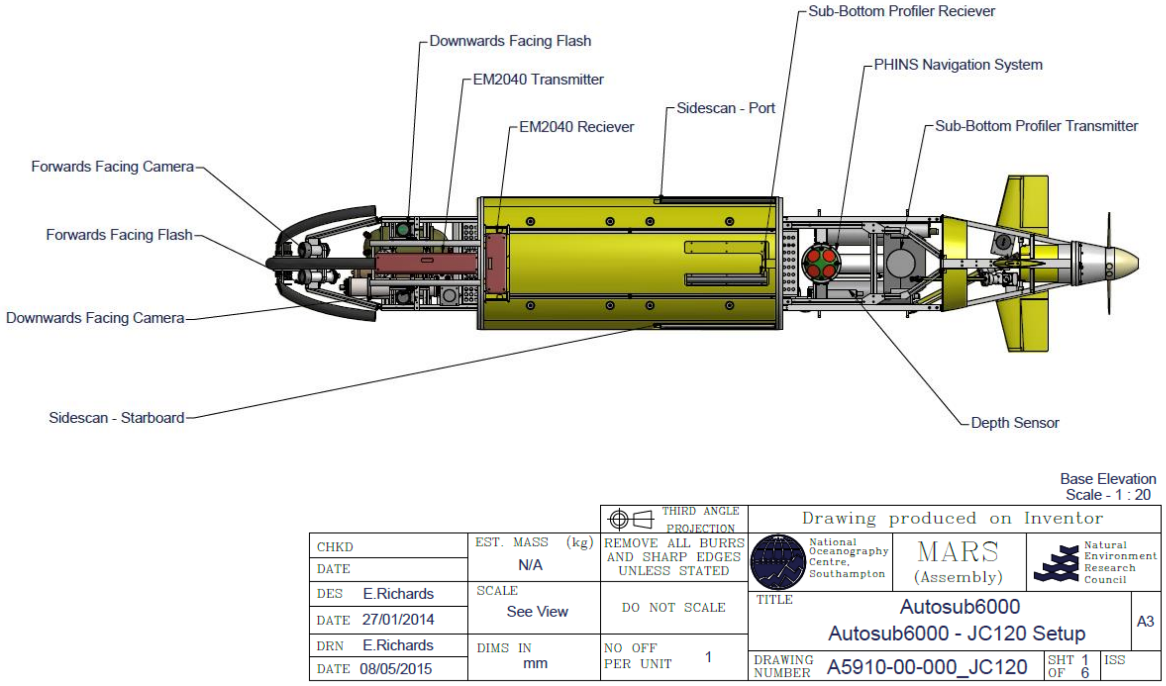

Figure 1.2. Sketch of the *Autosub6000* AUV from the National Oceanography Centre in Southampton. Positioning of different survey devices are indicated as set up during the JC120 research expedition (Jones 2015). Image courtesy of Ela Richards (Marine Autonomous and Robotic Systems, NOCS).

The usefulness of photogrammetric methods has led to megafauna being defined as those organisms large enough to be identified in deep-sea imagery (Grassle et al. 1975). This apparently simple and clear definition has though important methodological implications for the standardization of megafauna surveys. It implies that the minimum organism size considered in an image-based study, i.e. where we set the cut-off, is ultimately determined by survey features that condition organism identification, such as the image quality or the altitude above the seabed that these can be collected. Consequently, surveys conducted at closer distance will generally yield clearer organism identifications. But there are limits in the proximity to the seabed that AUV devices can reach, e.g. no less than 2 m, to avoid potential collisions (E. Richards, personal communication, April 28, 2015). Moreover, even if programed to survey at a fixed altitude, AUVs usually fluctuate vertically generating images at a range of altitudes above the seafloor (Morris et al. 2014). As a result, the minimum organism size considered in AUV photographic sampling is best considered *a posteriori*, once some preliminary data has been obtained from biological annotation to assess the consistency of faunal identifications. A simple yet thorough approach to tackle this issue is the exploration of potential biases in the detection of the smallest-sized taxa along the range of altitudes above the seabed where images were collected.

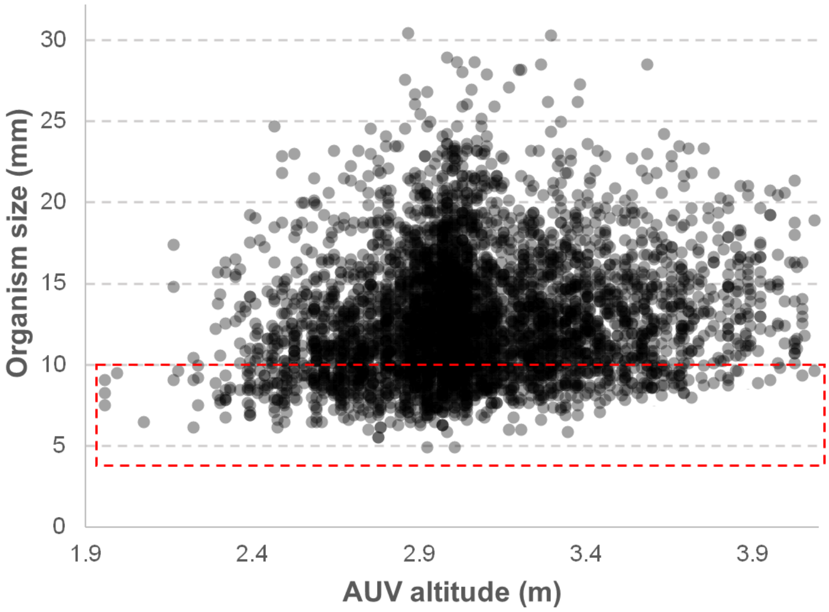

Figure 1.3. Variations in the detected organism sizes in images collected at different altitudes above the seabed. Plot shows the distribution of the sizes of the two smallest morphospecies detected in images collected at different AUV altitudes during JC120 expedition to the APEI6 of the CCZ (Jones 2015). Note the skewed distribution in the detection of the smallest organisms (i.e. < 10 mm) towards the images collected at lower altitudes (red-dashed rectangle).

For instance, Figure 1.3 shows the sizes of the smallest morphospecies identifiable in preliminary analysis of images collected between 1.9 and 4.1 m above the seabed using the *Autosub6000* during JC120 expedition (Jones 2015). This plot shows that organisms smaller than ~1 cm may be only detectable in those images collected in closer proximity to the seabed (i.e. ~1.9 – 3.4 m above seabed). This situation presents two main options to grant consistent standardization in organism detection across the image datasets collected; either retaining for analysis only those images taken below 3.4 m from the seabed, or retaining only organisms larger than 1 cm, which can be identified across the range of altitudes. Nevertheless, whichever way we choose, the use of images necessarily implies the risk of under-sampling the smallest populations in the community assessed, if only a fraction of their organisms (the largest) are detectable from images (Durden et al. 2016c). On the other hand, the minimal organism size considered ultimately affects the number of organisms that will be represented in image samples, i.e. the sample size, which can be key in the interpretation of results.

Larger samples, covering wider physical extensions and thus encompassing more specimens, characterise biological communities more precisely than smaller samples, but increases in precision are usually asymptotic with increasing sample unit size (Gotelli and Colwell 2001, Chao et al. 2009). Consequently, accuracy and precision of the parameters estimated in a study can be explored as a function of the sample size used, to support the reliability of the results obtained. This is a key concept in ecological sampling (Krebs 1999, Magurran 2004), largely explored in shallow marine or terrestrial systems (e.g. Andrew and Mapstone 1987, Hanberry et al. 2011), but barely tackled in deep-sea research (Soetaert and Heip 1990, Grassle and Maciolek 1992). Species accumulation curves are usually the only method applied to assess the representativeness of abyssal sampling, either in coring-based (De Smet et al. 2017, Pape et al. 2017) or image-based (Durden et al. 2015, Amon et al. 2016) assessments. However, the data contained in photographic samples can be readily decomposed in image sub-units or tiles, which makes these particularly well suited for the evaluations of sample-size derived precision in practically any estimated biological parameter. This can be implemented using data resampling techniques like bootstrap, the jack-knife, and randomization tests (Rodgers 1999), following similar approaches to those used in the evaluation of precision in species richness estimates (Crowley 1992, Chao et al. 2014). For instance, in the North Atlantic deep sea Durden et al. (2016c) and Benoist et al. (in press) have shown that parameters of conservation value exhibit various responses to the choice of sampling unit size, and that these are primarily linked to the number of specimens encompassed. In the CCZ, a key factor may be the very low numerical density of the megafauna, such that identifying an appropriate sampling unit size may be a particular issue. Studies that demonstrate appropriate sampling to support their conclusions are key in ecology, not least those concerned with the regulation of mining activities (Levin et al. 2016, Durden et al. 2017a).

1.3. Thesis overview

1.3.1. Research aims

This thesis aims to unfold the fundamental drivers of biological change in polymetallic nodule field ecosystems using acoustic and photographic data to investigate aspects of spatial heterogeneity in abyssal megabenthic community structure and distribution. Each experimental chapter (Chapters 2, 3, and 4) was devised to assess the influence of a different potential biological control on the distribution of megafauna: broad-scale seafloor geomorphological variations (Chapter 2); fine-scale hard substratum resource variations (Chapter 3); and different levels of presumed anthropogenic disturbance (Chapter 4). Numerical ecology methodologies based on strict quantitative hypothesis testing were carried out to detect patterns across space within polymetallic nodule field habitats, based on image-derived megafaunal samples collected using environmentally stratified random survey designs.

Chapters 2 and 3 were developed upon data collected within the APEI6 of the CCZ during *RRS James Cook* cruise JC120 (Jones, 2015). Both studies use the same biological dataset, yet a different approach in the survey design to assess the influence of each target environmental factor. Chapter 4 was developed upon data collected during *RV Sonne* cruise SO242-1 to the DISCOL site in the Peru Basin, where simulated mining impacts were still evident on the seafloor, 26 years after the disturbance experiment was performed (Greinert, 2015). Effects of each individual factor, and their combination where possible, are addressed with a particular focus on conservational aspects.

Chapter 2 explores megafaunal variations between three landscape types that commonly shape the seafloor of equatorial Pacific abyssal plains; a Ridge, a Flat and a Trough. These horst and graben reliefs are thought to be generally characteristic of the abyssal environment worldwide (Harris et al., 2014), and is particularly well defined in the CCZ (Olive et al. 2015), where the very low influx of terrigenous sediments prevents the blanketing of this topography (Smith and Demopoulos 2003). Habitat complexity derived from abrupt geomorphological variations can regulate standing stocks and diversity, i.e. seamounts and canyons (McClain 2007, De Leo et al. 2010), yet modest topographical variations can modulate similar variations, i.e. abyssal hills

(Durden et al. 2015, Morris et al. 2016), and may be hence particularly relevant to the ecology of the CCZ. Chapter 2 therefore addresses the following research question:

> **Q1- Are there differences in the megafaunal ecology between landscape types in polymetallic nodule fields?**

The CCZ megabenthos typically exhibits very low numerical density and a high species richness (Amon et al. 2016, Gooday et al. 2017), which could affect the estimation of ecological parameters, especially diversity estimations (Gotelli and Colwell 2001). Therefore, the chapter additionally examines the influence of the sampling unit size choice on a range of ecological parameters, to addresses the following research questions:

> **Q2- How sensitive are different ecological parameters to the size of the sampling-unit? How large has to be a photographic sample to reliably characterise CCZ megabenthic assemblages?**

Chapter 3 explores megafaunal variations across a gradient of polymetallic nodule occurrence. Nodules surfaces are typically inhabited by a diverse epi-growth that differs from that found in the surrounding sediment (Thiel et al. 1993, Veillette et al. 2007a). Although it has long been suggested that the hard substratum provided by nodules sustains the high biodiversity rates observed in polymetallic nodule fields (Mullineaux 1988, Veillette et al. 2007b, Amon et al. 2016, Vanreusel et al. 2016), logistical constrains in the mapping of nodule variations had so far limited the study of ecological pattern along continuous gradients of this resource. Chapter 3 therefore addresses the following research question:

> **Q3- Does the occurrence of nodule resource affect the ecology of megafauna across polymetallic nodule fields?**

To assess the potential influence of the landscape type (target of chapter 2) on ecological responses to the nodule cover gradient, separate analyses within each landscape type were additionally performed to addresses the following research questions:

> **Q4- Which aspects of the megabenthos in polymetallic nodule fields show a higher response to geomorphological variations? And in turn, which aspects show a higher response to nodule occurrence variations?**

Giant foraminifera (xenophyophores) are major constituents of the abyssal megafauna in the CCZ (Kamenskaya et al. 2013) and have been suggested to play a crucial role in polymetallic nodule field ecosystems (Gooday et al. 2017), i.e. providing habitat structures for meio- and macrofauna (Levin 1991). Although it is not possible to determine whether they are living from images (Hughes & Gooday, 2004), and hence these were not included in diversity assessments, additional analyses of the distribution of xenophyophore tests abundance were performed in both chapter 2 and chapter 3, with the aim to address the following research question:

> **Q5- Is there numerical evidence to hypothesise about a potential role of xenophyophore test occurrence in the structuring of metazoan megafauna assemblages?**

Chapter 4 explores long-term (>25 years) effects of simulated mining disturbance in the distribution of megafauna within polymetallic nodule fields. The DISCOL experiment conducted in the Peru Basin in 1989 (Thiel and Schriever 1990, Thiel et al. 2001) is the largest-scale disturbance experiment carried out to date. The revisit of the DISCOL site arranged over the course of the JPI Oceans project in 2015 provided hence a unique opportunity to investigate the potential long-lasting effects of simulated mining disturbance. Chapter 4 therefore addresses the following research question:

> **Q6. Are the effects of simulated mining impacts evident in the spatial distribution of megafauna within the DISCOL site, 26 years after disturbance?**

The DISCOL site was revisited in several occasions within the 7 year-period following the experiment and just before it started, with the objective of stablishing a temporal baseline of faunal response to disturbance (Ahnert and Schriever 2001, Bluhm 2001, Borowski 2001). The megafaunal community still showed evident signs of no recovery 7 years after disturbance, especially the suspension feeder fraction (Bluhm, 2001). Hence, Chapter 4 also addresses the following research question:

> **Q7. How do the current megafaunal distribution patterns compare to those observed in previous DISCOL revisits?**

1.3.2. Thesis structure

In accordance with the University of Southampton *Three-Paper Thesis* format requirements the content of the experimental chapters of this thesis are presented in exactly the same words as were used when these were submitted or as these are planned to be submitted to relevant journals. Hence, some overlap exists between chapters. Display materials have been renumbered and referring across chapters has been added to comply with thesis formatting regulations. For each chapter, the sections below provide an outline of the analytical approach, the author contributions, and the publication status. Collaborators are all from the National Oceanography Centre, Southampton, unless otherwise indicated.

1.3.2.1. Chapter 2: Megafaunal variation in the abyssal landscape of the Clarion Clipperton Zone

This chapter used swathe bathymetric survey data to objectively define three key landscape types in the APEI6 study area location (Flat, Ridge, Trough). Direct seabed sampling was additionally performed to further characterise the sedimentary environment in each landscape type. Variations in the megabenthos between landscape types were inferred from extensive photographic surveys collected following a stratified-random sampling design. To address **Q1**, different ecological parameters were calculated for each replicate sample, and variations of these between landscape types were statistically compared. To address **Q2**, different data resampling and rarefaction approaches were used to assess the precision and accuracy of a range of different parameters as a function of sample-unit size. Results of this analysis aid the interpretation of chapter 2 findings and the development of a robust survey design approach during chapter 3. Additionally, co-variation of xenophyophore test density with different ecological variables was assessed to address **Q5**.

This chapter was submitted to *Progress in Oceanography* as:

Simon-Lledó, E., J. M. Durden, R. M. Jeffreys, N. M. Benoist., T. Schoening, B. J. Bett, V. A. Huvenne, and D. O. Jones. Megafaunal variation in the abyssal landscape of the Clarion Clipperton Zone.

ESL annotated the photographs, analysed sediment samples, completed the subsequent data analysis and statistics, and wrote and edited the manuscript. R.M. Jeffreys (University of

Liverpool) performed nutrient analyses. T. Schoening (GEOMAR, Kiel) calculated nodule cover statistics. N.M. Benoist calculated biovolume metrics for each detected specimen. J.M. Durden (Univ. of Hawaii), B.J. Bett, V.A.I. Huvenne, and D.O.B. Jones provided advice on the data analysis and interpretation. All authors provided comments on the manuscript.

1.3.2.2. Chapter 3: Ecology of a polymetallic nodule occurrence gradient; implications for deep-sea mining

This chapter used image-based nodule-detection algorithms to classify the biological data inferred from each image during chapter 2 along a gradient of nodule cover occurrence. Using a modified form of bootstrapping, measures of variability (i.e. confidence intervals) in ecological characteristics between different nodule cover ranges were stablished, to address **Q3**. Homologous analyses were performed for each landscape type in chapter 2 separately, to address **Q4**. Additionally, co-variation of xenophyophore test density with different ecological variables was assessed to address **Q5**.

This chapter was submitted to *Limnology and Oceanography* as:

Simon-Lledó, E., T. Schoening, N. M. Benoist, B. J. Bett, V. A. I. Huvenne, and D. O. B. Jones. Ecology of a polymetallic nodule occurrence gradient: implications for deep-sea mining.

ESL annotated the photographs, completed the subsequent data analysis and statistics, and wrote and edited the manuscript. T. Schoening (GEOMAR, Kiel) calculated nodule cover statistics. N.M. Benoist calculated biovolume metrics for each detected specimen. B.J. Bett, V.A.I. Huvenne, and D.O.B. Jones provided advice on the data analysis and interpretation. All authors provided comments on the manuscript.

1.3.2.3. Chapter 4: Disturbance-mediated megafaunal variations in the Peru Basin

This chapter used seafloor photo-mosaics generated from extensive AUV surveys to objectively define four levels of potential disturbance across the DISCOL seafloor. Provided that disturbed plough-tracks are still readily observed in AUV imagery, target study areas were mapped as a function of the distance of the seafloor to the nearest disturbed track (i.e. within disturbed track; 1-10 m from disturbed track; 10-50 m from disturbed track,; and >3500 m from disturbed tracks: reference area). A stratified-random sampling design was applied to generate replicate sample sets by grouping randomly selected patches of seafloor from each disturbance level mapped, along with the megafauna detected in each. To address **Q6**, different ecological parameters were calculated for each replicate sample, and variations of these between disturbance levels were statistically compared. A particular focus was given to the relative variations of the most dominant taxonomic groups, to enable comparison with findings from previous DISCOL revisits, and address **Q7**.

This chapter was submitted to *Scientific Reports* as:

Simon-Lledó, E., K. Köser, T. Schoening, J. Greinert, B. J. Bett, V. A. I. Huvenne, and D. O. B. Jones. Biological effects 26 years after simulated deep-sea mining

K. Köser, T. Schoening, and J. Greinert (GEOMAR, Kiel) processed the imagery data, generated seafloor mosaics, and split those in tiles for subsequent ecological analysis. ESL annotated the tiles, performed the seafloor disturbance mapping based on full mosaic data, completed the subsequent data analysis and statistics, and wrote and edited the manuscript. B.J. Bett, V.A.I. Huvenne, and D.O.B. Jones provided advice on the data analysis and interpretation. All authors provided comments on the manuscript.

1.3.2.4. Megafauna morphospecies catalogue

Several taxonomic experts consulted (directly or indirectly) during the compilation and standardization of the megafauna catalogue used to identify specimens throughout this thesis, these were: Diva Amon, Tina Molodtsova, Andrey Gebruk, Andrew Gates, Sergi Taboada, David Billett, Henk-Jan T. Hoving, Tammy Horton, Tomoyuki Komai, Daniel Kersken, Pedro Martinez Arbizu, Christopher Mah, Michel Roux, Jeff Drazen, Rich Mooi, David Pawson, Tim O’Hara, Helena Wiklund, Mary Wicksten, Andrei Grischenko, Astrid Leitner, Craig Young, Dhugal Lindsay, and Janet Voight.

2. Chapter 2. Megafaunal variation in the abyssal landscape of the Clarion Clipperton Zone

2.1. Abstract

The potential for imminent polymetallic nodule mining in the Clarion Clipperton Fracture Zone (CCZ) has attracted considerable scientific and public attention. This concern stems from both the extremely large seafloor areas that may be impacted by mining, and the very limited knowledge of the faunistics and ecology of this region. The key environmental factors regulating local seafloor ecology are still very poorly understood. In this study, we focus on megafaunal ecology in the proposed conservation zone 'Area of Particular Environmental Interest 6'. We employ swathe bathymetric survey data to objectively define three key landscape types in the area (Flat, Ridge, Trough; water depth: 3950-4250 m) that are generally characteristic of the wider CCZ environment. We use direct seabed sampling to further characterise the sedimentary environment in each landscape type, detecting no statistically significant differences in particles size distributions or organic matter content. Additional seafloor environmental characteristics and data on both the metazoan and xenophyophore components of the megafauna were derived by extensive photographic survey from an autonomous underwater vehicle. Image data revealed that there were statistically significant differences in seafloor cover by nodules and in the occurrence of other hard substrata habitat between landscape types. Statistically significant differences in megafauna standing stock, functional structuring, diversity, and faunal composition were found between landscape types. Geomorphological variations presumably regulating local bottom water flows and the availability of nodule and xenophyophore test substrata between study areas may be the mechanism driving these assemblage differences. We also used these data to assess the influence of the sampling unit size choice on the estimation of ecological parameters. Sampling unit size evaluation supported our results, although each parameter exhibited a different sensitivity to this factor. All of these results are important to the appropriate management of potential mining activities in the CCZ and elsewhere in the deep ocean.

2.2. Introduction

The likelihood of polymetallic nodule mining in the Clarion Clipperton Fracture Zone (CCZ) has attracted considerable scientific attention (Levin et al. 2016, Van Dover et al. 2017). The potential impacts of mining are likely to extend over extremely large seafloor areas (Glover and Smith 2003, Aleynik et al. 2017). Such disturbance may lead to major change in the benthic fauna (Jones et al. 2017) and full recovery might take thousands of years (Glasby et al. 1982). Sixteen nodule mining exploration contract areas (150,000 km^2 each) were granted in the CCZ between 2001 and 2014 by the International Seabed Authority (ISA). The ISA also allocated a series of nine Areas of Particular Environmental Interest (APEIs) beyond these claim areas, where exploitation is prohibited (ISA, 2012) . The APEIs were designated to preserve source populations of species for future recolonization of disturbed areas (Lodge et al. 2014). However, the majority of these APEIs remain unstudied; it is not clear if their environmental conditions and faunas are similar to those of the mining claims (Glover et al. 2016a). As a result, improved knowledge of the drivers structuring biological communities in the CCZ is urgently needed to test the presumed functionality and current spatial arrangement of the APEIs system, and to re-assess the regional environmental plan (ISA, 2012).

The CCZ is generally considered as an extensive abyssal plain delimited by the topography of two WSW-ENE trending fracture zones, Clarion and Clipperton. There is a gradual increase in water depth from east (4000 m) to west (5000 m) owing to the sinking of older, cooler oceanic crust to the west (Pushcharovsky 2006). However, slight variations in spreading rate appear to have shaped the CCZ seafloor into a series of bathymetric highs and lows with a characteristic spacing of 1 to 10 km, elongated perpendicular to fracture zones (Klitgord and Mammerickx 1982, Olive et al. 2015). These horst and graben structures shape the CCZ seafloor as a succession of ridges, valleys, and intervening ‘flat’ zones. This topographic variation is thought to be generally characteristic of the abyssal environment worldwide (Harris et al. 2014). The very low influx of terrigenous sediments to the CCZ prevents the blanketing of this topography, as may occur on abyssal plains adjacent to continental margins (Smith and Demopoulos 2003).

Abyssal plains represent some 70% of the world’s seafloor (Harris et al. 2014) and are considered the largest contiguous feature in the Earth (Ramirez-Llodra et al. 2010). They are poorly explored but appear to have high species richness, including very many undescribed taxa (Smith et al. 2006). Despite their name, abyssal plains can have significant topography that influences the diversity and composition of deep-sea fauna (Durden et al. 2015, Stefanoudis et al. 2016, Leitner et al. 2017). This ecological variation appears to result from the interconnected effects of topographically-driven variation of local current dynamics (Thistle et al. 1991), sediment composition (Durden et al. 2015), and food supply (Smith and Demopoulos, 2003; Morris et al., 2016). However, habitat complexity derived from abyssal landscape geomorphology may have been underappreciated in global estimations of ecological heterogeneity at the deep-sea floor (Durden et al. 2015, Morris et al. 2016); a factor that might be particularly significant to the ecology of the CCZ.

The CCZ appears to have one of the highest levels of deep-sea megafaunal (>1 cm length) species richness (Kamenskaya et al. 2013, Tilot et al. 2018). Morphospecies richness estimations from imagery data can rise above 200 taxa in local assessments (Amon et al. 2016). True species diversity and genetic biodiversity is expected to be much higher (Glover et al. 2015). Given their smaller body size, even higher local diversity is to be expected in the meio- and macrofaunal assemblages of the CCZ (De Smet et al. 2017, Pape et al. 2017). Epifauna, particularly suspension feeders, appear to have higher numerical densities in locations with higher nodule coverage (Vanreusel et al. 2016), with nodule-free areas having an higher proportion of deposit feeders, such as holothurians (Stoyanova 2012). However, the precise role of nodules, and other local environmental factors, in the ecology of CCZ megafauna at the CCZ is still poorly understood. Faunal composition analyses are scarce, and most quantitative studies have been based on relatively small sample unit areas (<1000 m^2), and low replication levels. Meaningful comparison across the CCZ is also hampered by a lack of standardization between studies.

Reliable estimation of ecological parameters relies on appropriate sampling of the populations under investigation. It is often these parameters that serve as the sole basis for conservation management decisions (Andrew and Mapstone 1987, Magurran 2004). Investigation of the pros and cons of different sampling strategies is commonplace in terrestrial and shallow-water marine ecology (Heck Jr et al. 1975, Andrew and Mapstone 1987, Buckland et al. 2001) but rarely tackled in deep-sea studies, except for diversity estimators (Soetaert and Heip 1990, Grassle and Maciolek 1992, Etter and Mullineaux 2001). In part, this lack of research stems from logistic constraints, however, the need is no less. In the CCZ, a key factor may be the very low numerical density of the megafauna, such that identifying an appropriate sampling unit size may be a particular issue (Benoist et al., submitted; Durden et al., 2016). Studies that demonstrate appropriate sampling to support their conclusions are key in ecology, not least those concerned with the regulation of mining activities (Levin et al. 2016, Durden et al. 2017a).

Our study assesses the ecology of the megafauna in the dominant landscape types of APEI6 in the eastern CCZ. We define the landscape types by objective analysis of the bathymetry, establish corresponding sedimentary environmental conditions by direct sampling, and further environmental characteristics and faunal data by extensive seafloor photography from an autonomous underwater vehicle (AUV). In this contribution we examine landscape-type-related variations in standing stock, diversity, and faunal composition and how these parameters, and their interpretation, might vary with the choice of sampling unit size.

2.3. Materials and methods

Study area

The CCZ basin floor is covered by extensive polymetallic nodule fields that add to the seabed heterogeneity and constitute a unique deep-sea habitat (Radziejewska 2014a). Seafloor nodule coverage can be extremely patchy and change drastically over tens of metres (Peukert et al. 2018). Surface sediment is mainly composed of Cenozoic pelagic clays and radiolarian oozes (ISA, 2010). The average carbonate compensation depth (CCD) is around 4500 m (Mewes et al. 2014), although much shallower to the east (~3500 m) than the west (~5000 m) (Radziejewska 2014a). Bottom currents are generally weak (<10 cm s^{-1}), but direction shifts and periods of stronger flows are not infrequent (Aleynik et al. 2017). The supply of sinking food particles to the seafloor is extremely low (Lutz et al. 2007), although higher in the APEI6 area than in western areas (Veillette et al. 2007b).

All results reported here relate to the APEI6 area, and were acquired during RRS *James Cook* cruise 120 (Jones 2015). The survey represented a 5,500 km^2 rectangle of seafloor centred on 122° 55' W, 17° 16' N (Fig. 2.1), chosen to have similar topographic relief to mining contract areas in the central CCZ. Water depth ranged 3950-4250 m, and the seafloor landscape comprised a succession of crenulated ridges and shallow troughs oriented north-south between dispersed level-bottom (<3° slope) areas.

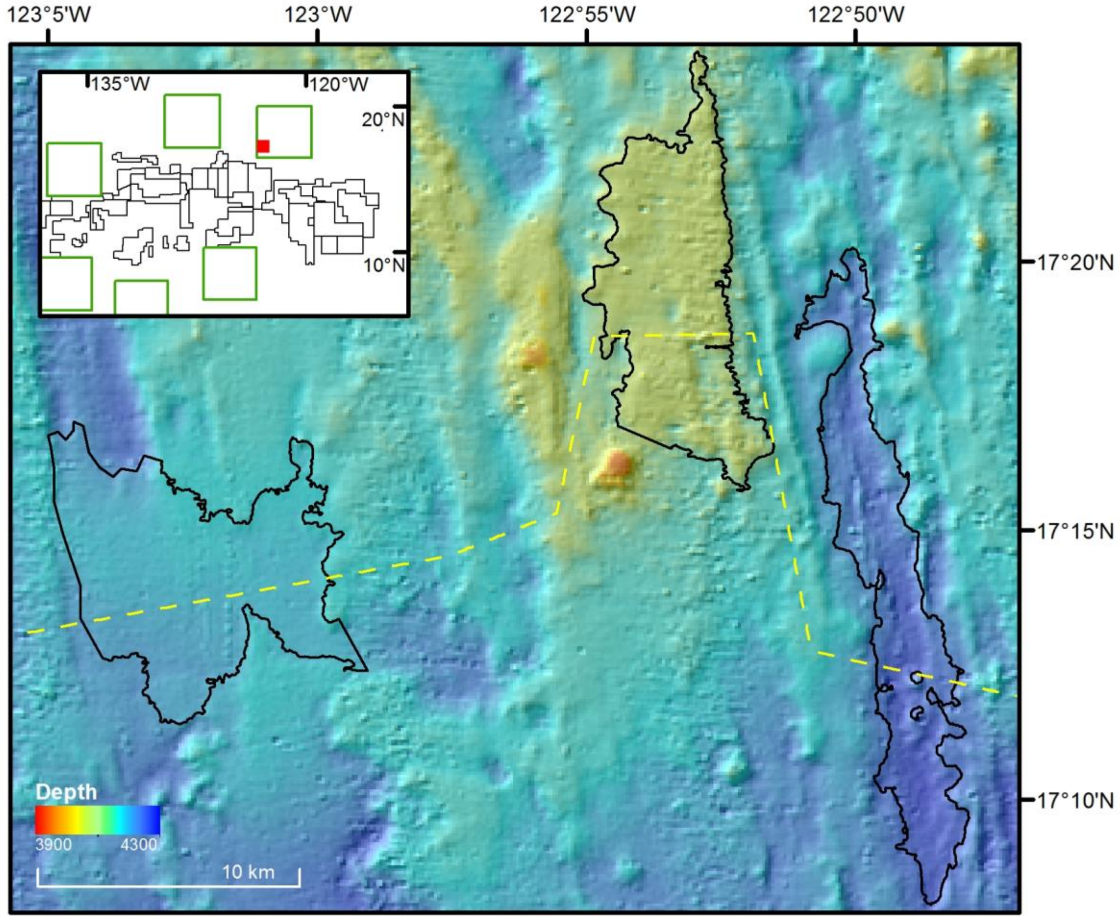

Figure 2.1. Bathymetric survey chart of the study location within the APEI6 of the CCZ (North Pacific Ocean). Landscape types mapped using objective classification depicted in dark lines. Yellow dashed line shows seafloor bathymetric profile depicted in Figure 2. A map of the eastern CCZ is inset, showing exploration licenced areas (black polygons), Areas of Particular Environmental Interest (green polygons), and study location (red square).

Survey design

Bathymetric mapping and landscape characterisation

Multibeam data were collected with the shipboard Simrad EM120 system (191 beams) and processed using CARIS HIPS and SIPS software (TeledyneCARIS; v8.0). The resultant digital elevation model (~100 m horizontal resolution) was used to calculate broad bathymetric position Index (bBPI) (Weiss 2001) and terrain ruggedness index (TRI) (Wilson et al. 2007) using SAGA v. 2.1.4 software (Conrad et al. 2015). BPI was calculated using an inner radius of 500 m and an outer radius of 10,000 m, and TRI was calculated with a 500 m radius circular neighbourhood. These areas were selected to be representative of the landscape-scale geomorphological variation that was the target of this study. After visual inspection of the generated datasets, classification thresholds were set to map ridge (bBPI: 50 to 100; TRI: 0 to 150), trough (bBPI: -100 to -50; TRI: 0 to 150), and flat (bBPI: -50 to 50; TRI: 0 to 50) areas. Contours were drawn using ArcGIS v10 (ESRI, 2011) along threshold values of each dataset, and used to delimit representative polygons. Three polygons each representing a characteristic landscape type were chosen for stratified-random sampling: Flat area, Ridge area, and Trough area (Fig. 2.2). Data were projected in Universal Transverse Mercator projection, Zone 10N, using the World Geodetic System 1984 datum.

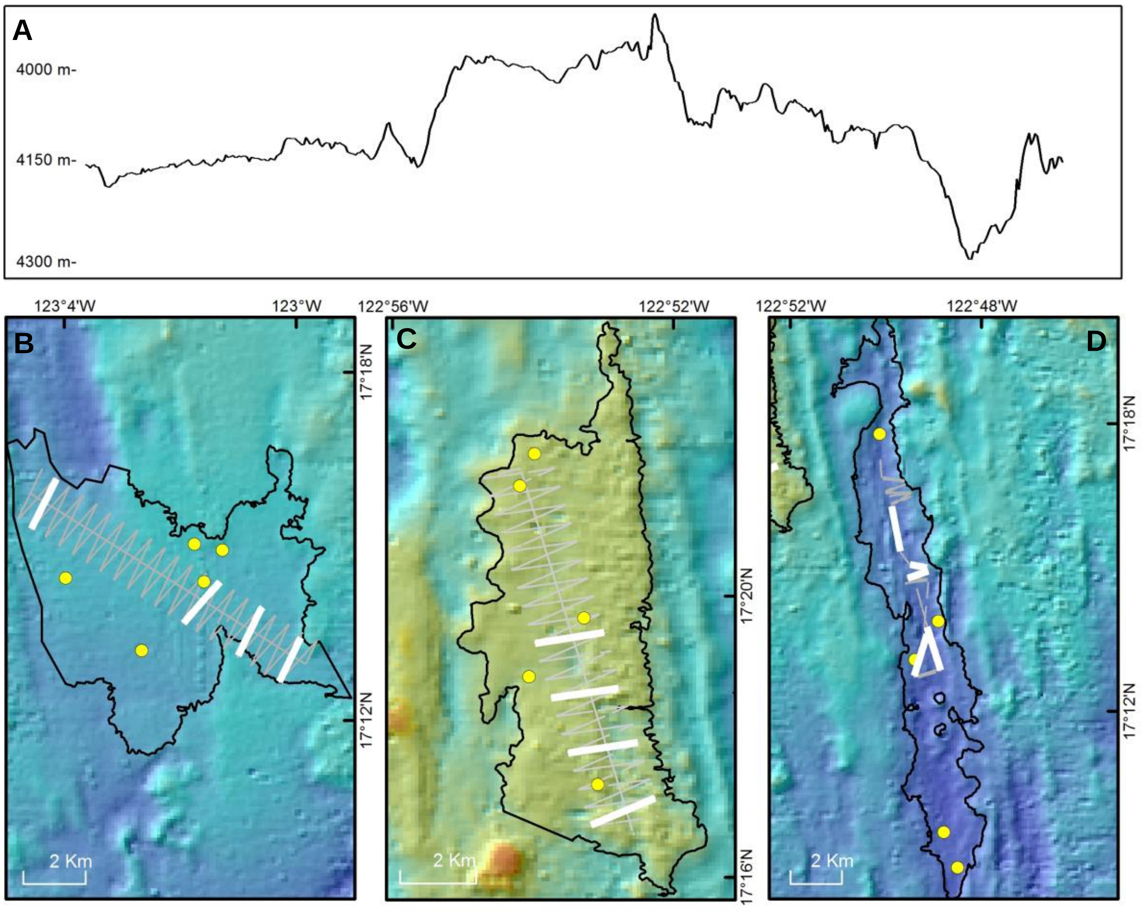

Figure 2.2. Survey Landscape type study areas investigated at the APEI6. **A)** Seafloor bathymetric profile depicted as yellow-dashed line in Fig 1. **B to D:** Detail of sampling operations: grey lines indicate full AUV image survey tracks, thick white lines highlight replicate sampling units selected for analysis, and yellow dots represent coring stations. Study areas surveyed: **B)** Flat area. **C)** Ridge area. **D)** Trough area.

Direct sampling

Five sediment sampling stations, with a minimum separation of 100 m, were randomly selected within each study area (Fig. 2.2B-D). Two Megacore (Gage and Bett, 2005; 10cm internal diameter) samples were collected per station. Each sample was initially sliced and split by sediment depth. Sediment grain-size distributions were assessed from one core in 0-5 and 5-10 mm depth horizons, by laser diffraction using a Malvern Mastersizer 2000 after homogenisation (grains >2 mm removed), dispersal in 0.05% $(NaPO_3)_6$ solution, and mechanical agitation. Grain-size distributions obtained for the two horizons were averaged for presentation. The 0-10 mm horizon from the second core were assessed for sediment chemistry. Total carbon (TC) and total nitrogen (TN) contents were measured in duplicate (reproducibility <±5%) using a Carlo Erba NC 2500 CHN Elemental Analyser. Total organic carbon (TOC) was determined after de-carbonation of the samples using the acid HCl vapour method of (Yamamuro and Kayanne 1995).

Photographic survey

Seafloor photographic images were collected using two digital cameras (FLIR *Grasshopper2*; 2448 x 2048 pixels), one mounted vertically, and one forward oblique facing on the autonomous underwater vehicle (AUV) Autosub6000 (Morris et al. 2014). The camera layout and the underwater navigation system were set as described in Morris et al. (2014). The AUV was programmed for a target altitude of 3 m above the seafloor, a speed of 1.2 m s^{-1}, and a photographic interval of 850 milliseconds. At the target altitude, individual vertical photographs imaged 1.71 m^2 of seabed.

In each area, a zig-zag survey design (Fig. 2.2B-D), with random start point, was chosen to maximise sampling efficiency while minimising design-based bias in the spatial distribution of the replicate sampling units (Buckland et al. 2001, Strindberg and Buckland 2004). A total of 40 sampling units, the straight line zig and zag sections, were surveyed in each area. Four sampling units were randomly selected in each area for subsequent analysis. Images taken as the vehicle changed course, i.e. junctions between sampling units, were discounted. In the remaining straight line sections, every second image was discounted to avoid overlap between consecutive images and the risk of double counting. To ensure consistency in specimen detection, images outside the altitude range 2-4 m were also discounted. The total seabed area analysed from each of the randomly selected sampling units was then standardised to c. 1320 m^2 (range 1321-1324 m^2) by random selection from the remaining constituent images, typically 715 photographs (range 555-

781). All images used for data generation were colour corrected as described by Morris et al. (2014).

Data analysis

Environmental assessment

Sediment grain size statistics were calculated using Gradistat v.8 software (Blott and Pye 2001), applying the geometric method of moments (Krumbein 1936). Mud content was calculated as the proportion of particles <63 µm. Carbonate content wet weight (% wt) was calculated from the difference between TC and TOC (assuming all carbonate was $CaCO_3$). The ratio of total organic carbon to total nitrogen (C:N) was calculated as the molar ratio.

Nodule seafloor coverage (% cover) and total surface covered by nodules (m^2) were quantified from AUV imagery using the Compact-Morphology-based poly-metallic Nodule Delineation (CoMoNoD) method (Schoening et al. 2017). CoMoNoD attempts to detect all polymetallic nodules present in an image and calculates their areal extent (cm^2) based on an ellipsoidal shape projection, to correct for potential underestimation resulting from sediment cover. Only nodules ranging from 0.5 to 60 cm^2 (i.e. with maximum diameters of ~1 to ~10 cm) were considered for analysis to avoid inclusion of large non-nodule formations. Angular-shaped cobbles to large rocks and whale bones (min. diameter >10 cm) coated in ferromanganese crust were manually counted and measured. Average nodule cover (%) and total nodule area extent (m^2) were calculated across the selected images of each sampling unit.

Megafauna assessment

Images used for megafauna data generation were reviewed in random order to minimise time or sequence-related bias (Durden et al., 2016). Specimens (>10 mm) were identified to the lowest taxonomic level possible (morphospecies: msp), measured using the BIIGLE 2.0 software (Langenkämper et al. 2017), and assigned to a “nodule-attached” (NA) or “Nodule-free-living” (NFL) life habit. To ensure consistency in identification, a megafauna morphospecies catalogue was developed based on an existing CCZ collation (see http://ccfzatlas.com), which was updated and maintained in consultation with international taxonomic experts and by reference to the existing literature (Dahlgren et al. 2016, Glover et al. 2016b, Amon et al. 2017). The likely feeding behaviour of each morphospecies was inferred from similar organisms described in the literature (i.e. Iken et al. 2001). Individual metazoan specimen biovolume was estimated, as a proxy for biomass, from two body measurements using the generalised volumetric method described of Benoist et al. (submitted). Despite being comparable in size to metazoan morphospecies, xenophyophores were analysed separately since it is not possible to determine whether they are living from images (Hughes and Gooday 2004).

A range of ecological parameters were calculated for each replicate sampling unit, including numerical density (ind m^{-2}) and proxy biomass density (ml $m^{-2} \approx$ g fresh wet weight m^{-2}). To examine the range of diversity characteristics, Hill's diversity numbers of order 0, 1, and 2 (Jost 2006) were calculated as morphospecies richness (S), the exponential form of the Shannon index (exp H´), and the inverse form of Simpson's index (1/D), using the 'vegan' package implemented in R (Oksanen et al. 2018). Additionally, sample-based morphospecies rarefaction curves were fitted using the analytical method proposed by Colwell et al. (2012), using Estimate S v.9.1 software (Colwell 2013), by randomly resampling sample data of each study area without replacement, while exp H´ and 1/D accumulation curves were calculated with replacement. *K*-dominance curves were also generated to explore dominance patterns (Clarke 1990).

Statistical analyses

Generalized linear models (GLM) (Dobson and Barnett 2008) were built to test whether statistically significant variation in environmental or biological parameters was apparent between study areas, using the 'car' package (Fox et al. 2016) implemented in R (R Core Team 2017). Models were fitted with quasi-Poisson errors in non-negative integer metrics (i.e. density, S) with over-dispersion (Gardner et al. 1995), and with normal errors applied to non-integer variables (i.e. mean grain size, exp H´, 1/D) (Freund and Littell 1981). Differences in proportional metrics (i.e. nodule coverage, mud content, or functional group percentages) were tested with beta-regression models (Ferrari and Cribari-Neto 2004) using the 'betareg' package (Cribari-Neto and Zeileis 2010). When statistically significant effects were detected in these global test, simultaneous tests were applied to make multiple comparisons between individual study areas, using the 'multcomp' package in R (Hothorn et al. 2008). Homogeneity of variance and normality assumptions were verified by visual inspection of model histograms and QQ plots. Statistical significance was reported for $p < 0.05$.

Variations in community composition between study areas were explored using a range of abundance-based multivariate approaches. The Bray-Curtis dissimilarity measure, based on square-root transformed faunal abundance, as calculated using the 'vegan' package in R, was used throughout these analyses. Non-metric multidimensional scaling (nMDS) ordination was used to visualise variations (‘vegan’ package in R). A one-way permutational MANOVA (PERMANOVA) analysis (Anderson 2001), with follow-up pair-wise tests, was used to test for statistically significant variations in assemblage composition between study areas, using PRIMER v.7 (Clarke and Gorley 2015). A SIMPER (‘’similarity percentages’’) analysis was performed to assess morphospecies contribution to between-group dissimilarity (‘vegan’ package in R).

Megafauna sampling effort evaluation

To assess the reliability of the biological survey developed in the present study, we investigated the effect of varying sampling unit size (seabed area or individuals covered per sample unit) on the accuracy (i.e. stabilization of mean value) and precision (i.e. coefficient of variation: CV) of different ecological parameters. Image data were first pooled within study area (i.e. across sampling units) and then randomly resampled 1000 times with or without replacement (depending on the target parameter and approach used: see below) into new sampling unit sets of increasing image number size. The mean (or median), the precision (CV), and the confidence intervals (95%) of each parameter were calculated at each sample unit size increase, together with the mean total seabed area and individuals represented by the images composing each subset.

Morphospecies rarefaction curves were fitted using the analytical method proposed by Colwell et al. (2012), using Estimate S v.9.1 software (Colwell 2013), by randomly resampling image sets of increasing size without replacement. Accumulation curves were interpolated and extrapolated up to 3000 individuals sampled, to balance for differences in fauna densities. Additionally, curves were extrapolated up to 15,000 m^2 per study area (see SM; Fig. 2.12). The autosimilarity approach proposed by Schneck and Melo (2010), as implemented in the seabed image case by Durden et al. (2016b), was applied to evaluate precision in assemblage description. At each sample size, Bray-Curtis dissimilarity was computed between two groups of images, each randomly selected without replacement and composed by half the total number of images of each set. Metazoan density, biomass density, and exp H´ and 1/D indexes were computed by bootstrapping image subsets resampled with replacement (Buckland et al. 2001). Custom R scripts and the ‘vegan’ package were used to process image data and calculate all ecological indices.

2.4. Results

Environmental assessment

Surface sediments (0-10 mm horizon) were dominated by radiolarian-bearing pelagic clay to fine silt particles (diameter <7.8 µm; 58-68% of particles), and medium to very coarse silt grains (diameter = 7.8-63 µm; 28-39% of particles). Mean and median particle size, and mud proportion showed no statistically significant variation between areas, though larger value ranges were evident among the Ridge area samples (Table 2.1). Subsurface sediments (>50 mm horizon) in the Ridge and Trough showed much greater variability in grain size distributions than those in the Flat area (SM; Fig. 2.11; Table 2.3). Relative proportions of TOC, TN, and $CaCO_3$ were almost homogenous across the study areas; no statistically significant differences were detected between study areas (Table 2.1).

The polymetallic nodules observed during the present study were of an ellipsoidal-flat shape with smooth surfaces. Mean nodule surface area was 2.5 cm^2, with most nodules <5 cm^2 (90%), and very few >10 cm^2 (1%). Nodules in the Flat were larger than in the other areas, though not significantly (Table 2.1). Average nodule cover was 6.4% and ranged from nodule-free to 38%. The highest mean nodule coverage was recorded in the Flat area (Table 2.1), although both the within-sampling unit and within-area deviations for this metric were high. Nodule coverage did exhibit a statistically significantly difference between study areas (Table 2.1), with a statistically significant pair-wise difference between the Flat and Trough areas (Tukey, $p < 0.05$). Larger (>60 cm^2 in surface) hard substratum formations coated in ferromanganese crust were especially common in the Ridge area, where angular shaped cobbles, boulders, and whale bones were about ten times more abundant than in the other study areas (Table 2.1). However, the inclusion of these structures (total survey area surface <6 m^2) to the total hard-substratum availability of each sample unit was negligible, even in Ridge samples.

Table 2.1. Environmental and biological features assessed for each landscape type of the APEI6, with detail on the general linear models (GLM) applied to explore variations of these parameters between study areas. **Sediment parameters:** measured from surface sediment (0-10 mm) and shown as: mean (minimum - maximum) obtained amongst all replicate Megacore samples (n=5) collected in each area. *Parameters*: particle size; mud content (particles <63 µm) percentage; percentages of total organic carbon (TOC) and $CaCO_3$; and molar C_{org}/Total nitrogen ratio. **Image parameters:** measured from seafloor imagery data and shown as: mean (95% confidence intervals: lower – upper) calculated amongst all replicate image samples (n=4) collected in each area. ***Parameters:*** seafloor percentage cover and total nodule area calculated using the CoMoNoD algorithm on seabed imagery (see text); density of non-nodule (>10 cm) hard substrata (boulders and whale bones); total density and proportion of metazoan and xenophyophore individuals (>10mm) split in different functional (SF: suspension feeders; DF: deposit feeders) and attachment-type (NA: nodule-attached fauna) categories; biomass (grams of fresh wet weight) density inferred using the generalised volumetric method (see text); and diversity: richness, exponential Shannon (exp H'), and inverse Simpson (1/D) indices.

	Flat	Ridge	Trough	Error fit	F-value
Sample parameters					**($F_{2,14}$)**
Sediment mean grain size (µm)	8.1 (7.7 - 8.2)	9.5 (6.8 - 17.6)	9.2 (8 - 12.2)	G	0.34
Sediment mud content (%)	92.6 (91.7 - 93.8)	92.5 (79.9 - 95.7)	90.7 (85.6 - 93.2)	B	1.01
Sediment TOC (%)	0.42 (0.39 - 0.44)	0.41 (0.35 - 0.45)	0.44 (0.39 - 0.49)	B	0.8
Sediment C_{org} TN^{-1}	4.0 (3.8 - 4.3)	3.8 (3.6 - 4.0)	4.1 (3.7 - 4.5)	B	0.85
Sediment $CaCO_3$ (%)	0.33 (0.24 - 0.53)	0.48 (0.26 - 0.66)	0.36 (0.26 - 0.48)	B	0.5
Image parameters					**($F_{2,11}$)**
Nodule surface size (cm^2)	2.6 (2.3 - 2.9)	2.0 (1.7 - 2.3)	2.1 (1.6 - 2.6)	G	2.57
Nodule seabed cover (%)	10.1 (7.2 - 12.3)	6.3 (4.3 - 8.6)	3.8 (1.9 - 6.5)	B	**6.73****
Nodule seabed cover (m^2)	133.8 (95 - 162)	83.0 (56.4 - 113.8)	50.1 (24.5 - 86.4)	G	**4.82***
Other hard-substrata (items ha^{-1})	62 (28 - 102)	682 (230 - 1132)	64 (30 - 102)	QP	**10.26****
Metazoan density (ind m^{-2})	0.49 (0.42 - 0.54)	0.47 (0.41 - 0.53)	0.32 (0.25 - 0.39)	QP	**5.23***
Metazoan biomass (g fwwt m^{-2})	1.6 (1.1 - 2.1)	2.9 (1.5 - 4.2)	2.1 (1.0 - 3.2)	G	0.79
Metazoan richness (S)	70.5 (67.2 - 74.0)	64.8 (61.0 - 68.5)	59.5 (50.5- 68.5)	QP	2.09
Metazoan exp H'	29.7 (27.0 - 32.3)	28.3 (25.5 - 31.5)	23.4 (18.3 -28.4)	G	2.33
Metazoan 1/D	16.4 (14.2 -18.5)	16.4 (13.2 - 19.6)	9.7 (6.2 -13.2)	G	**4.66***
Metazoan NA (ind m^{-2})	0.34 (0.29 - 0.38)	0.28 (0.23 - 0.35)	0.19 (0.13 - 0.25)	QP	**5.33***
Metazoan NA (%)	69.3 (60.9 - 74.4)	60.0 (50.2 - 67.3)	57.2 (48.2 - 65.5)	B	2.49
Metazoan SF density (ind m^{-2})	0.39 (0.34 - 0.44)	0.34 (0.29 - 0.39)	0.25 (0.19 - 0.31)	QP	**4.25***
Metazoan SF (%)	79.8 (77.9 - 81.6)	73.6 (69.6 - 76.1)	77.2 (74.8 - 79.5)	B	**5.33***
Metazoan DF density (ind m^{-2})	0.07 (0.07 - 0.08)	0.10 (0.09 - 0.11)	0.05 (0.04 - 0.07)	QP	**13.90****
Metazoan DF (%)	15.9 (14.4 - 17.4)	21.6 (18.5 - 24.8)	17.2 (14.9 - 19.4)	B	**5.56***
Xenophyophore density (ind m^{-2})	2.22 (1.54 - 2.99)	4.09 (3.55 - 4.60)	1.33 (0.48 - 2.6)	QP	**5.94****
Xenophyophore OHS (ind m^{-2})	1.15 (0.75 - 1.64)	1.36 (1.01 - 1.71)	0.52 (0.15 - 1.14)	QP	2.22
Xenophyophore OHS (%)	50.7 (47.5 - 54.2)	32.8 (28.3 - 37.2)	32.7 (24.3 - 41.3)	B	**10.22****

Figure 2.3. Examples of metazoan megafauna photographed at the APEI6 seafloor during AUV survey. Scale bars representing 50 mm. **A)** Actiniaria msp-6**. B)** Actiniaria msp-13**. C)** *Bathygorgia cf. profunda*. **D)** *Abyssopathes* cf *lyra*. **E)** Left: *Chonelasma sp.*; right: *Hyalonema sp*. **F)** *Cladorhiza* cf *kensmithi***. G)** *Bathystylodactylus* cf *echinus*. **H)** *Nematocarcinus* sp. **I)** Sabellida msp-1 (polychaete). **J)** Left: *Freyastera sp.*; right: *Caulophacus sp.* **K)** *Psychropotes* cf *longicauda* **L)** *Benthodytes* cf. *typica*. **M)** *Coryphaenoides* sp. **N)** *Typhlonus nasus* **O and P:** probable new *Mastigoteuthis sp.* same specimen photographed with different cameras. **O)** Vertical view **P)** Oblique view. Image taken ~1” prior to the vertical shot.

Table 2.2. Total abundance and taxonomical classification of metazoan morphospecies groups sampled at each APEI6 study area. Abundances show how specimens were found: sessile attached to hard-substratum (OHS); sessile on sediment or mobile fauna (OSS). (*) "Group" level taxonomical classification is not hierarchical, ranges from Class to Family level, to simplify tabulation.

Phylum/Class	**Group**	**Morphospecies**	**Flat**		**Ridge**		**Trough**	
	(*)	(n)	OSS	OHS	OSS	OHS	OSS	OHS
Ctenophora	Tentaculata	2	1		1			
Porifera	Porifera	10	26	45	33	40	52	35
	Desmospongidae	7	42	126	53	119	174	342
	Hexactinelidae	9	8	19	19	4	17	9
Cnidaria	Scyphozoa	2	5				6	
	Aff. Anthozoa	1		4		7	1	5
	Actiniaria	13	49	306	39	242	36	93
	Alcyonacea	6	107	821	125	633	52	252
	Antipatharia	1		1		1		
	Ceriantharia	2	8	3	2	1	5	1
	Pennatulacea	1	2	1	1		1	
Bryozoa	Cheilostomatida	4	19	251	44	226	25	95
Annelida	Echiura	3	21		20		10	
	Polychaeta	5	63	152	60	173	34	104
Mollusca	Bivalvia	1	74		140		66	
	Gastropoda	2	8		1		3	
	Octopoda	1			1		1	
	Scaphopoda	1	19		7		8	
	Teuthoidea	1	29		29		22	
Arthropoda	Aff. Crustacea	-	33		36		38	
	Amphipoda	3	12		11		11	
	Cirripeda	2	2	23	2	14	3	7
	Copepoda	2	12		2		8	
	Decapoda	8	43		20		30	
	Isopoda	1	16		17		14	
	Peracarida	1	7		8		3	
Echinodermata	Asteroidea	5	14		4		4	
	Crinoidea	6	1	12	4	20	5	19
	Echinoidea	5	60		79		45	
	Holothuroidea	11	32		19		16	
	Ophiuroidea	4	78		161		38	
Chordata	Urochordata	2	3	6	1	1	3	7
	Osteichthyes	7	23		18		15	
TOTAL		**129**	**817**	**1770**	**957**	**1481**	**746**	**969**

Megafauna assessment

Metazoan fauna

A total of 6740 megafauna individuals (>10 mm) were recorded in the 15,840 m^2 of seabed examined during the present study (Table 2.2). Megafauna were classified into 129 morphospecies and 11 higher taxonomic categories (i.e. Order, Family; Table 2.2). Rare taxa (≤ 3 records) represented a third of the total morphospecies richness. The fauna observed (Fig. 2.3) were predominantly cnidarians (25 msp; 0.18 ind m^{-2}, ~70% of which were Alcyonacea bamboo corals), sponges (27 msp; 0.07 ind m^{-2}), annelids (9 msp; 0.04 ind m^{-2}), bryozoans (4 msp; 0.04 ind m^{-2}), and echinoderms (32 msp; 0.04 ind m^{-2}). Mollusc, crustacean, fish, tunicate, and ctenophore morphospecies were also recorded at lower densities (<0.03 ind m^{-2}; Table 2.2). The metazoan fauna was primarily composed of suspension feeders (78%) and deposit feeders (16%), while predators and scavengers were scarce (4%). Almost 80% of suspension feeding individuals were found attached to polymetallic nodules or other hard substrata. The proportion of nodule-attached individuals was >70% of the total abundance in 37 morphospecies. These “nodule-dwelling” taxa constituted 70% of the total abundance, and 30% of the total richness recorded.

Patterns in faunal distribution

Mean metazoan density exhibited a statistically significantly difference between study areas (Table 2.1), with densities in Flat and Ridge areas higher than those in the Trough (Tukey, $p < 0.05$). We detected statistically significantly higher densities of suspension feeders in the Flat area compared to the Trough, and statistically significantly higher densities of deposit feeders in the Ridge than in the other study areas (Tukey, $p < 0.05$). Mean density and proportion of predators and scavengers was similar in all study areas (Table 2.1). Although the proportion of the fauna attached to nodules was not statistically significantly different between study areas (Table 2.1), the densities of nodule-attached individuals were statistically significantly higher in the Flat than in the Trough (Tukey, $p < 0.01$). The mean biomass density recorded across all sampling units was 1.22 g fwwt m^{-2} (in c. 1320 m^2 observed), with no statistically significant difference detected between study areas (Table 2.1).

Mean morphospecies richness (S) was higher in the Flat, though we found no statistically significant difference between study areas (Table 2.1). Sample-based morphospecies accumulation curves showed that this pattern was consistent at whole study areas sampling level (Fig. 2.4A), and extrapolation of image-based curves predicted the same scenario even when triplicating the total sampling performed per study area (SM; Fig. 2.12). Variations in diversity between study areas were more evident at progressively higher Hill's orders ($q > 0$). Mean exp H' and 1/D indices were higher in the Flat and the Ridge areas compared to the Trough, although these differences were statistically significant only in 1/D index (Table 2.1). These patterns were consistent at whole study areas sampling level (Fig. 2.4B-C). We also detected a higher morphospecies dominance in the Trough area, and more even abundances in the Flat and Ridge areas (Fig. 2.5A).

Variations in community composition

Cnidarians, sponges, bryozoans, and echinoderms showed the clearest variations in density between study areas (Fig. 2.6). In total, 54% of the morphospecies recorded were present in all three study areas, 22% were noted in only two areas, and 24% were detected in one area only area. Most (70%) of the single area records were singletons (SM; Fig. 2.13) and the rest rare morphospecies (≤ 5 occurrences). Nevertheless, a statistically significant difference in faunal composition was detected between the study areas (PERMANOVA, $R^2 = 0.39$, $p < 0.001$) (Fig. 2.7A), with statistically significant differences apparent in paired comparisons between the Trough and the other study areas (pair-wise PERMANOVA, R^2=0.36-0.37, $p < 0.05$). SIMPER analysis showed that variations in the density of 10-15 morphospecies were responsible for 70% of the dissimilarity between study areas, but three morphospecies, a sponge (Porifera msp-5) and two soft corals (*Lepidisis* msp and *Callozostron* cf. *bayeri*), contributed most to the significant dissimilarities. Total density of *Porifera* msp-5 in the Trough (8.7 ind 100^{-1} m^{-2}) was four times higher than in the Ridge and Flat areas; total density of *Lepidisis* msp in the Flat (3.8 ind $100m^{-2}$) was four times higher than in the Ridge and 20 times higher than in the Trough areas; while total density of *C*. cf *bayeri* in the Ridge and the Flat (~2.5 ind $100m^{-2}$) was four times higher than in the Trough area.

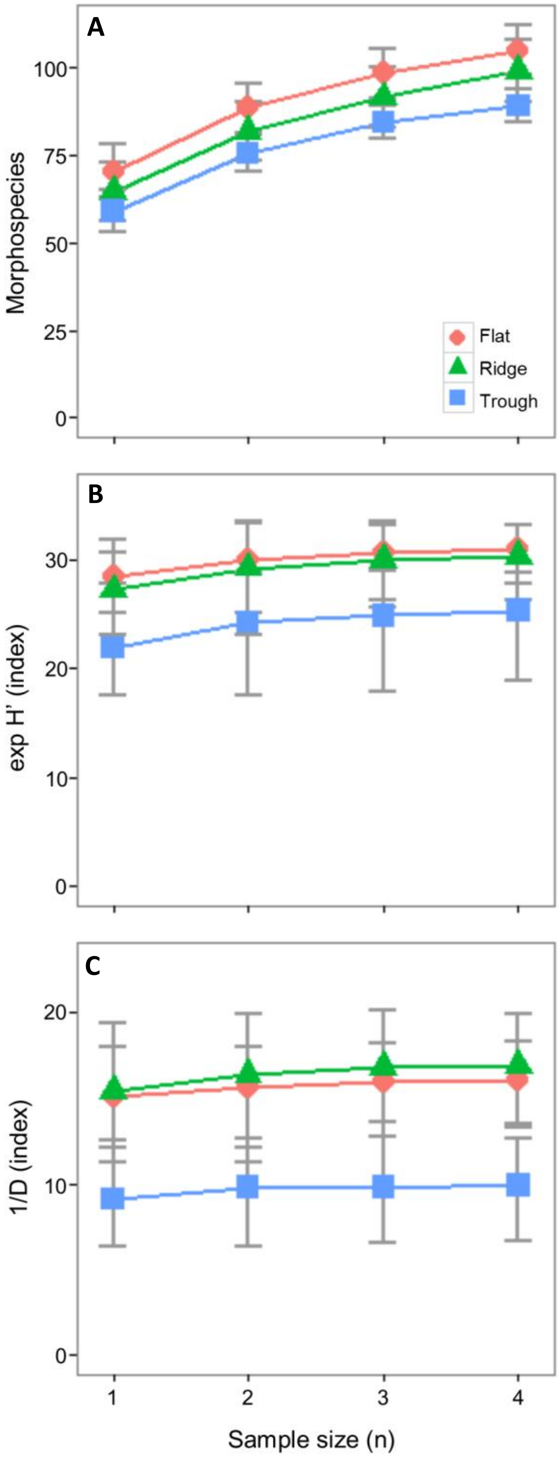

Figure 2.4. Sample-based diversity accumulation curves calculated for each APEI6 study area. Fauna occurrences of each replicate sample were randomly resampled (with or without replacement) 1000 times at each sampling effort level (n=1-4). **A)** Species rarefaction calculated without replacement. **B)** Exponential Shannon index, calculated with replacement. **C)** Inverse Simpson index, calculated without replacement. Error bars represent 95% confidence intervals between runs.

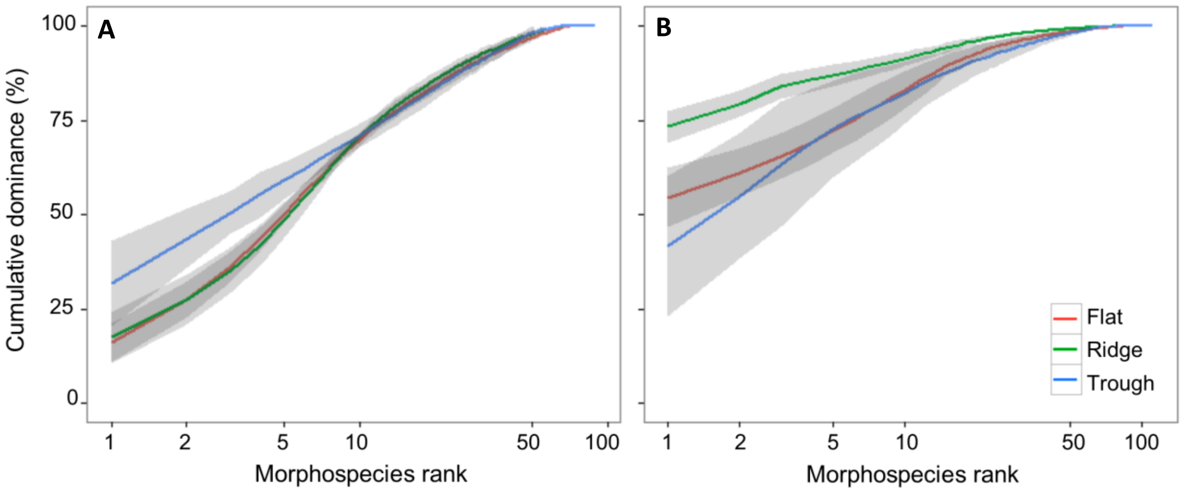

Figure 2.5. Morphospecies *k*-dominance curves calculated for each APEI6 study area. Curve lines represent cumulative rank abundances calculated as the mean amongst the four replicate samples analysed for each area. Shadowing represents 95% confidence intervals. **A)** Curves calculated including only metazoan fauna. **B)** Curves calculated including metazoans and xenophyophores.

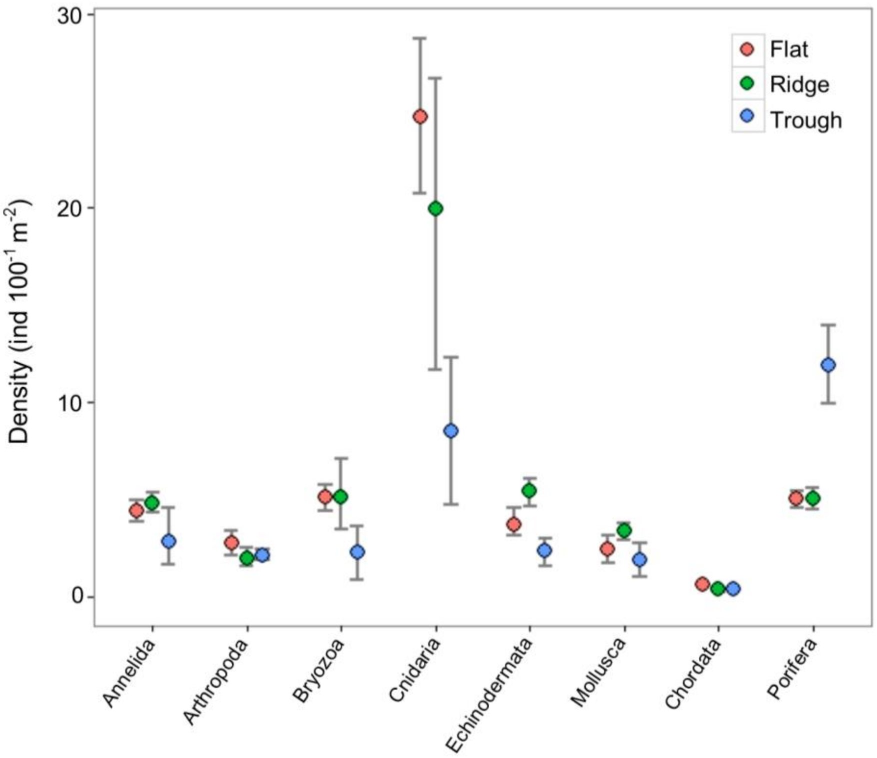

Figure 2.6. Density variations of different metazoan taxonomic groups between APEI6 study areas. Points represent the mean density of each group calculated amongst the four replicate samples analysed for each area. Error bars represent 95% confidence intervals.

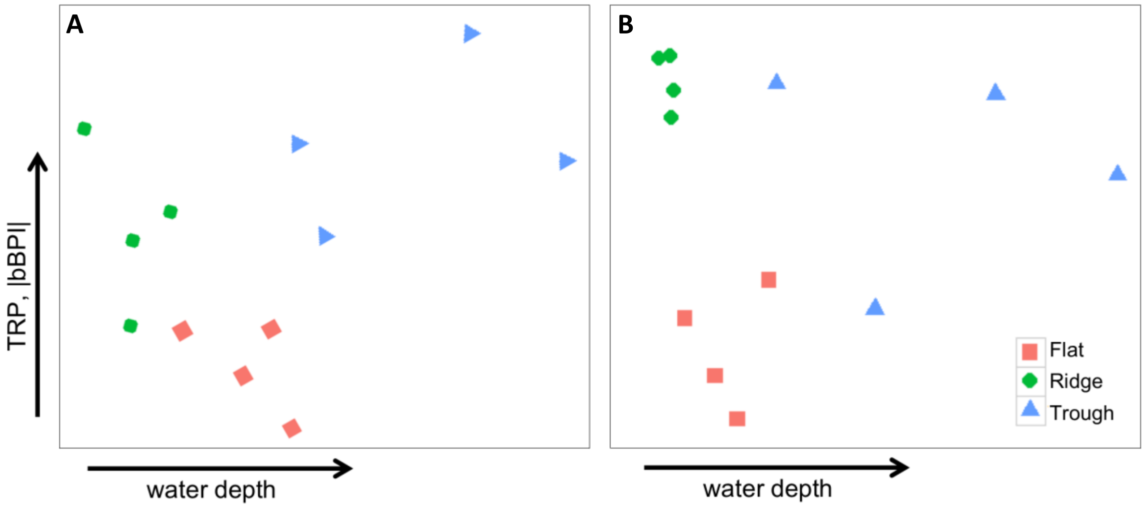

Figure 2.7. Interpreted megafauna morphospecies composition nMDS for APEI6 samples. Two-dimensional representations of nMDS developed on Bray-Curtis resemblance matrix calculated from square-root transformed megafauna composition by abundance data. **A)** nMDS plot developed including only metazoan fauna. **B)** nMDS plot developed including metazoans and xenophyophores. Arrows indicating the (non-linear) trend in water depth and bathymetric derivatives suggested for each axis.

Sample unit size evaluation

Estimates of most of the ecological parameters assessed were consistent at the sample unit size used in the present study (c. 1320 m^2 of seabed) (Figs. 2.8 and 2.9). The maximum precision (CV) reached by each parameter with increasing sample unit size ranged from 0.02 to 0.30 (SM; Fig. 2.14), yet increases in precision were relatively minor for most parameters with unit sizes >300 individuals (700-900 m^2), except for autosimilarity, which required much smaller sizes (>150 individuals; 300-450 m^2) to reach an almost constant precision rate (SM; Fig. 2.15). Analysis of accuracy yield more variable results. Estimation of mean taxa richness required the largest unit size to stabilise (>500 individuals; 1000-1500 m^2) (Fig. 2.8A-B), while fauna density required the smallest (>30 individuals; 50-100 m^2) (Fig. 2.9A-B). Mean autosimilarity required unit sizes >500 individuals (1000-1500 m^2) to stabilise (Fig 2.9C-F). At this size, mean within-sample similarity was >70% (i.e. two sub-samples of 250 individuals randomly generated from 500 individuals yield an average similarity >70%). Accuracy of biomass density estimates differed between study areas: sample unit sizes >500 individuals were required for stabilisation of median values in the Flat and Trough samples, while stabilisation in the Ridge occurred >250 individuals. Mean exp H' stabilized with unit sizes >350 individuals (700-1000 m^2) (Fig. 2.8C-D), while mean 1/D stabilised with >200 individuals (400-600 m^2) (Fig. 2.8E-F).

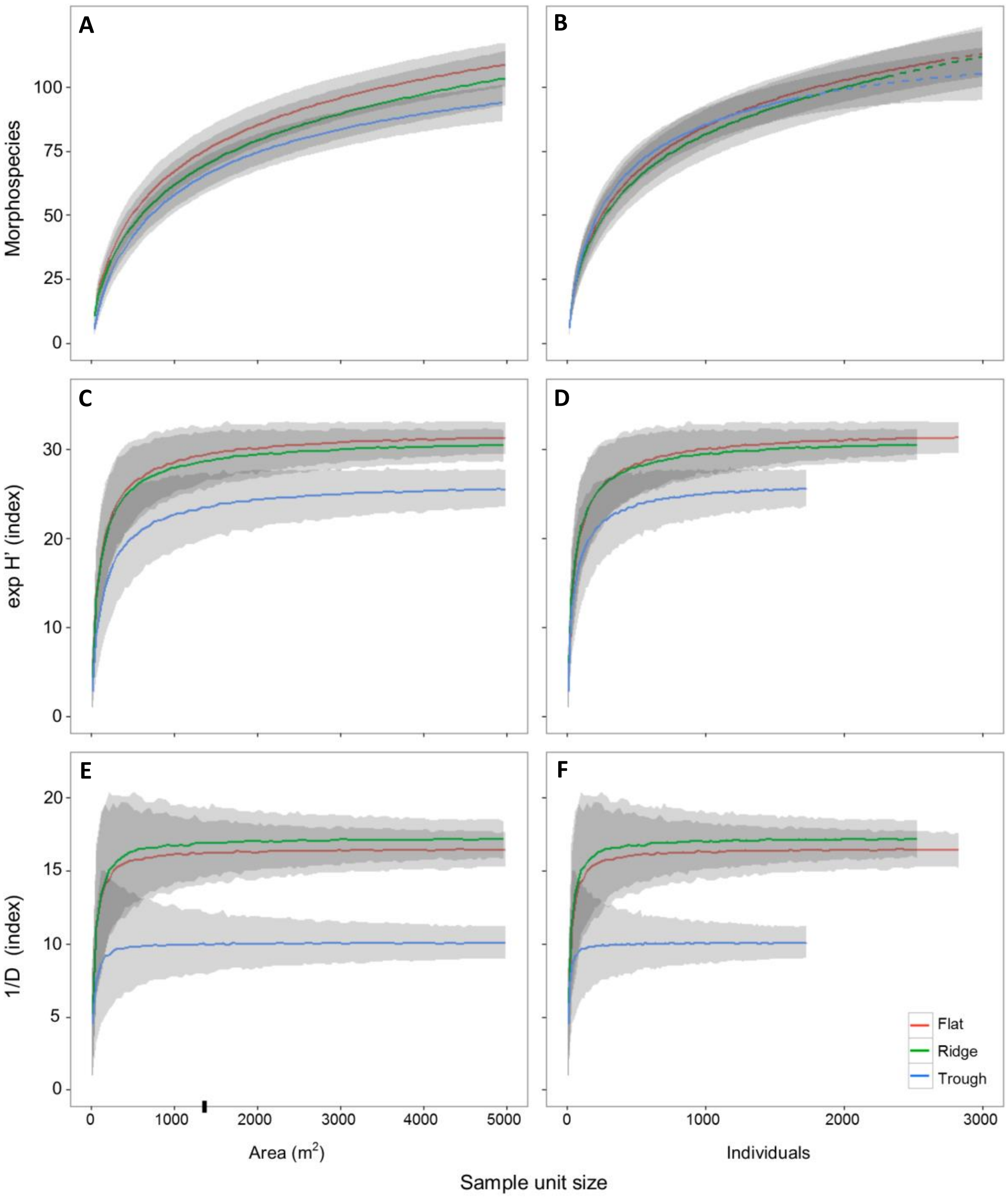

Figure 2.8. **Variation of the different metazoan community diversity indices used in the present study, as a function of the seabed area or number of individuals encompassed by the sample unit size**. Lines represent mean values across the 1000 randomisations performed at each sample unit size increse, for each study area collated sample (n=3) (see methods). Shadowing representing 95% confidence intervals. Ticks on x-axis indicate the sampling unit size used in the present study (replicate sample areas = 1320 m^2). **A and B:** Rarefied metzaoan morphospecies accumulation curves. **A)** Area-based accumulatiuon curves. **B)** Individual-based accumulation curves. Dashed lines represent sample extrapolation. **C and D:** Variation of metazoan exp H’ diversity index. **E)** Area-based mean exp H’**. F)** Individual-based mean exp H’**. E and F:** Variation of metazoan 1/D diversity index. **I)** Area-based mean 1/D**. J)** Individual-based mean 1/D.

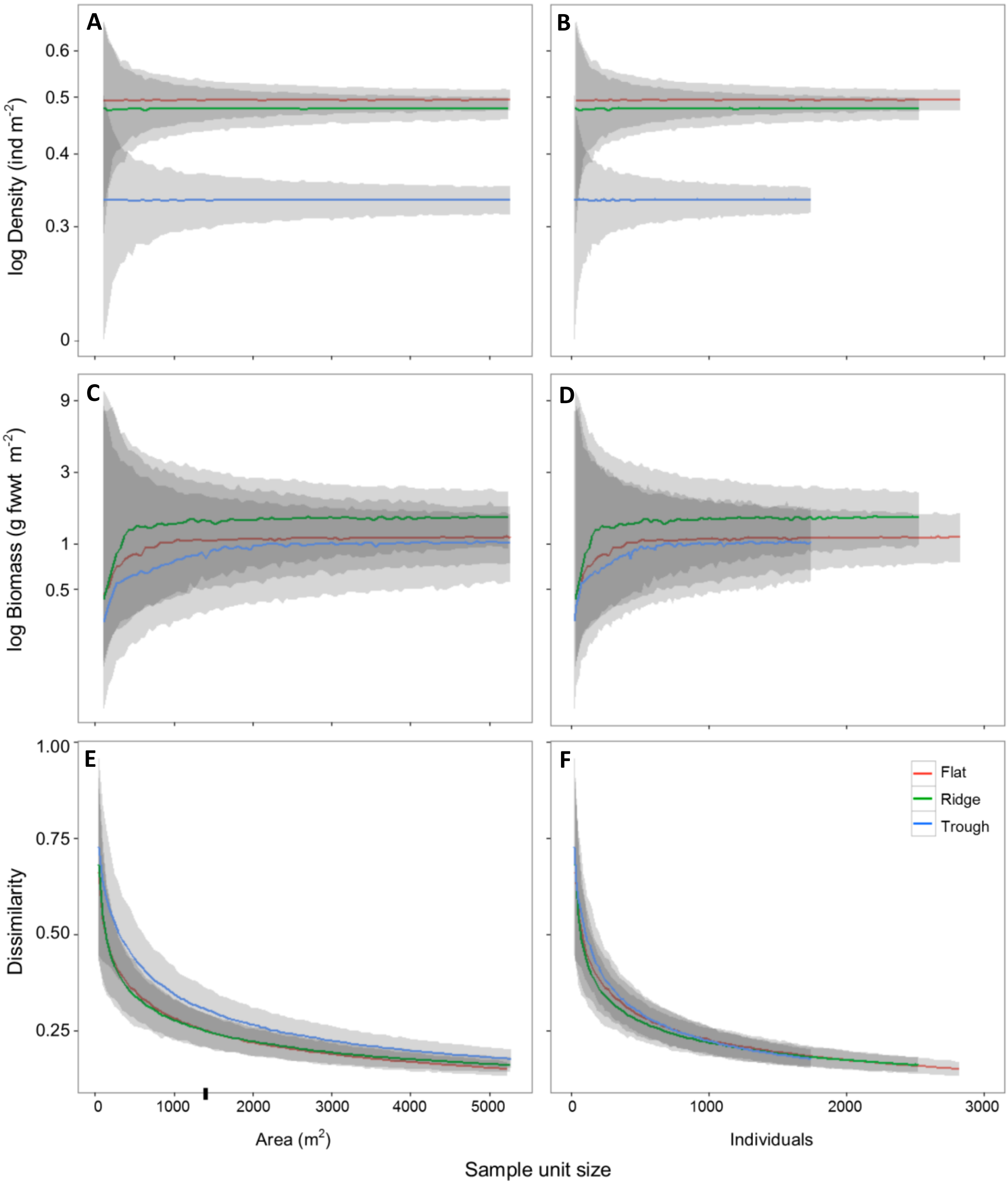

Figure 2.9. **Variation of the different metazoan community parameters used in the present study as a function of the seabed area or number of individuals encompassed by the sample unit size.** Lines represent mean or median values across the 1000 randomisations performed at each sample unit size increse, for each study area collated sample (n=3) (see methods). Shadowing representing 95% confidence intervals. Ticks on x-axis indicate the sampling unit size used in the present study (replicate sample areas = 1320 m2). **A and B:** Variation of mean metazoa density**. A)** Area-based mean density**. B)** Individual-based mean density.**C and D:** variation of median metazoan biovolume concentration**. A)** Area-based median biovolume**. H)** Individual-based mean biovolume. **E and F:** autosimilarity curves showing mean Bray-Curtis dissimilarity index calculated amongst pairs of metazoan samples. **E)** Area-based autosimilarity curves. **F)** Individual-based autosimilarity curves.

Xenophyophore fauna

Xenophyophore tests (Fig. 2.10) numerically dominated the megafauna recorded during the present study; being overall, six times more abundant than metazoans, and reaching a peak density of 17 ind m^{-2} in an image from the Ridge area. Mean xenophyophore density exhibited a statistically significantly difference between study areas (Table 2.1), with densities in the Ridge higher than those in the Trough (Tukey, $p < 0.01$). The recently described species *Aschemonella monile* (Gooday et al. 2018) (Fig. 2.10B) dominated the fauna, having mean densities of 3.27, 1.51, and 0.85 ind m^{-2} in the Ridge, Flat, and Trough areas respectively. The numerical dominance of xenophyophores has substantial impact on the perception of relative faunal diversity among the study areas (Fig. 2.5), inclusion of foraminiferal taxa markedly increased rank 1 dominance (Berger-Parker index) in the Flat and Ridge areas, indicating a very substantial reduction in diversity in the Ridge area particularly.

Xenophyophores were classified in 23 morphospecies. Xenophyophore faunal composition exhibited statistically significant variation between study areas (PERMANOVA, $R^2= 0.55$, $p < 0.001$), and statistically significant differences detected in all paired comparisons (pairwise PERMANOVA, $R^2= 0.39\text{-}0.61$, $p < 0.05$). Joint analysis of xenophyophore and metazoan faunal composition yielded comparable results to those obtained from the analysis of metazoan taxa only (Fig 2.7); statistically significant variations between study areas (PERMANOVA, $R^2= 0.48$, $p < 0.001$) were led by statistically significant differences between the Trough and the other study areas (pairwise PERMANOVA, $R^2= 0.37\text{-}0.45$, $p < 0.01$).

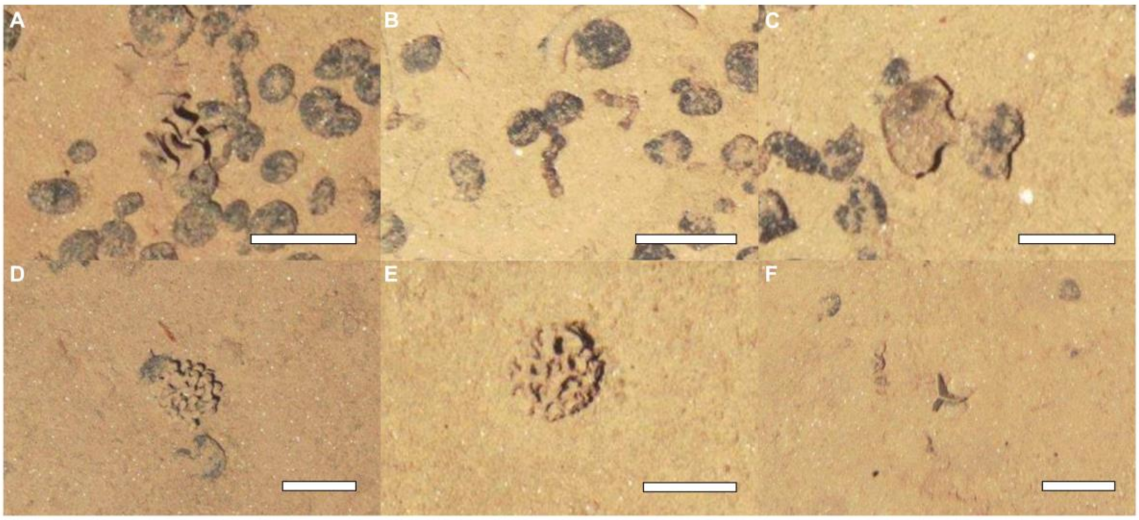

Figure 2.10. Examples of xenophyophore megafauna photographed at the APEI6 seafloor during AUV survey. Scale bars representing 50 mm. **A)** *Reticulammina* msp. **B)** *Aschemonella monile.* **C)** Fan-shaped *Psammina* msp. **D)** Indeterminate Psamminid msp, possibly *Shinkaiya* or *Syringammina.* **E)** *Syringammina* cf *limosa.* **F)** Triradiate *Psammina* msp, possibly *P. multiloculata*.

2.5. Discussion

Environmental setting at the APEI6

The high homogeneity in particle size and nutrient availability found across the APEI6 study areas suggests that these factors may be consistent over scales broader than the tens of kilometres between areas studied here. Our results were somewhat unexpected since variations in sediment grain-size distributions and particulate organic matter have commonly been reported between landscape types in previous assessments in the north Atlantic abyss (Durden et al. 2015, Morris et al. 2016), where bottom current speed ranges are comparable (Vangriesheim et al. 2001) to those expected at the APEI6, but sediments were coarser and more heterogeneous. Surface sediment particle sizes at the APEI6 were comparable in range to those found in eastern CCZ contract areas (Khripounoff et al. 2006, Mewes et al. 2014, Pape et al. 2017). Although sediments in these -more southerly- areas exhibit bimodal particle size distributions, being primarily composed of clays and fine silts (<6.3 µm), but with higher proportions of sands (>63 µm) than at the APEI6. Ranges of TOC (0.41-0.44%) and C:N ratios (3.8-4.1) were also comparable to those reported in eastern CCZ contract areas (Khripounoff et al. 2006, Mewes et al. 2014, Pape et al. 2017). This suggests that the sedimentary environment of the APEI6 may be generally representative of the environment found at a larger scale (i.e. eastern CCZ), although further exploration in other contract areas would be required to draw more precise conclusions in this regard.

Variations in nodule abundance could be indicative of environmental change between study areas. Locally stronger bottom-water currents reducing deposition rates are presumed to enhance nodule formation (Skornyakova and Murdmaa 1992, Mewes et al. 2014). Higher nodule abundances in mild slopes and elevated seafloors, such as the Flat and the Ridge areas, have commonly been linked with low sedimentation rates (Frazer and Fisk 1981, Mewes et al. 2014). Yet convergent channelling of bottom currents in bathymetric valleys, such as the Trough area, has also been suggested to limit deposition enhancing nodule growth (Peukert et al. 2018). The more irregular nodule coverage observed in the Ridge concurs with previous descriptions of hilltop environments at the CCZ (Margolis and Burns 1976, Skornyakova and Murdmaa 1992, Jung et al. 2001). In these, current circulation over rugged seafloor can generate scattered redistribution of surface materials (Jung et al. 2001, Nasr-Azadani and Meiburg 2014, Peukert et al. 2018), which may have reduced the sediment blanketing of hard structures (i.e. rock fragments, whale bones) and trace fossils (Durden et al. 2017b) within the Ridge.

Sample unit size evaluation

Narrowing of the precision range with increasing sample unit size was apparent in all parameters (SM; Fig. 2.15), as was expected from previous image-based assessments (Durden et al. 2016c), but the accuracy of each parameter (Figs. 8-9) showed a different sensitivity to this factor. The sample unit size we used in this study (c. 1320 m^2 of seafloor) was therefore sufficiently large for reliable estimation of fauna density, diversity of higher orders, and community dissimilarity, but was arguably too small for the assessment of taxa richness and biomass density patterns, as not all samples collected contained the minimum of 500 individuals (three samples contained < 500 ind) suggested by our analysis for a reliable characterisation of these two parameters.

It is conceivable that the higher sensitivity to sample size was a “rarity-driven” effect. On the one hand, the low density combined with the high taxa richness we found at the APEI6 yield high rates of taxon rarity in our assessment. This is commonplace in abyssal sampling (Smith and Demopoulos 2003), but has a negative effect on the accuracy of those diversity indices more sensitive to rare taxa, such as richness (Soetaert and Heip 1990, Magurran 2004). On the other hand, the high rarity of particularly large individuals appeared to restrict the accuracy of biomass density assessment, especially within the Flat and the Trough areas, were larger-sized fauna were even rarer. Predominance of the smaller taxa is common in low-productivity abyssal habitats (Rex et al. 2006, Smith et al. 2008a), yet large megafaunal species have an important ecological role in these environments (Billett et al. 2001, Stratmann et al. 2018b), and these appear to require rather large sample unit sizes to be best characterised (i.e. 500 ind: this study). Higher rarity rates are therefore expected in abyssal megafauna surveys as an artefact of lower sample unit sizes, which can influence other parameters such as diversity or community composition analysis.

Our results underline that sampling unit evaluation is important for assessing the reliability of ecological patterns inferred from abyssal sampling. Minimum sample sizes for accurate estimation exhibited by different parameters were extremely variable (range: 30-500 individuals; 100-1500 m^2 of seafloor per sample unit). This means that with sampling units <400 m^2, most biological parameters estimated here would have been largely inaccurate and imprecise. For instance, it is likely that no variation in diversity nor community composition between areas might have been detected if transect size of this study had been set below 600 m^2, which would have biased the overall conclusions. This underlines the importance of appropriate tuning of the sampling unit size in abyssal ecology, especially at the CCZ, where these may have a paramount influence on conservation policy (Levin et al. 2016, Durden et al. 2017a). However, sample unit analyses have been commonly ignored in most assessments of megafauna at the CCZ (Wang and Lu 2002, Stoyanova 2012, Vanreusel et al. 2016, Tilot et al. 2018). This adds a level of difficulty to the already constrained comparability between studies in the region (Amon et al. 2016), and bounds the study of ecological patterns at the regional scale.

The use of different sampling devices and methods (i.e. definition of megafauna size, camera altitude, sampling unit size), is an ongoing issue for the comparability of image-based analyses (Durden et al. 2016c), especially at the CCZ (Amon et al. 2016). For example, megafauna assessments performed by Tilot et al. (2018) and Stoyanova (2012) using a different camera set-up reported densities ten times lower than those reported by Vanreusel et al. (2016) at the same contractor areas (IFREMER-2 and IOM-2, respectively). The application of improved imaging systems may have increased the apparent megafauna densities, influencing diversity estimations. This stresses the need for a standardization of both assessment method and morphotype taxonomy across the CCZ, to enable more reliable comparisons between the various APEI and claim areas, and simplify the detection of possible biogeographical boundaries across the CCZ.

Landscape ecology of metazoan megabenthos

Differences in megafauna density across the landscape types studied were predominately driven by variations in suspension feeder abundance (Table 2.1), particularly sessile cnidarians (Fig. 2.6). Potential topographically-enhanced bottom water current speeds have previously been suggested to promote the development of suspension feeding fauna in the abyss (Thistle et al. 1985, Smith and Demopoulos 2003, Durden et al. 2015). Suspension feeders usually dominate the megabenthos in the CCZ and show higher abundances in areas with higher nodule density (Stoyanova 2012, Amon et al. 2016, Vanreusel et al. 2016). Factors promoting higher nodule densities also enhance the development of suspension feeders (Vanreusel et al. 2016); for example, in the present study most suspension feeders (80%) were attached to nodules. Suspension feeder density, and relative abundance, may therefore be related to both the availability of hard substrata and local enhancements in bottom water currents, and that the latter two factors may themselves be related. These factors suggest that low slopes or elevated topographies, as found at the Flat and Ridge areas, enhance suspension feeder densities increasing the overall metazoan standing stock of these areas, as compared to depressions, like the Trough area.

Variations in functional composition between study areas were driven by the distribution of deposit feeder fauna, suggesting enhanced resource availability for this group in the Ridge. This could indicate a higher food supply at the more elevated seafloor of the Ridge, owing to less particulate organic carbon loss during sinking (Smith et al. 2008a), but this is likely a small effect at abyssal depths for changes of few hundred meters (Lutz et al. 2007). Moreover, sediment TOC exhibited no statistically difference between study areas, nor was there a statistically significant difference in the C:N ratio. This suggests that, if there were variations in food supply for deposit feeders, these may either have occurred at a finer spatial scale (i.e. patch accumulations: Lampitt, 1985; Smith et al., 1996), or be related with the quality rather than the quantity of the available resource (Ginger et al. 2001).

Deposit feeder abundance was predominantly composed by ophiuroids (Table 2.2), and the density of these was both positively correlated with xenophyophore test abundance (r_s= 0.77-0.79, $p < 0.01$), as was the density of predator and scavenger fauna, although at a weaker level (r_s= 0.65, $p < 0.05$). Biological structures can be important in the generation of habitats in the deep-sea (Buhl-Mortensen et al. 2010). Such associations are common in the in the north-eastern

Pacific abyss, for instance, sponge stalks can serve as microhabitats for species-rich assemblages of suspension-feeder epifauna (Beaulieu 2001), or for the attachment of octopod egg clutches during brooding (Purser et al. 2016). Co-occurrence of xenophyophores and ophiuroids has been previously documented in eastern Pacific seamounts (Levin et al. 1986, Levin and Thomas 1988a). Levin (1991) suggested that xenophyophore tests represent a stable substratum that can function as refuge from predators and or nursey habitat for juvenile mobile metazoans, like ophiuroids. Xenophyophore test substratum has shown to play a crucial role in the regulation of meiofauna and macrofauna communities at the CCZ (Gooday et al. 2017), and our results suggest that these may also be important in the functional structuring of megafauna.

Heterogeneity diversity measures indicated clearly reduced diversity in the Trough relative to Flat and Ridge areas, markedly so in the case of 1/D index (Fig. 2.4C). The dominance component of diversity was higher in the Trough (Fig. 2.5A) unless xenophyophores were included (Fig. 2.5B). The lower metazoan heterogeneity diversity of the Trough was caused by a general decrease in the density of most morphospecies, combined with a clearly higher abundance of the sponge *Porifera msp-5*, possibly better adapted to a presumably more disturbed environmental regime in this area. *Porifera msp-5* was amongst the smallest morphospecies we detected (mean diameter: 13.1 ± 3.1 mm; without elimination of individuals >10 mm: 8.8 ± 3.4 mm) and was predominantly found (>70%) encrusting nodules. A recent study revealed a similar dominance, also exhibited by a small nodule-encrusting sponge (*Plenaster craigi*) in the eastern CCZ (Lim et al. 2017). Our results highlight the importance of a standardized detection of small -and usually predominant-taxa for robust assessment of heterogeneity diversity in CCZ megafauna communities.

Previous CCZ megafauna studies related the presence of nodules with increased metazoan richness (Amon et al. 2016, Vanreusel et al. 2016, Tilot et al. 2018). Although we found no direct correlation between nodule availability and sample diversity (of any order), it is possible that the overall lower nodule availability of the Trough played an important role in the reduction of evenness we observed there, since most of the APEI6 metazoan abundance was composed by nodule-dwelling taxa. However, the survey design applied in this study was optimised for the detection of patterns at a relatively broad scale (few kilometres), compared to the tens of meters at which nodule coverage variations usually occur at the CCZ (Peukert et al. 2018). Moreover, our sampling effort evaluation highlighted that two samples did not contain a sufficiently large specimen coverage (<500 ind) to reliably assess richness patterns, and that this may also have affected the estimation of richness in previous studies. Further analysis of the APEI6 dataset at a finer spatial scale (Chapter 3) shall further expand and contextualize the precise relation between nodules and both the richness and evenness components of megafauna diversity.

Statistically significant differences in megafaunal density, functional composition, evenness and taxon composition were variously apparent between the landscape types studied. Previous studies showed that even modest topographic elevation (i.e. hills) has substantive effect on abyssal megafaunal compositions (Durden et al. 2015, Stefanoudis et al. 2016, Leitner et al. 2017). However, in this study the assemblages of the Flat and Ridge (in previous studies: plain and hill areas, respectively) showed a higher similarity, as compared to the Trough area, where most taxa densities were somewhat reduced and the dominant morphospecies shifted from colonial bamboo corals to a small-encrusting sponge. The higher availability of nodule and xenophyophore-test substrata in the Ridge and the Flat possibly increase the heterogeneity of these areas, enhancing the development of a more even assemblage type. Variations in habitat heterogeneity commonly regulate niche diversification processes (Tews et al. 2004), exerting a fundamental influence on the diversity and structure of deep-sea benthic communities (Levin et al. 2001). Thus, our results suggest that by regulating nodule and xenophyophore test availability - and presumably bottom current speeds- geomorphological variations play a crucial role in the structuring of the CCZ megabenthos at the landscape scale.

Ecological significance of megafaunal xenophyophores

Test densities were almost four times higher in Ridge samples than in the Trough, and almost twice as dense as within the Flat area. Previous studies have also described higher relative xenophyophore densities in sites with sloping topography and enhanced water motion (Levin and Thomas 1988a, Stefanoudis et al. 2016). The feeding modes and strategies of xenophyophores remain uncertain (Gooday et al. 1993, Laureillard et al. 2004), with passive particle-trapping, suspension or deposit feeding mechanisms noted (Levin and Gooday 1992, Kamenskaya et al. 2013). Accepting our inability to distinguish living specimens, that *A. monile* specimens alone represent over 70% of all megafauna observed in the Ridge area suggests considerable ecological significance for this taxon, and the xenophyophores as a group. Note that our identification of 23 xenophyophore morphospecies is undoubtedly an underestimate of their true species diversity, particularly in the CCZ where these are exceptionally diverse (Kamenskaya et al. 2013, Gooday et al. 2017).

Inclusion of xenophyophores substantially affected the assessment of biological diversity, particularly in respect to heterogeneity diversity. It is conceivable that this was a 'true body size' mismatch effect. For example, Levin and Gooday (1992) suggest a protoplasm volume of 1 to 0.01% of test volume. This means that the mean test biomass of *A. monile* at the APEI6 was possibly <1 mg fwwt ind^{-1} - provided its devoid of protoplasm test interior (Gooday et al. 2018)- while the mean biomass of the smallest taxa recorded in the metazoan fraction ranged between 40-60 mg fwwt ind^{-1}. As smaller individuals are largely more abundant in the abyss (Smith et al. 2008a), it is likely that the inclusion of xenophyophores artificially reduced the heterogeneity diversity, given that ~ 1 mg fwwt sized individuals from other taxa were not possible detect and hence not represented in analyses. Consequently, general interpretation of diversity is probably best limited to the metazoan only assessments.

2.6. Conclusions

This paper presents an ecological assessment of megabenthic faunal distribution in response to seafloor geomorphology at the CCZ. Differences in the megafaunal ecology between landscape types of the APEI6 manifested as changes in standing stock, functional structure, diversity, and community composition. This shows that local geomorphological variations can play an important role in the structuring of the CCZ megabenthos. Our assessment somewhat concurs with previously reported differences between abyssal hills and adjacent plains in North Atlantic megafauna (Durden et al. 2015), and in fish populations at the CCZ (Leitner et al. 2017). Yet we have added a level of abyssal landscape heterogeneity (troughs), where megafauna showed the clearest variations. Analyses of sampling effort support our results: the collected sample size enabled a stable estimation of key biological metrics, but also highlighted limitations in understanding of some parameters.

Benthic ecology has been suggested to be regionally controlled by a gradient of POC-flux to the seafloor at the CCZ (Veillette et al. 2007b, Smith et al. 2008b). However, local environmental factors presumably regulated by local geomorphology, such as bottom water flows (Mewes et al., 2014), or the availability of nodule (Peukert et al., 2018) and xenophyophore test (this study) substrata may play a key role at the local level, possibly influencing habitat heterogeneity across the CCZ. This complexity needs to be reflected in both local (claim-scale) and regional (CCZ-scale) management plans (Levin et al. 2016, Durden et al. 2017a) and in the design of future monitoring strategies aimed to characterise and preserve biodiversity in the CCZ.

2.7. Supplementary material: Chapter 2

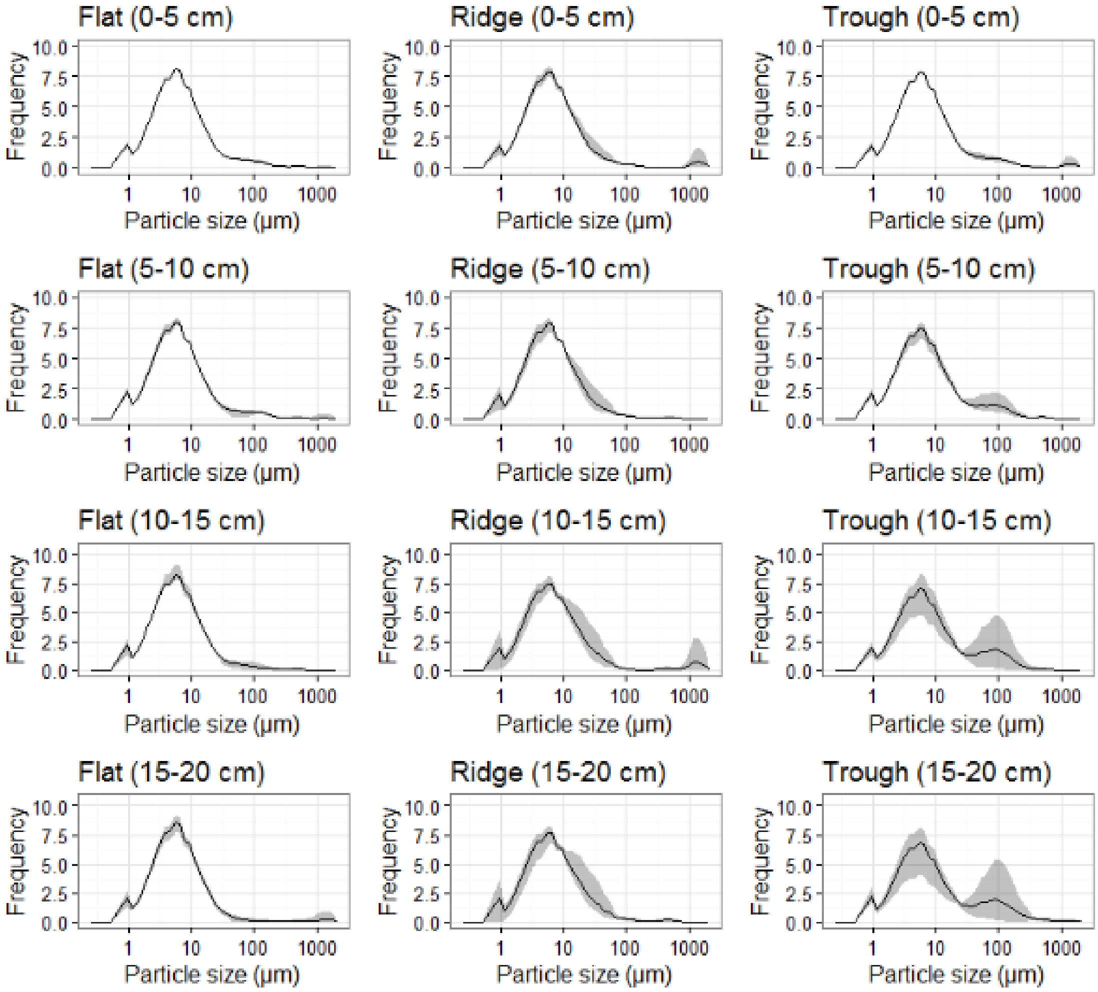

Figure 2.11. Sediment grain-size distributions plots generated for different sediment horizons sampled at the APEI6 seafloor. Lines representing mean frequency across each of the five replicate megacore samples collected per landscape type. Shadowed areas representing maximum and minimum values per replicate set. Each core was initially sliced and split into nine different sediment depths (0-5, 5-10, 10-15, 15-20, 20-30, 30-50, 50-100, 100-150, and 150-200 mm). Sediment grain-size distributions at each horizon were measured independently by laser diffraction. Horizons 0-5, 5-10, 10-15, 15-20, 20-30, 30-50 were averaged into a 0-50 mm depth.

Table 2.3 Particle size statistics calculated applying a geometric method of moments for different sediment horizons sampled at the APEI6 seafloor. Values representing maximum and minimum ranges across each of the five replicate megacore samples collected per landscape type. Each core was initially sliced and split into nine different sediment depths (0-5, 5-10, 10-15, 15-20, 20-30, 30-50, 50-100, 100-150, and 150-200 mm). Sediment grain-size distributions at each horizon were measured independently by laser diffraction. Horizons 0-5, 5-10, 10-15, 15-20, 20-30, 30-50 were averaged into a 0-50 mm depth, prior to the statistical processing.

Horizon	Statistic	Flat	Ridge	Trough
0 to 5 cm	Mean	7.15 - 7.61	6.71 - 9.21	7.60 - 8.50
	St dev	2.82 - 3.03	2.54 - 4.77	2.99 - 4.04
	Skewness	0.96 - 1.50	0.46 - 2.02	0.86 - 1.86
	Kurtosis	4.50 - 7.35	3.22 - 8.29	3.79 - 7.50
	Mode	7.19	7.19	7.19
	D_{50}	6.47 - 6.70	6.29 - 7.40	6.61 - 7.03
5 to 10 cm	Mean	6.50 - 8.52	6.56 - 8.72	7.49 - 11.16
	St dev	2.73 - 3.66	2.71 - 2.78	2.95 - 3.97
	Skewness	0.89 - 1.56	0.46 - 1.15	0.67 - 1.07
	Kurtosis	4.18 - 6.60	3.20 - 5.82	2.73 - 5.20
	Mode	7.19	7.19	7.19
	D_{50}	5.97 - 6.89	5.98 - 7.95	6.63 - 8.17
10 to 15 cm	Mean	6.06 - 7.24	6.33 - 11.67	6.47 - 20.08
	St dev	2.10 - 3.00	2.43 - 6.73	2.48 - 4.72
	Skewness	0.06 - 1.08	0.12 - 1.64	0.06 - 0.90
	Kurtosis	2.75 - 5.02	2.34 - 6.26	1.79 - 6.14
	Mode	7.19	7.19	7.19
	D_{50}	6.04 - 6.48	5.87 - 9.50	6.29 - 16.45
15 to 20 cm	Mean	5.77 - 8.55	6.07 - 10.61	6.35 - 20.15
	St dev	2.19 - 4.28	2.50 - 2.94	2.56 - 5.07
	Skewness	0.01 - 1.93	0.13 - 1.18	- 0.14 - 1.85
	Kurtosis	2.59 - 7.50	2.35 - 6.17	1.77 - 8.79
	Mode	7.19	7.19	7.19 - 115.00
	D_{50}	5.69 - 6.63	5.70 - 10.28	5.93 - 31.85

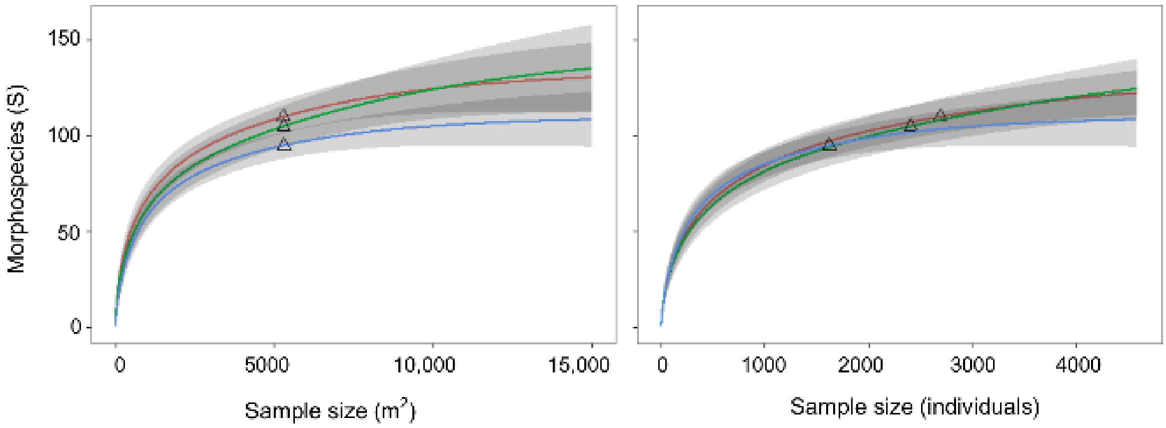

Figure 2.12. Extrapolated metazoan morphospecies rarefaction curves for each APEI6 study area. Triangles showing the total size of the sample analysed at each geomorphology. Expected richness with sample coverages of 15,000 m^2 show a lower richness at the Trough (~107 msp) compared to the Flat (~130 msp) and the Ridge (~134 msp) areas, but confidence intervals continued to overlap between curves. Whole geomorphological units sample size (5280 m^2) covered 85-90% of the expected richness > 15,000 m^2.

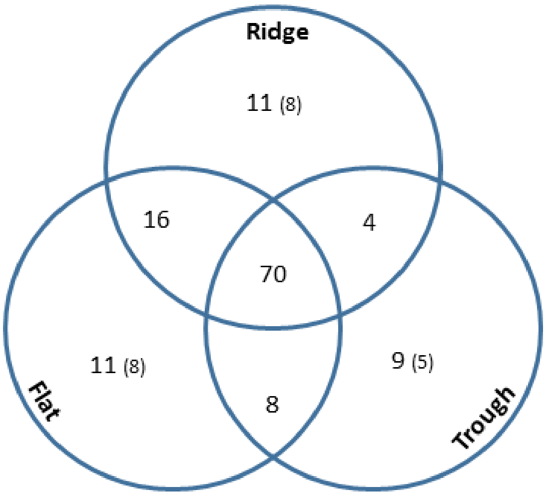

Figure 2.13. Metazoan morphospecies composition overlap between APEI6 study areas. Venn diagram showing the total number of metazoan taxa shared between each combination of landscape types of the APEI6. *In brackets*: singleton morphospecies.

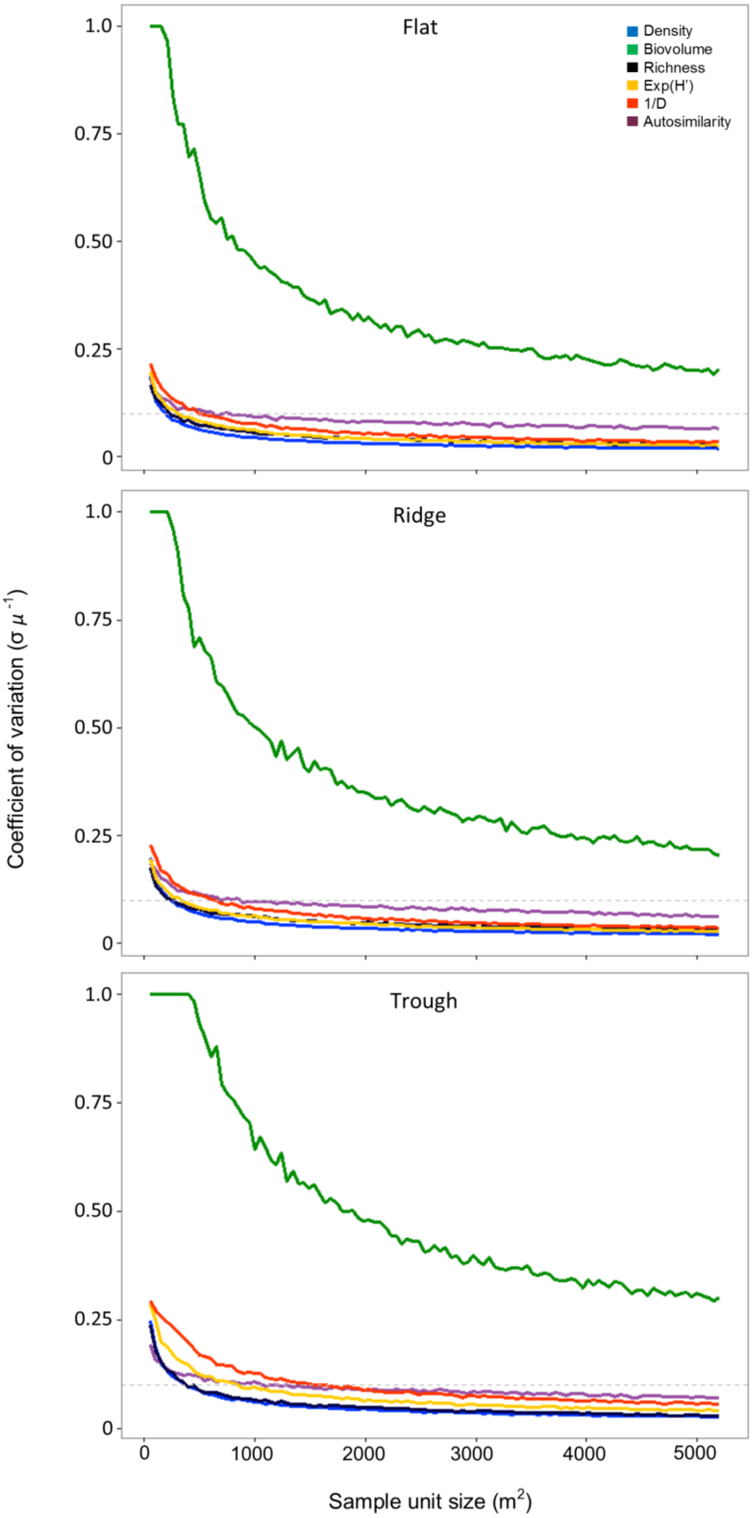

Figure 2.14. Variations of the coefficient of variation with increasing sample size calculated for the main ecological parameters calculated in the present study. Coefficients of variation were calculated as the standard deviation divided by the mean of each metric at each different sampling effort (see methods), for the whole metazoan dataset collected for each landscape type of the APEI6.

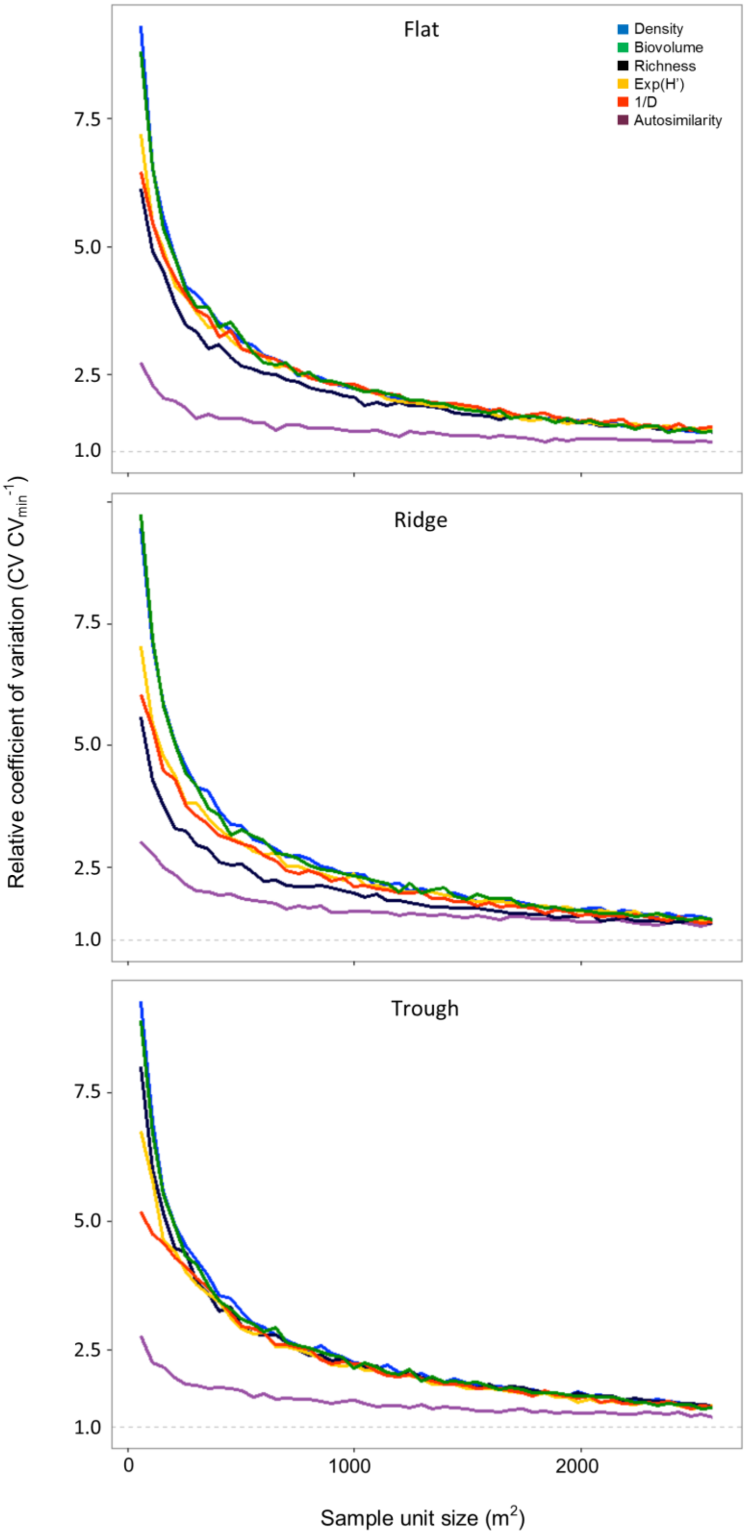

Figure 2.15. Relative variations of the coefficient of variation with increasing sample size calculated for the main ecological parameters calculated in the present study. Coefficients of variation were calculated as the standard deviation divided by the mean of each metric at each different sampling effort (see methods), for the whole metazoan dataset collected for each landscape type of the APEI6, and then divided by the minimum value exhibited in each along the sample size spectrum assessed.

3. Chapter 3. Ecology of a polymetallic nodule occurrence gradient: implications for deep-sea mining

3.1. Abstract

Abyssal polymetallic nodule fields constitute an unusual deep-sea habitat. The mix of soft sediment and the hard substratum provided by nodules increases the complexity of these environments. Hard substrata typically support a very distinct fauna to that of seabed sediments, and its presence can play a major role in structuring deep-sea assemblages. We assessed the influence of seafloor nodule cover on the ecology of the larger fauna (megafauna) of a marine conservation area (Area of Particular Environmental Interest 6, APEI6) in the Clarion Clipperton Zone (CCZ, 122° 55' W 17° 16' N, 3950-4250 m water depth) using extensive photographic surveys from an autonomous underwater vehicle. Variations in nodule cover (1-20%) appeared to exert statistically significant differences in faunal standing stocks, some biological diversity attributes, faunal composition, functional group composition, and the distribution of individual species along the nodule cover gradient. The standing stock of both the metazoan fauna and the giant protists (xenophyophores) doubled with a very modest initial increase in nodule cover (from 1 to 3%). Notably, faunal density determined by sample-based rarefaction, was positively correlated with nodule cover, while taxon richness, determined by individual-based rarefaction, was invariant (c. 60 taxa among 500 individuals). Faunal composition varied continuously, describing a step change, along the nodule cover gradient. We discuss these results in the context of potential seabed-mining operations and the associated sustainable management and conservation plans. We note in particular that successful conservation actions will likely require the preservation of areas comprising the full range of nodule cover and not just the low cover areas that are least attractive to mining.

3.2. Introduction

Polymetallic nodule fields represent a unique abyssal habitat (Radziejewska 2014b). The hard substratum provided by the nodules combined with the background soft sediment seabed acts to increase habitat complexity, and is thought to promote the occurrence of some of the most biologically diverse seafloor assemblages in the abyss (Amon et al. 2016, Gooday et al. 2017). This unusual and diverse habitat is potentially subject to imminent large-scale human impacts in the form of seafloor mining (Kuhn et al. 2017). Mining disturbances are likely to extend over extremely large seafloor areas (Aleynik et al. 2017) and have a clear potential to drive major changes in the resident fauna (Jones et al. 2017). Predicting the nature of such changes remains difficult; the ecology of this remote habitat is poorly understood, in particular, very little is known of the biodiversity associated with nodules (Veillette et al. 2007b, Vanreusel et al. 2016).

The presence of hard substratum is thought to be a key factor in structuring heterogeneous deep-sea habitats (Buhl-Mortensen et al. 2010, Bell et al. 2016). For example, modest variations in the availability and the composition of hard surfaces can influence the larval settlement processes of the seafloor fauna (Van Dover et al. 1988, Roberts et al. 2006). Substratum selectivity is commonly exhibited by many deep-sea species, including soft corals (Sun et al. 2011), sponges (Lim et al. 2017), and foraminifera (Gooday et al. 2015). The presence and extent of hard substratum is therefore expected to exert a significant control on the composition of deep-sea benthic assemblages (Levin et al. 2001, Smith and Demopoulos 2003). Seafloor environments in the deep sea with extensive hard substratum range in nature from landscape-scale features such as seamounts (Clark et al. 2010b) and canyons (De Leo et al. 2010), to widely dispersed pebbles, cobbles, and boulders referred to as iceberg drop-stones (Meyer et al. 2016), and the similar human artefact habitat produced by steamship clinker (Ramirez-Llodra et al. 2011). While individual polymetallic nodules are generally small, 1-20 cm in diameter, nodule fields can extend over extremely large areas, many hundreds of km^2, as occurs in the CCZ of the central Pacific Ocean (Kuhn et al. 2017).

Polymetallic nodules in the CCZ are thought to support a specialised fauna that differs from that of nodule-free sediment areas (Thiel et al. 1993, Gooday et al. 2015). Nodule-dwelling meiofauna such as nematodes, tardigrades, harpacticoids, and foraminifera inhabit the crevices (Veillette et al. 2007b, Miljutina et al. 2010), while sessile macro- and megafauna such as polychaetes, sponges, cnidarians and xenophyophores are commonly found attached to nodule surfaces

(Gooday et al. 2015, Amon et al. 2016). Consequently, nodule occurrence has been linked with variations in faunal standing stocks and distributions (Amon et al. 2016, Vanreusel et al. 2016). However, logistic constrains have limited the detailed monitoring of nodule cover (Vanreusel et al. 2016, Tilot et al. 2018), restricting the assessment of seafloor ecology along nodule occurrence gradients.

Recent advances in large-scale seafloor visual imaging (Durden et al. 2016c), coupled with automated nodule-detection algorithms (Schoening et al. 2016, Schoening et al. 2017) now make such studies possible. Here, we combine extensive nodule coverage and faunal data obtained by photography from an AUV to examine the effect of nodule occurrence on the ecology of megafauna in the CCZ. We include protozoan, invertebrate, and fish species that can be distinguished in photographs, having body length-scales >1 cm, as members of the megafauna. In particular, we consider variations in their standing stock, biological diversity, and faunal composition along a nodule cover gradient. This work is carried out within an 'Area of Particular Environmental Interest' (APEI), a form of marine protected area designed as a conservation measure in response to potential future seabed mining in the region (ISA 2012). Consequently, we also cast our results in the context of the sustainable management and conservation of this unusual abyssal habitat.

3.3. Materials and Methods

Study area

Our initial study area was a 5500 km^2 rectangular region of seafloor centred on 122° 55' W 17° 16' N within the APEI6 region (Fig. 3.1). This location was selected to have similar topographic relief to mining contract areas in the central CCZ. Water depth ranged 3950-4250 m, and the seafloor landscape comprised a succession of crenulated ridges and shallow troughs oriented north-south between dispersed level-bottom (<3° slope) areas. General seafloor conditions were described in Chapter 2, and are only briefly summarised here. Surface sediments (0-1 cm) were homogenous across the study area, dominated by very fine silt and clay particles (58-68% <7.8 µm diameter), and having a very low content of total organic carbon (TOC, 0.44 ± SD 0.05 %). The polymetallic nodules present were of a flattened, ellipsoidal form with smooth surfaces. The seafloor exposed mean individual nodule area was 2.5 cm^2, with most nodules <5 cm^2 (90%), and very few >10 cm^2

(1%). In individual seafloor photographs, average nodule cover was 6.4% and ranged from nodule-free to 37%. Nodule cover was patchy, with extremes of variation occurring at metre-scales (Fig. 3.1). All results reported here were acquired April-May 2015, during RRS *James Cook* cruise JC120; additional supporting technical detail is provided by Jones (2015).

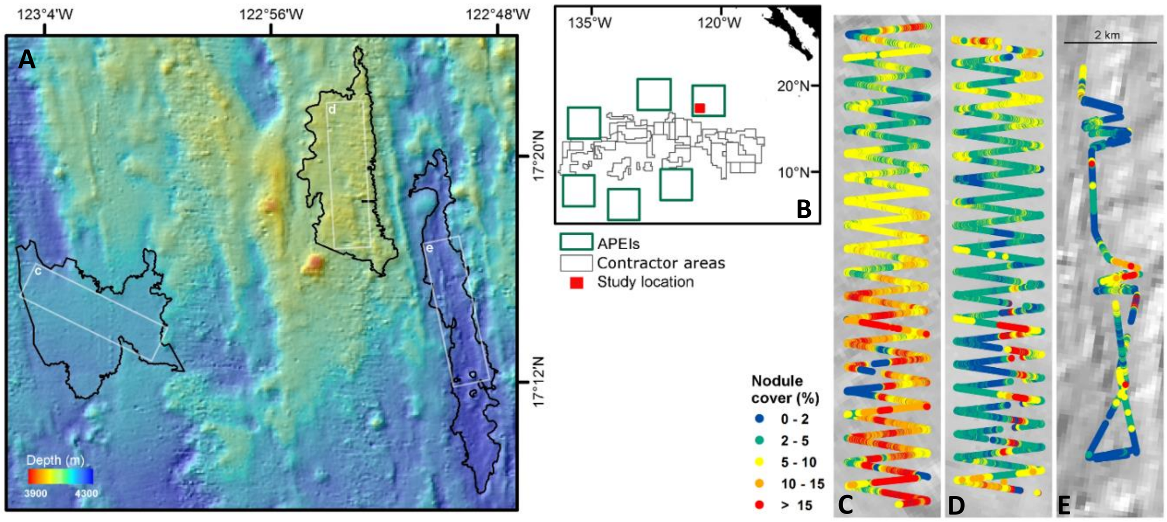

Figure 3.1. Study area location and sampling operations within the APEI6 of the CCZ (North Pacific Ocean). **A)** Bathymetric survey chart of the study location. Landscape types depicted in dark lines (left to right: Flat, Ridge, and Trough). White rectangles indicate AUV sampling areas targeted within each landscape. **B)** Map of the eastern CCZ showing contractor areas, Areas of Particular Environmental Interest, and study location. C to E) Full AUV imagery dataset collected at each landscape type. Colour of survey tracks represents the nodule coverage level of the seabed, obtained from automatic detection in survey images using the CoMoNoD algorithm (Schoening et al. 2017). **C)** Flat survey. **D)** Ridge survey. **E)** Trough survey.

Data collection and processing

Seafloor images were collected using a digital camera (FLIR Integrated Imaging Solutions Inc. *Grasshopper2*; 2448 x 2048 pixels) mounted vertically beneath the AUV Autosub6000 (Morris et al. 2014). The AUV was programmed for a target altitude of 3 m above the seafloor, a speed of 1.2 m s^{-1}, and a photographic interval of 850 milliseconds. At the target altitude, individual vertical photographs imaged 1.71 m^2 of seabed. Three landscape types (Ridge, Flat, and Trough), delimited by objective analysis of bathymetric data, were surveyed using zig-zag designs with random start points (Strindberg and Buckland 2004) as detailed in Chapter 2. A total of 40 individual image transects were surveyed in each landscape-type. Images taken as the vehicle changed course, i.e. junctions between transects, were removed. In the remaining straight-line sections, every second image was removed to avoid overlap between consecutive images and to prevent double counting. To ensure consistency in specimen and nodule detection, images outside the altitude range 2-4 m were also removed. Four transects were randomly selected from each landscape-type for subsequent analysis. The full resultant dataset was composed of data from 10,052 non-overlapping images, representing a seafloor area of 18,580 m^2.

All images were colour corrected, as described by Morris et al. (2014), before manual and automated analyses were performed to obtain biological and environmental data. Nodule cover (%) was quantified using the Compact-Morphology-based poly-metallic Nodule Delineation method (CoMoNoD, Schoening et al. 2017). The CoMoNoD algorithm calculates the size of each nodule (i.e. seafloor exposed area size) detected in an image, enabling the calculation of descriptive nodule statistics. Megafauna specimens were identified to the lowest taxonomic level possible (see below), and their physical dimension measured, using BIIGLE 2.0 (Langenkämper et al. 2017). Each specimen was assigned to a ‘nodule-attached’ (NA: nodule-dwelling sessile fauna) or ‘nodule-free-living’ (NFL: sediment-dwelling sessile or unattached mobile fauna) life-habit category. The biovolume of individual metazoan specimen was estimated as a proxy for biomass, using the generalised volumetric method described by Benoist et al. (submitted).

To ensure consistency in specimen identification, a CCZ-standardised megafauna morphospecies (msp: taxa identified on the basis of evident morphological traits) catalogue was developed upon a pre-existent megafauna compilation (see http://ccfzatlas.com), that we further expanded in consultation with international taxonomic experts and by reference to existing literature (Amon et al. 2017, Kersken et al. 2018). The likely feeding behaviour of each morphospecies was inferred from similar organisms described in the literature (Iken et al. 2001). The full dataset comprised 7837 metazoan specimens across 133 morphospecies, and 47133 xenophyophore specimens across 22 morphospecies.

Data analysis

To perform an initial general assessment of the potential influence of seafloor nodule cover on the ecological characteristics of the megafauna, all images from the three landscape types were pooled. This total image set was ordered by estimated nodule cover, and then divided into ten subsets at nodule-cover breakpoints chosen to yield approximately equal numbers of megafaunal observations in each image subset. Metazoan and xenophyophore data were processed separately on the basis that it was not possible to determine whether the latter were living from the images (Hughes and Gooday 2004). Across the ten resultant nodule-cover classes, metazoan megafauna counts ranged 784-787, and xenophyophore counts 4714-4719. To establish measures of variability in ecological characteristics within the nodule-cover classes, the corresponding image subsets were resampled using a modified form of bootstrapping (Davison and Hinkley 1997). Each image subset was randomly resampled with replacement until a minimum of 500 specimens were encountered, and that process was repeated 1000 times for each nodule-cover class. This resampling process yielded bootstrap-like samples that ranged in metazoan specimen counts 500-565, and xenophyophore counts 500-587. We adopted these specimen-count based methods to recognise and control the impact of specimen number on the estimation of biological diversity and faunal composition parameters (Sanders 1968, Forcino et al. 2015).

A range of ecological parameters was calculated for each of the 10 × 1000 bootstrap-like samples, including metazoan and xenophyophore numerical density (ind m^{-2}) and metazoan biovolume density (ml m^{-2} ≈ g fresh wet weight m^{-2}). To examine the range of diversity characteristics, Hill's diversity numbers of order 0, 1, and 2 (Jost 2006) were calculated as metazoan morphospecies richness (S_N), the exponential form of the Shannon index (Exp H'), and the inverse form of Simpson's index (1/D). We also calculated morphospecies density (S_A), based on an additional set of bootstrap-like samples generated following the same procedure, but with a controlled minimum seabed area encompassed by each sample, that was set to the smallest seabed area (c. >700 m^2) obtained in the specimen-controlled set of bootstrap-like samples used to calculate the rest of parameters. Variation in metazoan community composition was assessed by 2d non-metric multidimensional scaling (nMDS) ordination of all 10000 bootstrap-like samples, based on square-root transformed faunal density and use of the Bray-Curtis dissimilarity measure (Clarke 1993). The resultant dimension 1 scores (MDS-d1) were used as a univariate measure of faunal composition.

Mean (median in the case of biovolume assessment) values of these various parameters were calculated from each bootstrap-like sample set, together with corresponding 95% confidence intervals based on the simple percentile method (Davison and Hinkley 1997). In addition to the general analyses of ecological responses to the nodule cover gradient, we considered landscape-type-related variations in those responses by undertaking a separate analysis within each landscape-type. This material is provided in the Supplementary Material 1 (SM1) of this Chapter. Data processing and analyses described above were performed using a custom R (R Core Team, 2014) script incorporating multiple functions of the 'vegan' package (Oksanen et al. 2018).

3.4. Results

Standing stocks

Metazoan and xenophyophore density were significantly and substantially lower in the lowest nodule-cover class (Fig. 3.2A). We found no significant correlation between density and nodule availability (Table 3.1); density variation of both groups across the nodule gradient described a rapid asymptote, stabilising in cover levels >2-3%. In contrast, metazoan biomass density showed a high dispersion rate and no significant variations along the nodule cover gradient (Fig. 3.2A).

Biological diversity

Diversity measures calculated with controlled number of individuals exhibited no significant correlation with nodule cover (Table 1). Morphospecies richness (S_N) was near constant across nodule-cover classes with no indication of any significant difference between any pair of classes (Fig 3.2B). Exp *H'* was more variable across classes, but exhibited no coherent substantive change across the nodule gradient. In contrast, 1/D showed a significantly lower value in the lowest nodule class. On the other hand, morphospecies density (S_A; calculated with controlled seabed area) was significantly correlated with nodule cover (Table 3.1). S_A was consistently lower than S_N across the nodule gradient, though marginally (confidence intervals overlapped), except in the lowest nodule class, where S_A was significantly and substantially lower than S_N.

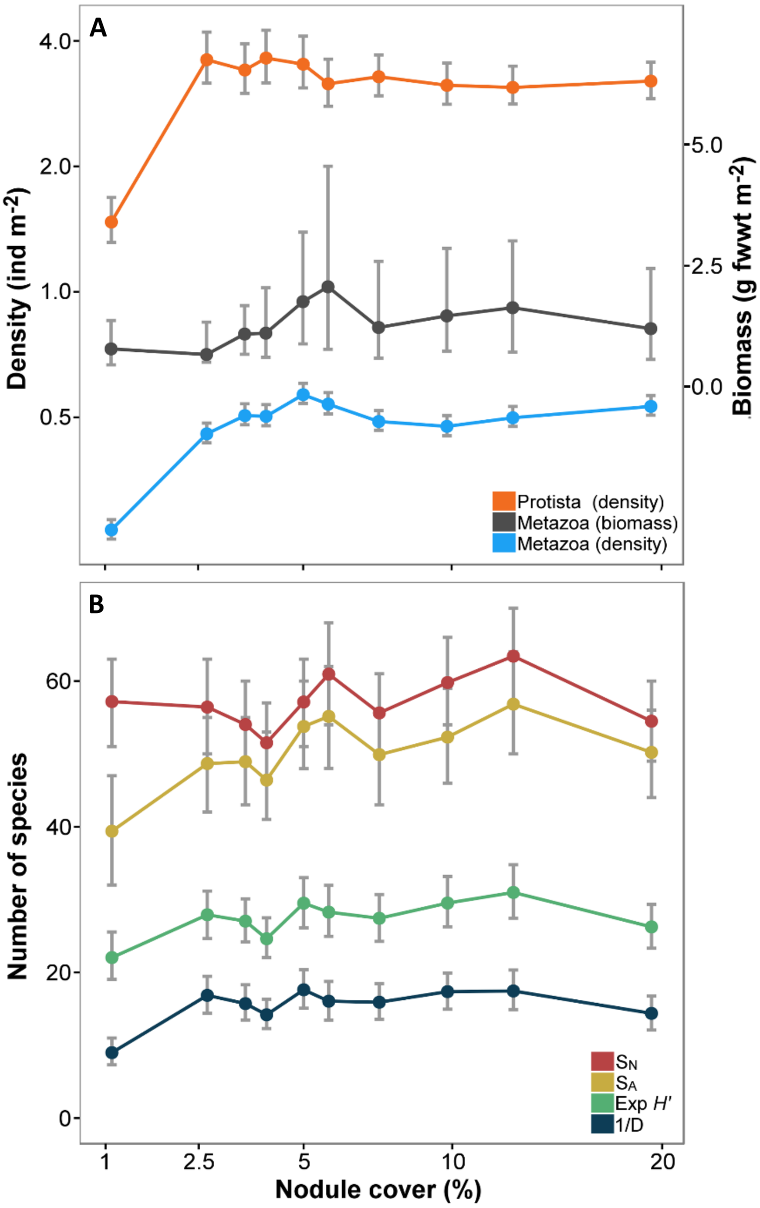

Figure 3.2. Variation in standing stock and diversity with nodule cover at the APEI6 seafloor. Points indicate mean (median for metazoan biomass) values of each parameter calculated from each nodule-cover class bootstrap-like sample set. Error bars represent 95% confidence intervals. **A)** Density of metazoans and xenophyophores (left y-axis), metazoan biomass density (right y-axis). **B)** Metazoan diversity: morphospecies richness (S_N), morphospecies density (S_A), Exponential Shannon index (Exp *H'*), and Inverse Simpson index (1/D).

Table 3.1. Spearman's rank correlations with nodule cover. Summary results of tests performed between mean (or median, for biomass) values of each investigated ecological parameter calculated from each nodule cover class bootstrap-like sample set, with detail of significant differences between nodule class 1 (mean cover= 1.1%) and the rest of classes (cover >2%). Distinct class 1: no overlap of the confidence interval of the lowest nodule cover class with any other class. Note that correlation approach fails to detect significance of variations in unimodal responses.

	Distinct class 1	**Correlations**	
		r_S	p-value
Standing stock			
Xenophyophores (ind m^{-2})	**yes**	-0.297	0.404
Metazoans (ind m^{-2})	**yes**	0.345	0.328
Metazoan biomass (g fwwt m^{-2})	no	0.624	0.053
NA metazoa (ind m^{-2})	**yes**	0.466	0.174
SA-FL metazoa (ind m^{-2})	**yes**	0.224	0.533
Porifera msp-5 (ind m^{-2})	no	-0.976	**<0.001*** **
C. cf *bayeri* (ind m^{-2})	no	-0.6	0.067
Lepidisis msp (ind m^{-2})	no	0.952	**<0.001*** **
Diversity and composition			
Morphospecies richness (S_N)	no	0.248	0.405
Morphospecies density (S_A)	no	0.721	**0.018***
Exponential Shannon (Exp *H*')	no	0.478	0.161
Inverse Simpson (1/D)	**yes**	0.345	0.328
MDS-dimension 1	**yes**	0.891	**0.001****

Faunal composition

Assemblage

Two-dimensional nMDS ordination of bootstrap-like samples showed that metazoan assemblages differed across the nodule gradient (Fig. 3.3A); the lowest and the highest nodule-cover classes yield the largest dissimilarity rates, and both were substantially different than the asseamblages found in mid-nodule cover classes (i.e. nodule classes 3 to 8). MDS-d1 was strongly and significantly correlated with nodule cover (Table 3.1). MDS-d1 score in the lowest nodule class was substantially and significantly different from all other cover classes (Fig. 3.3B).

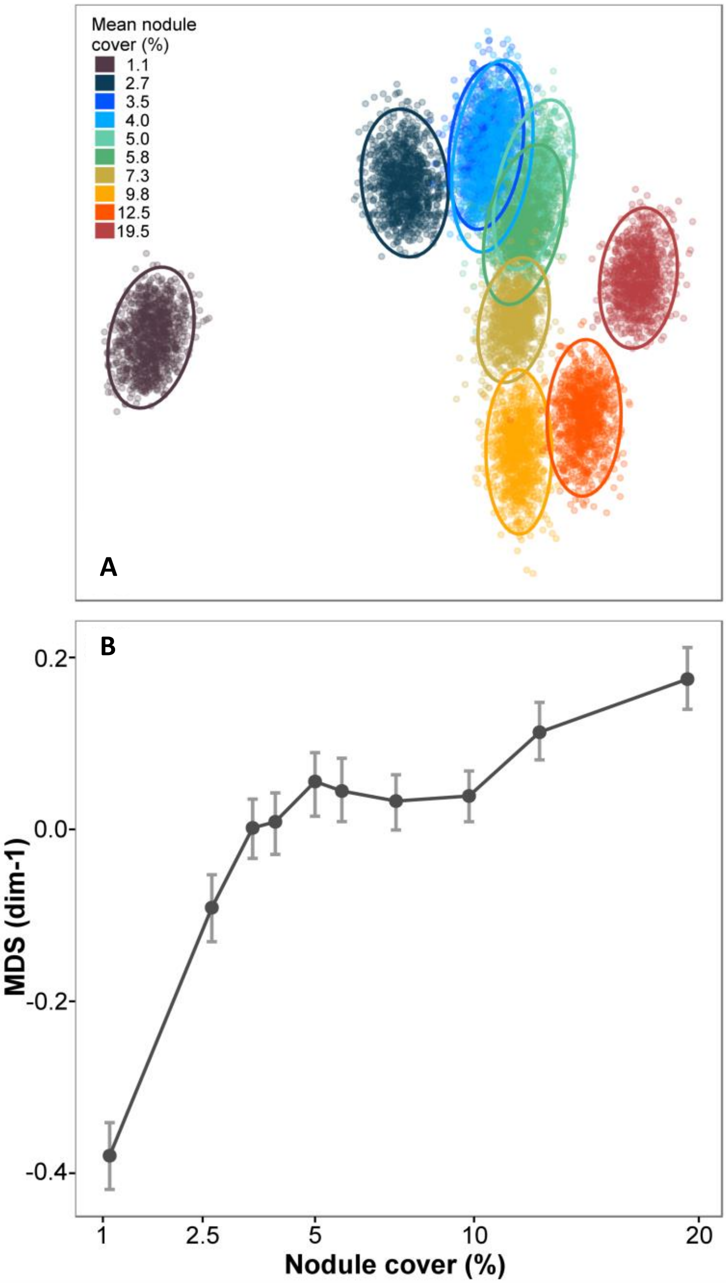

Figure 3.3. Variations in metazoan faunal composition with nodule cover at the APEI6 seafloor. **A)** nMDS plot describing 2-dimensional ordination of dissimilarity (distance) between the assemblages of each bootstrap-like sample. Ellipses represent 95% confidence intervals for each nodule cover class bootstrap-like sample set. **B)** Variation of NMDS dimension-1 with nodule cover. Points indicate mean values of this parameter calculated from each nodule cover class bootstrap-like sample set. Error bars represent 95% confidence intervals.

Functional groups

Neither nodule-attached (NA) nor nodule-free-living (NFL) faunal density was significantly correlated with nodule cover (Table 3.1). However, in both cases density in the lowest nodule-cover class was significantly lower than in any other class (Fig. 3.4A). Both deposit-feeder and suspension-feeder faunal density was significantly and substantially lower in the lowest nodule-cover class, while predator and scavenger density showed no significant variations across the nodule cover gradient (SM2; Fig. 3.8). Variation in suspension and deposit-feeder density across the nodule gradient described a rapid asymptote, yet none of the three functional groups densities exhibited a significant correlation with nodule cover (SM2; Table 3.2).

Taxonomic groups

Among the 15 most abundant morphospecies (SM2; Fig. 3.10) a graded series of distributions across nodule-cover classes was apparent (SM2; Fig. 3.11 and Table 3.2). For example (Fig. 3.4B): (i) negative monotonic, Porifera msp-5, strong and statistically significant correlation with nodule cover (Table 3.1); (ii) unimodal, *C.* cf *bayeri*, statistically significant difference between tails (classes 1, 8-10) and centre (classes 2-6) of the distribution; (iii) positive unimodal, *Lepidisis* msp, strong and statistically significant correlation with nodule cover (Table 3.1). The density of Polychaete msp-5 and Actinia msp-18 was significantly and substantially lower in the lowest nodule-cover class, while density of *Ophiosphalma* sp., *Columnella* msp, and Irregularia msp-1 was also lower in the lowest nodule-cover class, though marginally (SM2; Fig. 3.11). Among major taxa levels (i.e. most dominant phyla) a graded series of distributions across nodule-cover classes was also apparent (SM2; Fig. 3.9 and Table 3.2).

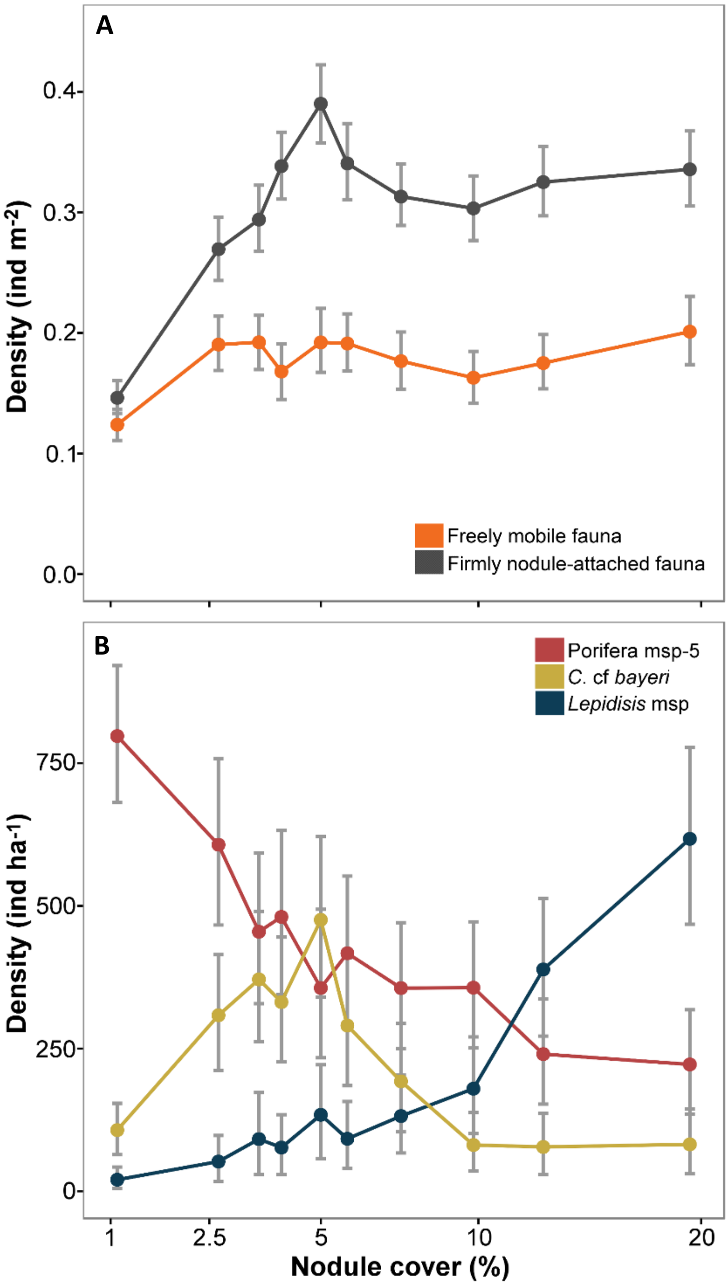

Figure 3.4. Variations in density of metazoan (A) life modes, and (B) selected morphospecies (the sponge: Porifera msp-5; the primnoid soft-coral*: Callozostron* cf *bayeri*; and the bamboo soft-coral: *Lepidisis* msp) with nodule cover. Points indicate mean values of each parameter calculated from each nodule cover class bootstrap-like sample set. Error bars represent 95% confidence intervals.

3.5. Discussion

We found substantial and statistically significant variations in megafaunal standing stock, biological diversity, and faunal composition along a gradient of seafloor nodule cover. These responses were generally graded with nodule cover. However, in many cases the magnitude of change between the first two cover classes was particularly marked. Both of these observations are of direct relevance to sustainable management and conservation concerns in relation to seabed mining in the CCZ and similar environments elsewhere.

Standings stocks

Differences in metazoan density across the nodule cover gradient were predominately driven by variations in suspension feeder abundance, particularly anthozoans living attached to nodules; the abundance of which was substantially and statistically significantly reduced in the lowest nodule class (SM2; Fig. 3.8 and Fig. 2.9B). Hard substrata provide a stable anchor point for suspension feeders and enable the placement of food-catching structures into faster off-bottom currents (Wildish and Kristmanson 2005). Enhanced densities of hard substratum attached fauna has been observed on bedrock in seamounts or canyons (Clark et al. 2010b, Baker et al. 2012, Jones et al. 2013), in areas with drop-stones (Jones et al. 2007, Meyer et al. 2016), and in polymetallic nodule fields (Amon et al. 2016, Vanreusel et al. 2016). Our results provide additional detail that suggests a non-linear, asymptotic relationship between standing stock and nodule cover (Fig. 3.2A). This response may be simply explained by resource limitation (Tilman 1982), i.e. hard substratum is initially limiting, but food resource (i.e. advecting organic particles) becomes limiting as attached suspension feeder density increases (Jeffreys et al. 2009). Variation in suspension-feeder density at the landscape-type scale sustains this hypothesis and suggest that the transition between limiting resources (i.e. from nodules to food) occurs at nodule cover >2-3% (Fig. 3.5A).

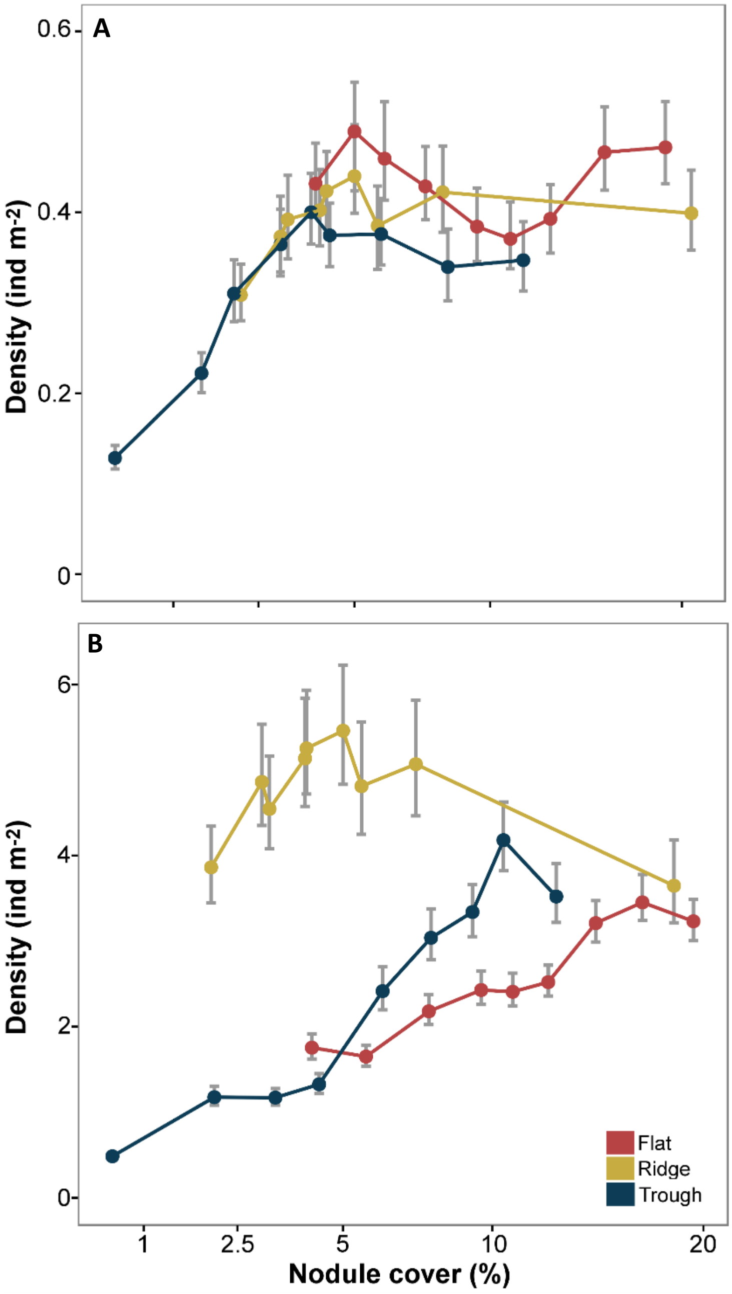

Figure 3.5. Example of landscape-type variation in faunal response to nodule cover. Variations in density of **(A)** suspension feeder metazoans, and **(B)** xenophyophores with nodule cover. Points indicate mean density values calculated from each nodule cover class bootstrap-like sample set for each separate landscape type analysis (Flat, Ridge, and Trough). Error bars represent 95% confidence intervals.

Xenophyophore density showed a rapid asymptotic relationship with nodule cover in the broad assessment but a different pattern in each area when investigated at the landscape-type level, with a clearly higher abundance in the Ridge (Fig. 3.5B). Other studies have documented enhanced xenophyophore density on elevated terrain, e.g. seamounts (Levin and Thomas 1988a, Wishner et al. 1990) and abyssal hills (Stefanoudis et al. 2016), and their dominance in the megafauna and high taxonomic diversity in the CCZ (Amon et al. 2016, Gooday et al. 2017). Although sediment-dwelling species are well-known, nodules clearly represent a very important habitat for xenophyophores (Gooday et al. 2015, Kamenskaya et al. 2015). While the specific feeding modes of xenophyophores remain uncertain (Gooday et al. 1993, Laureillard et al. 2004), the nodule-attached forms are most likely suspension feeders, and the sediment-dwellers most likely deposit feeders (Gooday et al. 2017). Yet our results suggest that, although nodule resource may limit the development of a part of the xenophyophore fraction (i.e. suspension feeder forms), geomorphological variations are a stronger control on the overall xenophyophore standing stock.

Biological diversity

Variation between morphospecies richness and morphospecies density was evident in the lowest nodule class (Fig. 3.2B), suggesting either a lower faunal density and/or a lower evenness between taxa abundances where nodule resource is limiting, yet no reduced taxa richness, as previous CCZ megafauna assessments suggested (Amon et al. 2016, Vanreusel et al. 2016, Tilot et al. 2018). However, previous studies typically used fixed-area samples, in fact reporting taxa density. For instance, Tilot et al. (2018) compared richness between areas with varying nodule abundance based on subsample units with fixed seabed areal cover, yet ranging in size from ~150 to ~450 individuals, which possibly generated strong biases in richness estimations as these are highly sensitive to the number of individuals surveyed (Gotelli and Colwell 2001). Distinction between morphospecies richness and density becomes particularly relevant in the assessment of nodule-field communities, as the lower megafaunal density characteristic of areas with low nodule cover can lead to the underestimation of taxonomic richness. In turn, if richness appears to be essentially invariant with respect to nodule cover, indices more sensitive to the variation in taxa evenness (i.e. heterogeneity diversity) may consequently be more appropriate monitoring targets.

Heterogeneity diversity measures indicated a clearly reduced diversity in the lowest nodule class, markedly so in the case of 1/D index (Fig. 3.2B). Our results concur with Amon et al. (2016) that nodule availability does not need to be high to promote higher megafauna diversity (although not necessarily richness), and with Vanreusel et al. (2016) that suspension feeder abundance distribution appears to lead (most) of this variation. Lower diversity in the lowest nodule class was predominantly generated by two combined factors: (i) general reduction in the abundance of almost all suspension feeder taxa, and (ii) extremely high numerical dominance of one taxon (Porifera msp-5), possibly better adapted to the environmental conditions in the lowest nodule class. On the other hand, landscape-type level analyses showed a clearly higher diversity in the Ridge compared to the Trough in areas with low nodule cover (2-3%, see SM1; Fig. 3.7E-F), possibly resulting from a more balanced taxa evenness, generated by the higher deposit feeder taxa abundance within the Ridge (Chapter 2). Structurally more complex habitats can provide a wider range of niches and diverse ways of exploiting the environmental resources, promoting species coexistence in the deep-sea benthos (Levin et al. 2001). Hence, our results suggest that nodules may act as 'keystone structures' (Tews et al. 2004) in the regulation of habitat complexity at fine scales (tens of meters), while geomorphological variations presumably modulating bottom water flows and deposition patterns (Mewes et al. 2014, Peukert et al. 2018), may play an important role at larger scales (few kilometres) (Chapter 2).

Faunal composition

Our data suggest that faunal composition changes continuously, yet not gradually nor proportionally, describing step changes with nodule cover across the full spectrum of the gradient studied. The first two steps on that gradient, i.e. from nodule class 1 to 2, and from nodule class 2 to 3, were, however, substantially greater than the other step change that followed these. i.e. from nodule class 8 to 9-10 (Fig. 3). This initial 'jump' is consistent with the change from an overwhelmingly background sedimentary habitat to a mosaic habitat with a varying admixture of nodule hard substrata to that sediment background. A higher dissimilarity of the lowest nodule-class assemblage was somewhat expected, since most of the APEI6 megafaunal community (70% of taxa richness) were nodule-dwelling taxa (Chapter 2) with reduced abundance in the lowest nodule class (SM2; Fig. 3.11). These populations may simply not find enough suitable substratum to develop where nodules are limited, as typically occurs in the smaller-sized meio- and macrofaunal communities (Mullineaux 1987, Veillette et al. 2007b). This first, sharply defined, faunal composition change numerically supports that even subtle increases in nodule availability can drive substantial variations in megafaunal communities (Amon et al. 2016). Yet the following, step variations, suggest a potential diversification of habitats along the nodule gradient beyond the simple presence or absence of a minimum nodule resource level.

We found a clear shift in dominance from sponges (predominantly Porifera msp-5) in the lowest nodule class to cnidarians in the remaining classes, and within the latter, an alternation of dominance between primnoid soft corals, anemones, and bamboo corals with increasing nodule cover. This suggests that other environmental drivers may potentially co-vary along the nodule cover gradient. For instance, nodule size was positively linearly correlated with nodule cover (r_P=0.72, p <0.001), with mean surface areas of nodules found in the lowest cover class (median: 1.66 cm^2; IQR: 0.44) being almost half the size of those in areas with the highest coverage (median: 2.87 cm^2; IQR: 0.42). Such comparably larger nodule sizes are commonly found in areas with lower sediment accumulation rates and relatively stronger bottom-current speeds (Skornyakova and Murdmaa 1992, Mewes et al. 2014). Variable development of particular deep-sea suspension feeder populations can be regulated by bottom current speeds (Thistle et al. 1985, Smith and Demopoulos 2003), and also by the size of the available hard structures (Meyer et al. 2016), especially in soft corals (Watanabe et al. 2009). Areas with larger and hence potentially more physically stable nodules possibly provide a more suitable long-term anchoring point for bamboo coral taxa, enabling their greater final colony height compared to, for example, primnoid soft corals (Lapointe and Watling 2015, Cairns 2016). In turn, the presumably stronger bottom current speeds in areas with large nodule size perhaps limits the development of primnoids, which appear to find a suitable habitat in areas with comparably lower nodule availability (4-6%). Therefore, we hypothesise that factors interrelated with nodule availability, like nodule size or bottom current speeds possibly act as environmental filters, ultimately controlling population recruitment rates.

Sustainable management and conservation

Our results suggest that areas less likely to be exploited by deep-sea mining (i.e. low to intermediate nodule-cover classes) would not serve the preservation of the full range of taxa that live in polymetallic nodule fields. Although these may act as source populations of taxa that also lives in high nodule abundance areas (i.e. actinians or bryozoans), our results show that these cannot support abundant populations of the fauna found in high nodule cover areas (i.e. bamboo corals). Moreover, the potential deposition of sediment plumes in non-directly exploited areas (Aleynik et al. 2017) may also compromise the preservation of source populations for most suspension feeder taxa (Bluhm 2001), that represent the vast majority of the metazoan standing stock at the CCZ (Amon et al. 2016, Vanreusel et al. 2016), and appear to be the most sensitive fauna to variations in nodule cover (i.e. this study). This suggests that the combined effects of nodule removal and sediment plume deposition are likely to generate biodiversity and standing stock losses at the landscape scale, with the corresponding loss in rate processes and ecosystem services provided by the megafauna.

Simplistically, a nodule field could be considered as two habitats: (a) the background sedimentary habitat, and (b) the hard substratum environment of the nodules. More realistically, and certainly at the physical scales inhabited by megafauna, the nodule field is likely better considered as a mosaic habitat comprising those two components. However, our results make clear that the mosaic habitat does not support a single biotope, nor indeed two biotopes; within the limits of the nodule cover gradient that we have been able to study, faunal composition exhibits step change variation. Equally, it is also clear that we do not yet fully understand the drivers of ecological variation along the nodule cover gradient. Consequently, sustainable management and conservation plans (Levin et al. 2016, Durden et al. 2017a), together with the monitoring programmes that support them, must recognise this complexity and uncertainty if they are to be effective.

In closing, we should note that our primary analyses have concerned a broad assessment of nodule cover using data drawn from three distinct abyssal landscape types. These landscape-scale variations in environmental and ecological characteristics (Chapter 2, SM1) add an additional layer of complexity that can be expected to operate at the physical scale of individual conservation areas (Area of Particular Environmental Interest in the CCZ) and potential mining operation areas.

3.6. Supplementary Material: Chapter 3

3.6.1. SM1: Additional analyses within landscape type

The dataset was collected in three landscape types, ‘Flat’, ‘Ridge’, and ‘Trough’ (main text, Fig. 3.1). To assess the potential influence of geomorphology on ecological responses to the nodule cover gradient, we additionally carried out separate analyses within each landscape type. As in our broad analysis, images were ordered by nodule cover and divided into nine cover classes at breakpoints to yield an approximately equal number of megafauna specimens in each class. Megafauna data from each cover class, in each landscape type, was then subjected to a boostrap-like resampling procedure to produce 1000 targeting a minimum of 250 specimens per sample. Faunal density and diversity measures (as in main text) were calculated for each boostrap-like subsample, and 95% confidence intervals derived by the simple percentile method (see main text).

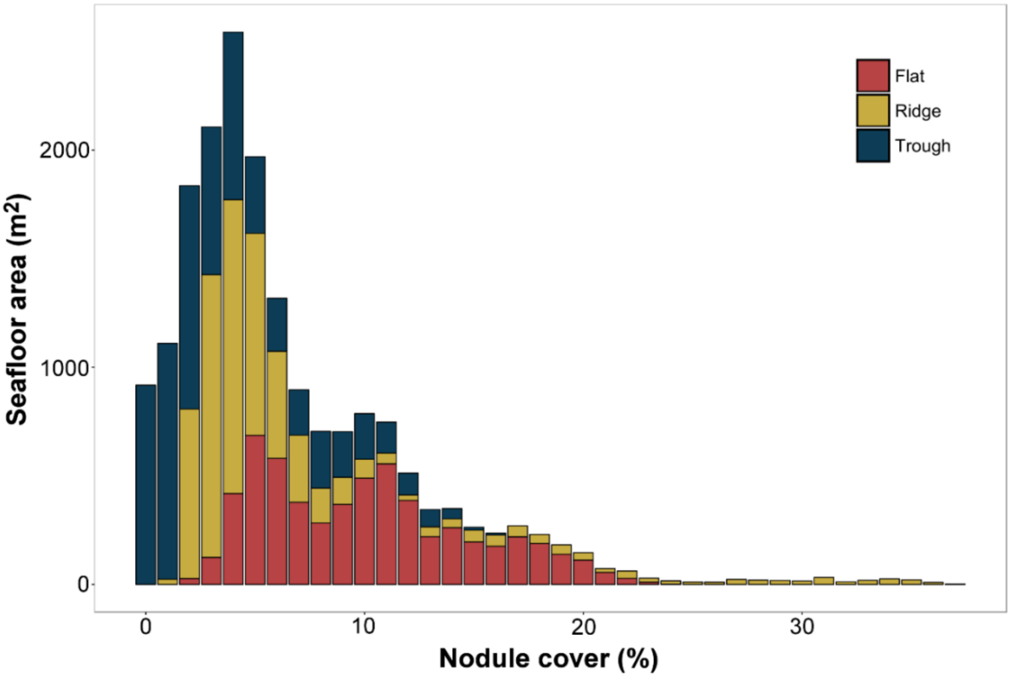

Figure 3.6. **Areal distribution of nodule cover within each landscape type of the APEI6.**

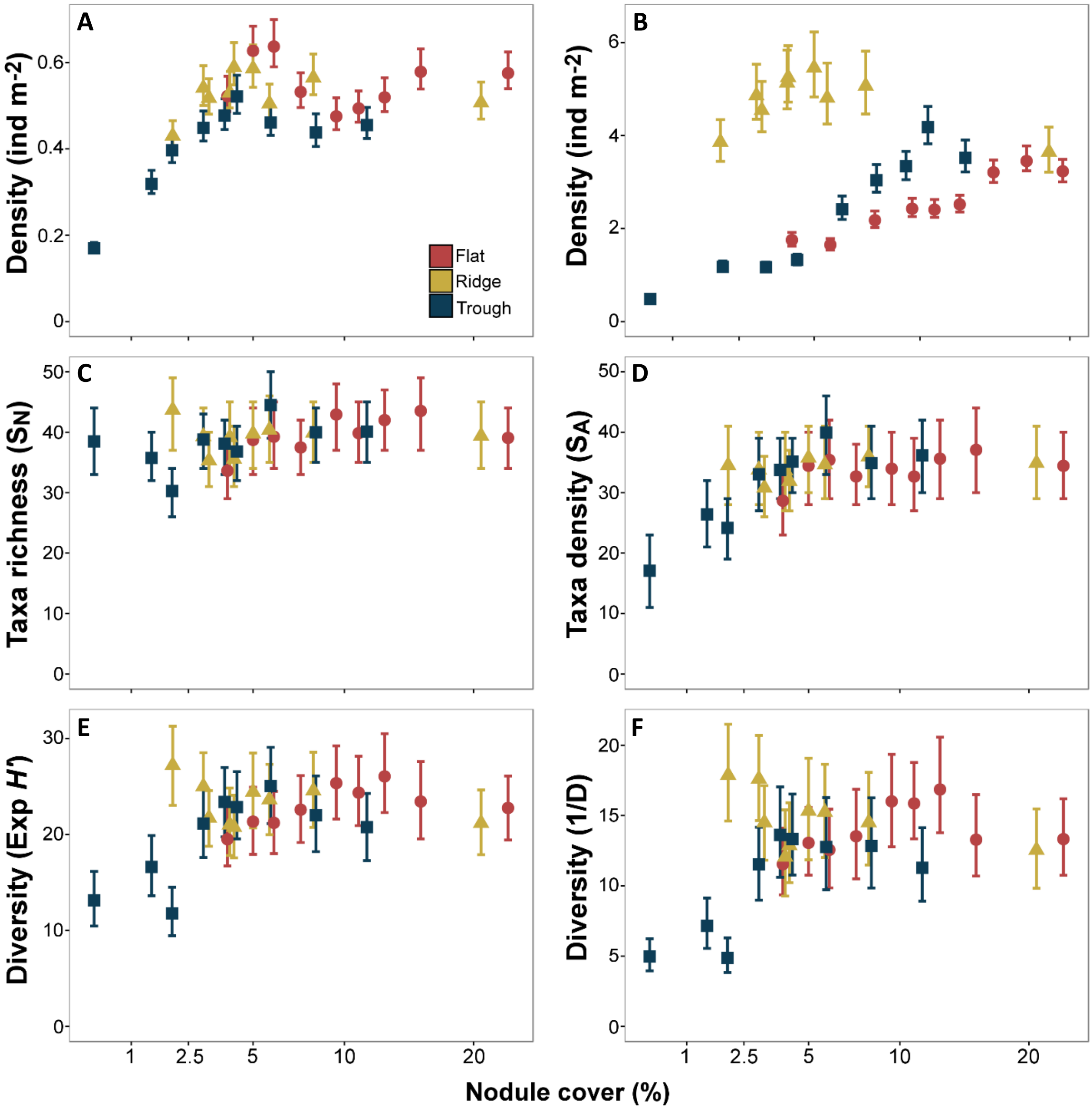

Figure 3.7. Variation of different ecological parameters across the nodule coverage gradient of each different APEI6 landscape type. Data are mean values of each parameter as calculated from each nodule cover class bootstrap-like sample set. Error bars represent 95% confidence. **A)** Metazoan density. **B)** Xenophyophore test density. **C)** Morphospecies richness. **D)** Morphospecies density. **E)** Exponential Shannon index. **F)** Inverse-Simpson index.

3.6.2. SM2: Additional results of general ecological assessment

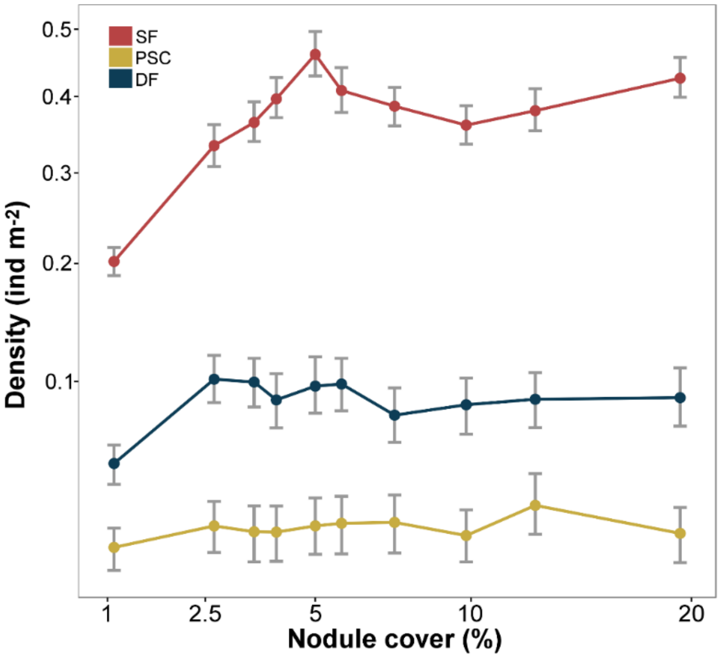

Figure 3.8. Variation in the density of three functional groups with nodule cover at the APEI6 seafloor. Data are mean density values of different metazoan types (SF: suspension feeders; PSC: predators and scavengers; DF: deposit feeders) calculated from each nodule cover class bootstrap-like sample set. Error bars represent 95% confidence intervals.

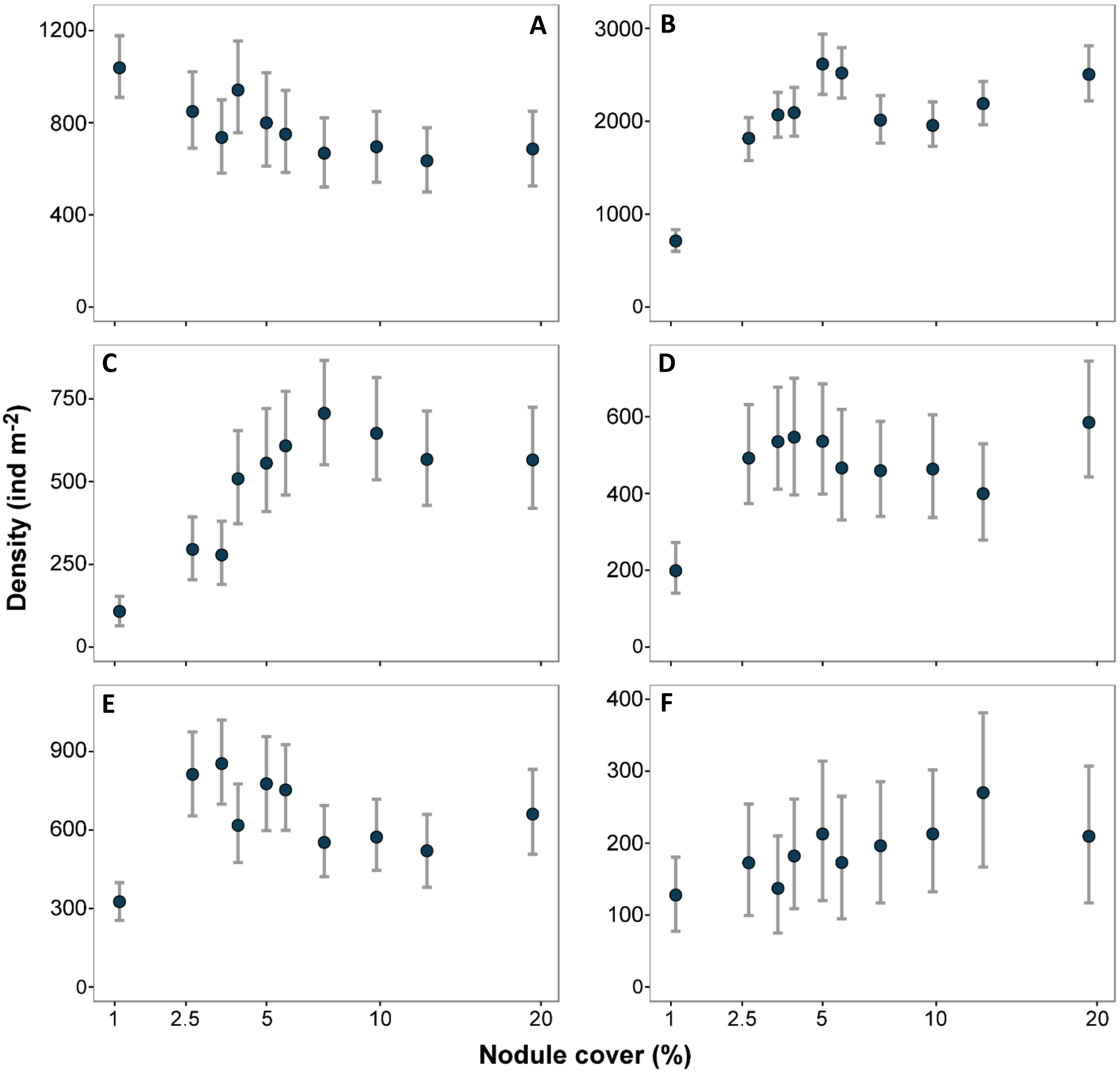

Figure 3.9. Variation in the density of taxonomical groups with nodule cover at the APEI6 seafloor. Data are mean density values of the six most dominant metazoan phyla as calculated from each nodule-cover class bootstrap-like sample set. Error bars represent 95% confidence intervals. **A)** Sponges. **B)** Cnidarians. **C)** Bryozoans. **D)** Annelids. **E)** Echinoderms. **F)** Arthropods: crustaceans.

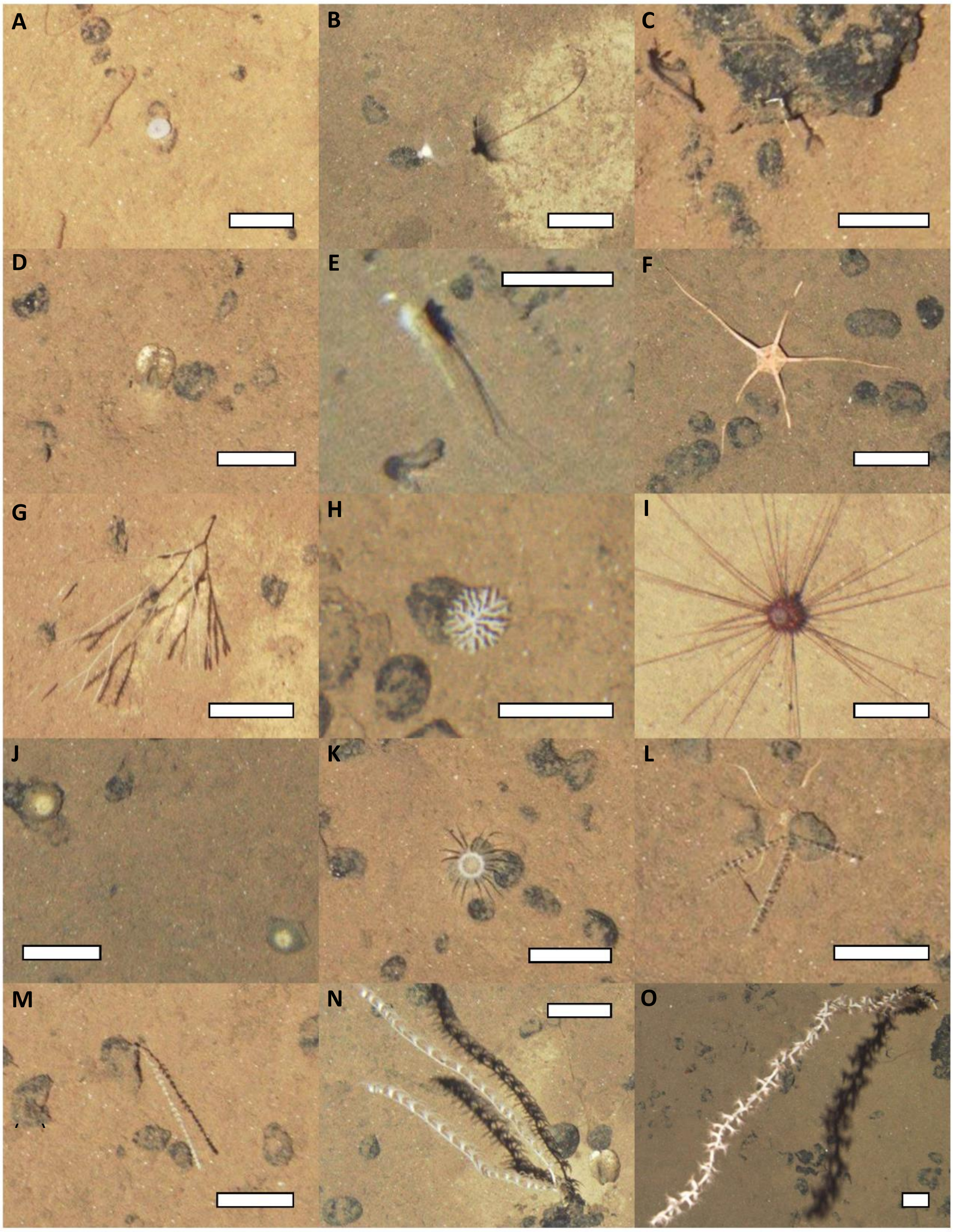

Figure 3.10. Top-15 most abundant metazoan morphospecies recorded at the APEI6 seafloor. Scale bars indicate 50 mm. **A)** Porifera msp-5. **B)** *Cladorhiza* cf *mexicana*. **C)** Polychaete msp-5. **D)** Irregularia msp-1. **E)** *Munnopsis* msp-2. **F)** *Ophiosphalma* sp. **G)** *Columnella* msp (Bryozoa). **H)** *Smithsonius* msp (Bryozoa). **I)** Aspidodiadematidae msp. **J)** Actinia msp-18. **K)** Actinia msp-22. **I)** *Callozostron* cf *bayeri*. **M)** *Calyptrophora* cf *persephone*. **N)** *Bathygorgia* cf *profunda*. **O)** *Lepidisis* msp.

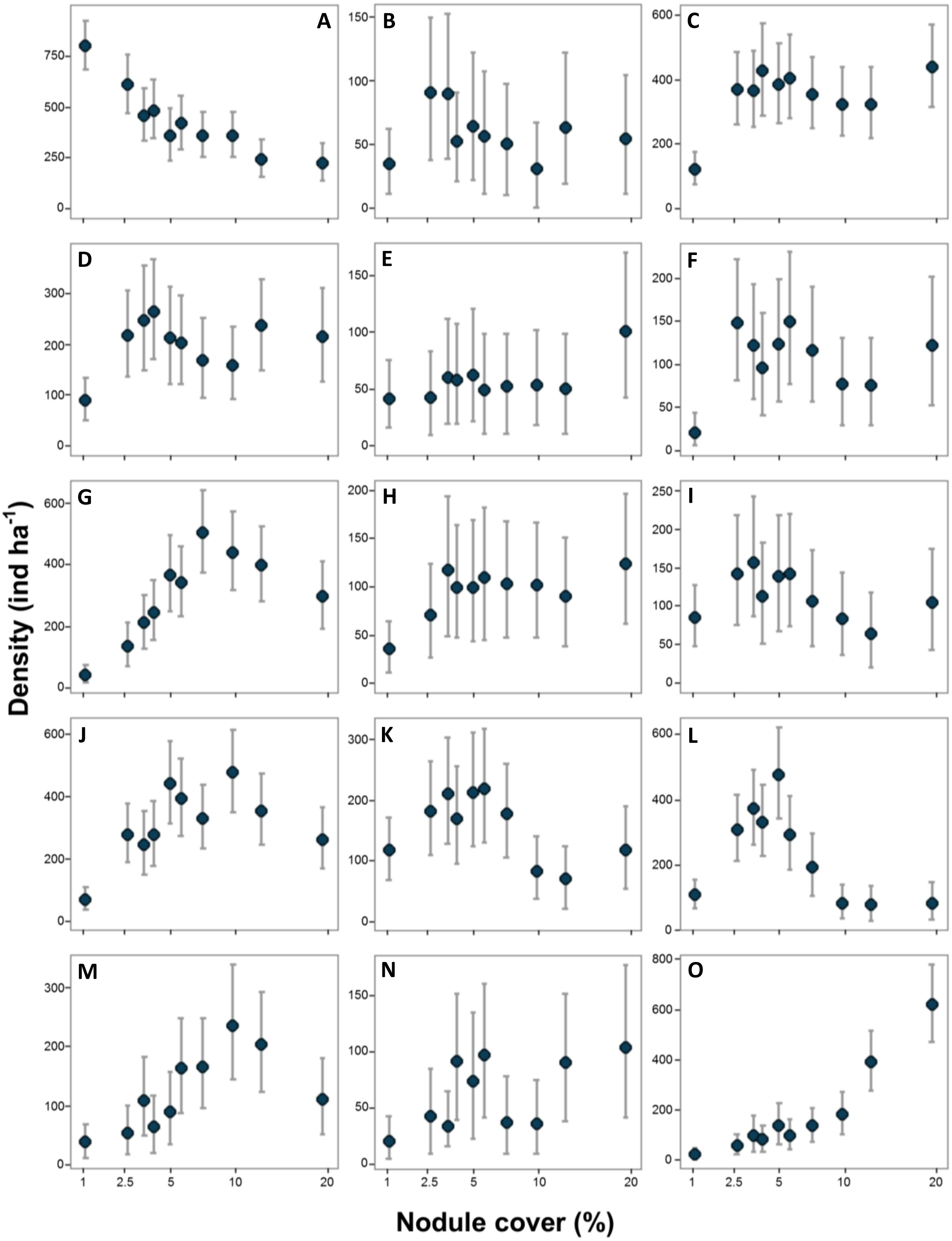

Figure 3.11. Variation in morphospecies density with nodule cover at the APEI6 seafloor. Data are mean density values of top-15 most abundant metazoan morphospecies as calculated from each nodule cover class bootstrap-like sample set. Error bars represent 95% confidence intervals. **A)** Porifera msp-5. **B)** *Cladorhiza* cf *mexicana*. **C)** Polychaete msp-5. **D)** Irregularia msp-1. **E)** *Munnopsis* msp-2. **F)** *Ophiosphalma* sp. **G)** *Columnella* msp (Bryozoa). **H)** *Smithsonius* msp (Bryozoa). **I)** Aspidodiadematidae msp. **J)** Actinia msp-18. **K)** Actinia msp-22. **I)** *Callozostron* cf *bayeri*. **M)** *Calyptrophora* cf *persephone*. **N)** *Bathygorgia* cf *profunda*. **O)** *Lepidisis* msp.

Table 3.2. Spearman's rank correlations of all ecological parameters with nodule cover. Results of tests performed between mean density (ind m^{-2}) values of different metazoan groups as calculated from each nodule cover class bootstrap-like sample set and nodule cover variation, with detail of significant differences between nodule class 1 (mean cover = 1.1%) and the rest of classes (cover >2%). Distinct class 1: no overlap of class 1 confidence interval with any other class.

	Distinct class 1	**Correlations**	
		r_S	p-value
Functional group			
Deposit feeders	**yes**	-0.15	0.676
Predators and scavengers	no	0.28	0.425
Suspension feeders	**yes**	0.50	0.138
Taxonomic Phylum			
Annelida	**yes**	0.10	0.777
Bryozoa	**yes**	0.78	**0.008****
Cnidaria	**yes**	0.49	0.150
Arthropods: crustaceans	no	0.83	**0.003***
Echinodermata	**yes**	-0.25	0.489
Porifera	no	-0.84	**0.002***
Morphospecies			
Polychaete msp-5	**yes**	0.18	0.627
Columnella msp	**yes**	0.76	**0.011***
Smithsonius msp	no	0.50	0.138
Actinia msp-18	**yes**	0.47	0.174
Actinia msp-22	no	0.83	**0.003***
C. cf *persephone*	no	-0.36	0.310
B. cf *profunda*	no	0.55	0.098
Lepidisis msp	no	0.95	**<0.001*****
C. cf *bayeri*	no	-0.60	0.067
Irregularia msp-1	no	-0.03	0.934
Aspidodiadematidae msp	no	-0.54	0.108
Ophiosphalma sp	no	-0.03	0.934
Porifera msp-5	no	-0.93	**<0.001*****
*C.*cf *mexicana*	no	-0.24	0.511
Munnopsis msp-2	no	0.44	0.200

4. Chapter 4: Disturbance-mediated megafaunal variations in the Peru Basin

4.1. Abstract

The potential start of abyssal polymetallic nodule exploitation has raised considerable scientific attention. The interface between the targeted nodule resource and sediment in this unusual mosaic habitat promotes the development of some of the most biologically diverse megabenthic communities in the abyss. However, the ecology of these remote ecosystems is still poorly understood, so it is unclear to what extent and timescale these ecosystems will be affected by, and could recover from, mining disturbance. We revisited the area within the Peru Basin (E Pacific; 3800-4300 m water depth) where the "DISturbance and reCOLonization experiment" (DISCOL) was conducted in 1989, and 26 years after simulated mining impacts were induced we investigated whether the effects of disturbance were still evident in the megabenthos. Using seafloor photo-mosaics generated from extensive AUV surveys, we objectively mapped the spatial distribution and magnitude of potential seafloor disturbance from plough tracks. Distinct ecological patterns were found across different seafloor disturbance levels. Suspension feeder standing stock remained significantly reduced in disturbed areas. However, deposit feeder and predator & scavenger fauna showed no diminished presence in disturbed areas, the first time this has been shown since the experiment began. Nevertheless, we found significantly lower heterogeneity diversity across differently disturbed areas compared to a nearby reference site, and markedly distinct faunal compositions along different disturbance levels. Our results show that the megabenthos of the DISCOL area has not yet recovered from simulated mining impacts. If the results of this experiment at DISCOL can be extrapolated to the Clarion-Clipperton Zone, the impacts of polymetallic nodule mining there may be much larger than so far expected, and could potentially lead to an irreversible loss of some ecosystem functions, especially in directly disturbed areas.

4.2. Introduction

Abyssal polymetallic nodule mining has attracted considerable scientific and public attention (Levin et al. 2016, Van Dover et al. 2017, Niner et al. 2018). The potential impacts of mining are likely to extend over extremely large seafloor areas (Aleynik et al., 2017) and lead to major changes in the benthic fauna (Jones et al. 2017), some of which may be long-lasting (Gollner et al. 2017). Polymetallic nodule fields are an unusual mosaic habitat (Chapter 3) where the hard substratum resource provided by nodules combined with the background soft sediment increase habitat complexity and promote the development of some of the most biologically diverse megabenthic communities in the abyss (Amon et al. 2016, Gooday et al. 2017). Nodules occur in densities commercially viable for potential exploitation in the central Indian Ocean basin, along the Cook Islands (equatorial Pacific), in the Clarion-Clipperton Zone (CCZ; NE Pacific), and in the Peru Basin (E Pacific) (Kuhn et al. 2017). Despite the effects of mining impacts having been investigated for decades (Roels 1974, Ozturgut et al. 1981, Thiel and Schriever 1990, Gollner et al. 2017), the ecology of these remote areas is still poorly understood. To date, it is largely unclear to what extent and timescale these ecosystems would be affected by and could recover from mining disturbance.

Besides the initial depletion of benthic fauna within machinery tracks, exploitation of polymetallic nodules is expected to change seafloor features (Morgan et al. 1999). Collector vehicles will remove the hard substratum provided by nodules, which is a basic resource for many sessile organisms and for small motile fauna inhabiting the crevices (Thiel et al. 1993, Veillette et al. 2007a, Vanreusel et al. 2016, Lim et al. 2017). Nodule-dwelling taxa can represent 50-70% of the megafaunal populations in polymetallic nodule fields (Amon et al. 2016, Chapter 2), and hence nodules are thought to play an important role in maintaining local and regional biodiversity (Vanreusel et al. 2016, Chapter 3). In addition to nodule removal, the top ~10-15 cm of the sediment, containing much of the organic material and biomass, will be re-suspended into sediment plumes (Aleynik et al. 2017). Sediment plumes and their re-deposition can affect the feeding activities of suspension feeder fauna and limit the recolonization of disturbed areas by affecting larval dispersal, mortality and settlement success (Gollner et al. 2017). Moreover, physical and chemical alteration of surface sediments appears to be also long-lasting (>20 years), even in areas only affected by particle re-deposition (Paul et al. 2018).

Several deep-sea mining simulations have been performed to investigate ecosystem responses to artificial disturbance of the seabed (Jones et al. 2017). The "DISturbance and reCOLonization experiment" (DISCOL), conducted in the Peru Basin in 1989 (Thiel and Schriever 1990, Thiel et al. 2001), is the largest-scale disturbance experiment carried out to date. For this experiment, an 8 m-wide plough-harrow device was towed 78 times on diametric courses across a 10.8 km^2 circular area, named the DISCOL Experimental Area (DEA), to simulate some of the impacts that would be expected from the movement of a polymetallic nodule collector vehicle (Thiel et al. 2001). Physical disturbance of two forms resulted: i) within the plough tracks (PT), most polymetallic nodules were buried and the surface sediment structure became a mosaic of clasts of previously buried consolidated 'clay' and flocculent, redeposited material with a high water content (Thiel et al. 2001), and ii) unploughed areas, which were also subject to sediment deposition. About 20% of the DEA was directly ploughed, the remainder was blanketed in a re-deposited sediment layer up to 30 mm-thick (Schriever 1992). Four areas located approximately 4 km from the DEA, and presumed beyond the influence of the plume re-deposition, served as reference sites during the investigations that monitored the recolonization patterns of the DISCOL area, 0, 0.5, 3, and 7 years after the disturbance (Ahnert and Schriever 2001, Bluhm 2001, Borowski 2001, Vopel and Thiel 2001).

Simulated mining impacts at the DEA generated variations in meio-, macro- and megafaunal communities, but the effect of disturbance differed among size classes and functional groups. For example, abundance of meiofaunal harpacticoids became ~ 20% lower within PTs than outside these in the DEA immediately after disturbance, and remained significantly reduced after 7 years (Ahnert and Schriever 2001). Macrofaunal density within PTs became ~70 % lower than outside these within the DEA immediately after disturbance, but densities within and outside PTs were balanced 3 years after (Borowski 2001). In contrast, megafaunal density was dramatically reduced within PTs immediately after disturbance, and remained substantially reduced 7 years after (Bluhm 2001), with density recovery of only ~ 9% for sessile taxa and 49% for the mobile taxa within PTs compared to pre-disturbance levels (Gollner et al. 2017). Megafaunal richness recovery within PTs was ~ 16% for sessile taxa, and 33% for mobile taxa after 7 years (Gollner et al. 2017). Outside PTs, megafaunal density slightly declined immediately after disturbance but was greater than in the reference areas after 3 years (Bluhm 2001), yet anthozoan abundance was still reduced compared to reference sites and to pre-disturbance levels after 7 years (Gollner et al. 2017). However, these megafaunal analyses were performed upon seafloor pictures that were taken non-randomly (Bluhm and Gebruk 1999), and hence likely overestimated rare and charismatic invertebrate megafauna and probably underestimated dominant fauna (Stratmann et al. 2018a). Moreover, natural variations between DISCOL revisits, possibly generated by temporally enhanced food supply (Ahnert and Schriever 2001, Bluhm 2001, Borowski 2001), constrained the temporal comparison of megafaunal data, particularly the assessment of community composition and heterogeneity diversity. Consequently, to date, despite all research performed, we still lack a full picture on how key ecological aspects of the megabenthos were affected by disturbance across the DEA.

We revisited the DISCOL site 26 years after the mining simulation experiment to investigate whether past disturbance still influences the megabenthic ecology of this area. Complete-coverage seafloor photo-mosaics generated from autonomous vehicle (AUV) imagery allowed us to simultaneously determine the present level of seafloor disturbance and link this to the spatial distribution of megafauna. We assessed the temporal and spatial responses to disturbance of dominant megafauna groups, as well as community diversity and composition. These results are used to understand better the context and scale of potential commercial mining disturbance.

4.3. Materials and Methods

Study area

All data used for the present study were acquired during RV *Sonne* expedition SO242-1 to the DISCOL site in the Peru Basin (Greinert 2015). The seafloor landscape in the DISCOL area ranges from 3800 to 4300 m water depth and is characterized by a succession of crenulated hills and shallow troughs between dispersed level-bottom (<5° slope) areas (Greinert 2015). The DEA and the south reference area (hereafter, REF) are located on a relatively smooth, slightly elevated part of the DISCOL seafloor, where water depths range from 4160 to 4140 m (Fig. 4.1). Within this area, average bottom water temperature was 1.8 °C, salinity was 34.6 PSU, and oxygen concentration was 139 µM L^{-1} (Greinert 2015). Bottom water currents are generally weak and alternate between periods of slow (1-3 cm s^{-1}) and modest (5-10 cm s^{-1}) current flows without a predominant direction (Klein 1993). Surface sediments have an average organic carbon content of 0.64% wt and are typically composed by silty clays or clayey silts (Clay: 65%; Silt: 20%; Sand: 15%) with little regional variation (Grupe et al. 2001, Marchig et al. 2001). Polymetallic nodule mass density averages > 10 kg m^{-2} in the DEA (beyond PTs) and REF sites, although may reach up to 30-40 kg m^{-2} locally (Thiel and Schriever 1989, Greinert 2015).

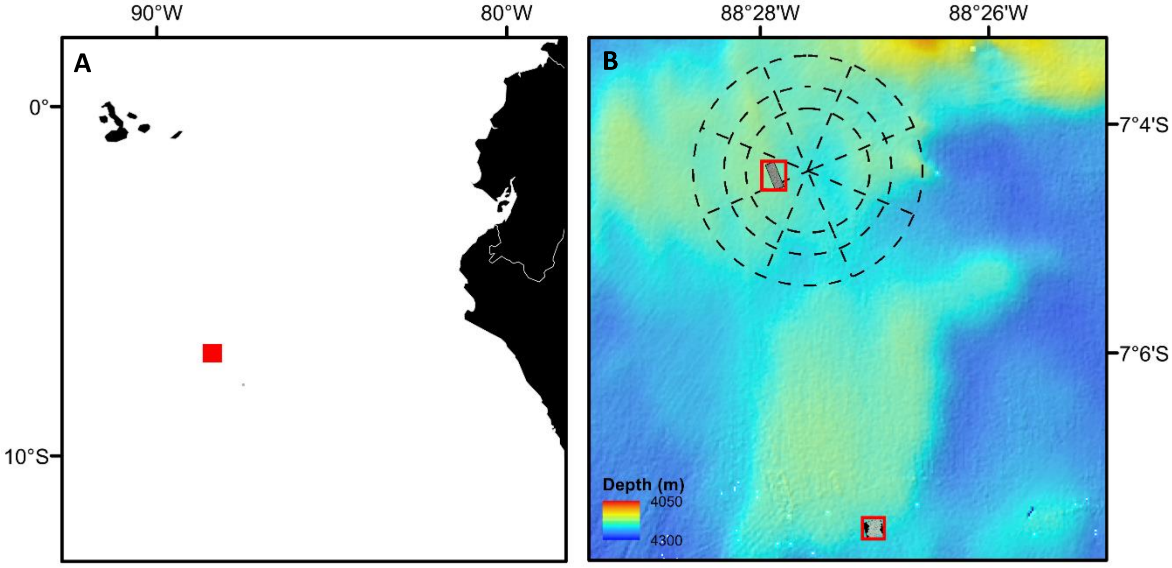

Figure 4.1. Study location and areas targeted for study along the DISCOL site in the Peru Basin. **A)** Location of DISCOL experimental area (red square). **B)** Map of the DEA (dashed lines) and REF site within the DISCOL area. Red polygons delimit the seabed areas targeted for AUV imagery collection and subsequent mosaic generation.

The DEA plough tracks are still readily observed in AUV imagery, 26 years after their generation (Fig. 4.2B). Consequently, seafloor areas are readily classified into three categories: i) apparently undisturbed areas (all of REF), ii) areas apparently subject to sediment re-deposition (adjacent to, and beyond, PTs, in DEA), and iii) areas of physically disturbed sediment (within DEA PTs).

Data processing

Image collection and mosaic generation

To assess the potential continuing influence of the original DISCOL disturbance on megafaunal assemblages, we conducted AUV-based visual surveys of the seafloor in the centre of the DEA (88.465° W, 7.074° S) and in the REF (88.450° W, 7.126° S). The AUV Abyss (Geomar Kiel) equipped with a *Canon* EOS-6D camera system with 8–15 mm f4 fisheye zoom lens, and 24 LED arrays for lightning, flew approximately 4.5 m above the seafloor at a speed of 1.5 m s^{-1} taking a picture every second along parallel transects with an average seafloor coverage overlap of 80%

(Kwasnitschka et al. 2016). Machine-vision processing was used to generate photo-mosaics (Kwasnitschka et al. 2016) of the targeted DEA and REF seafloor, each of 5-6 ha in spatial extent (Fig. 4.2A) and with a resolution of 3 mm pixel^{-1}.

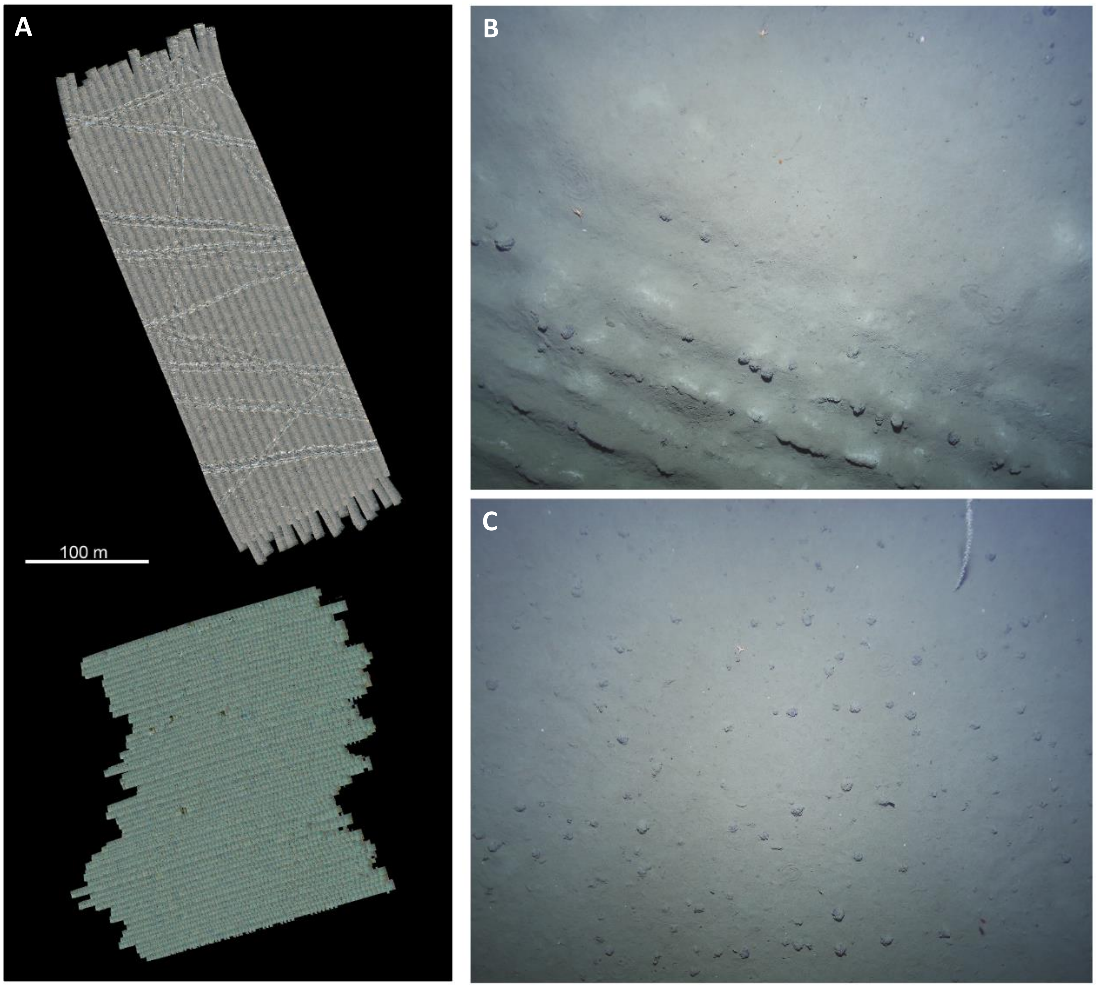

Figure 4.2. Mosaics generated from AUV imagery collected within the DISCOL area, and example images depicting the seafloor of each area. **A)** Mosaics of the DEA (top) and REF (bottom) study areas. **B)** Image of the DEA seafloor showing a still visibly disturbed PT generated during the DISCOL experiment in 1989, 26 years later. **C)** Image of the undisturbed REF area seafloor.

Megafauna detection

Mosaics were split into georeferenced tiles (c. seafloor area: 10.1 m^2) for megafauna data generation to facilitate data visualisation and avoid double counting. Tiles were analysed in random order to minimise sequence- or time-related bias (Durden et al. 2016). Metazoan specimens were identified to the lowest taxonomic level possible (morphospecies: msp), and measured using BIIGLE 2.0 (Langenkämper et al. 2017). To ensure consistency in specimen identification, a standardised megafauna catalogue was developed based upon pre-existent megafauna compilations (see http://ccfzatlas.com and https://www.discol.de/megafauna), which we expanded in consultation with international taxonomic experts and by reference to existing literature (Amon et al. 2017, Kersken et al. 2018). The likely feeding behaviour of each morphospecies was inferred from similar organisms described in the literature. Only specimens with a dimension >5 cm were retained for analysis to maximise the taxonomic resolution of specimen identifications, given the relatively high operating altitude above the seabed and the rather low resolution of mosaicked imagery data. The geolocation of each detected specimen was estimated from AUV navigation data based on their locations within individual image tiles, and recorded in Universal Transverse Mercator projection coordinates (Zone 16S) referenced to the World Geodetic System 1984 datum.

Disturbance levels mapping

We generated a polygon shapefile to map the spatial allocation of disturbed PTs within the DEA mosaic using ArcGIS software v.10. This shapefile was used as input to calculate a raster (cell resolution: 10 cm) of the distance (in m) of each cell to the closest PT, using the 'Euclidean Distance' tool in ArcMap, which covered the full extent of the DEA mosaic. A new raster was generated reclassifying raster cell distances to PTs into a range of hypothetical seafloor disturbance levels: level-A: within PTs and up to 1 m alongside these; level-B: 1-10 m from PT; level-C: 10-50 m from PT; while the whole REF seafloor was considered level-D: >3500 m from PT (Fig. 4.3). Each faunal record was assigned to the location where these were found within each study area, either at the DEA (levels A-C) or the REF site (level-D), using ArcMap. This spatially aligned environmental and biological dataset was used for subsequent analyses.

Data analysis

Semi-quantitative analysis: selected taxonomic groups

We selected the six most abundant (>100 occurrences per study area) taxonomic classes (Table 4.1) out of the 11 most-dominant megafauna groups examined by Bluhm (1995, 2001) in previous DISCOL revisits. These were: anthozoans, sponges, holothurians, ophiuroids, crustaceans and fishes (Fig. 4.4). Variations in the total density of each of these six groups across the disturbance levels mapped were assessed based on the total number of occurrences of each group and the total seafloor area encompassed within each disturbance level, which we calculated using ArcMap. Heat maps showing the distribution of density (ind ha^{-1}) of these six groups were calculated based on the spatial distribution of each group within the DEA. Raster maps (cell resolution: 1 m) were generated calculating the density of each group in each cell of the DEA, based on a circular neighbourhood radius of 50 meters, using the 'Kernel Density' tool in ArcMap.

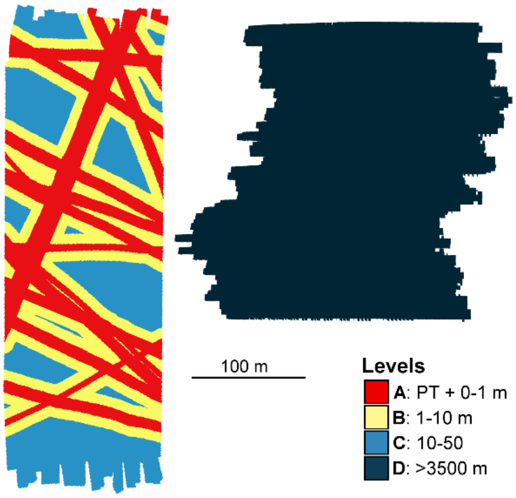

Figure 4.3. Disturbance levels mapped within each study area (left: DEA; right: REF) based on relative distances of the seafloor to the nearest PT.

Quantitative analyses: full community

We applied a stratified-random sampling design to investigate variations in the megabenthic community across the range of seafloor disturbance levels mapped. We split the full area covered by the DEA and REF mosaics, and corresponding faunal occurrence data, into quadrat-shaped units (cells) covering c. 0.25 m^2 of seabed, assigning each cell to the disturbance level where its centroid coordinates fell. Replicate sample sets were generated by grouping randomly selected cells from each disturbance level without replacement, up to a total of 3500 m^2 of seafloor surveyed (14,000 cells per replicate), using a custom R script (R Core Team, 2017). This ensured a minimum of 5 replicate samples generated for each DEA disturbance level (levels A-C). Ten replicates were generated this way within the REF site (level-D). Faunal data contained in each cell was pooled for each replicate sample. Samples typically contained 197-299 individuals.

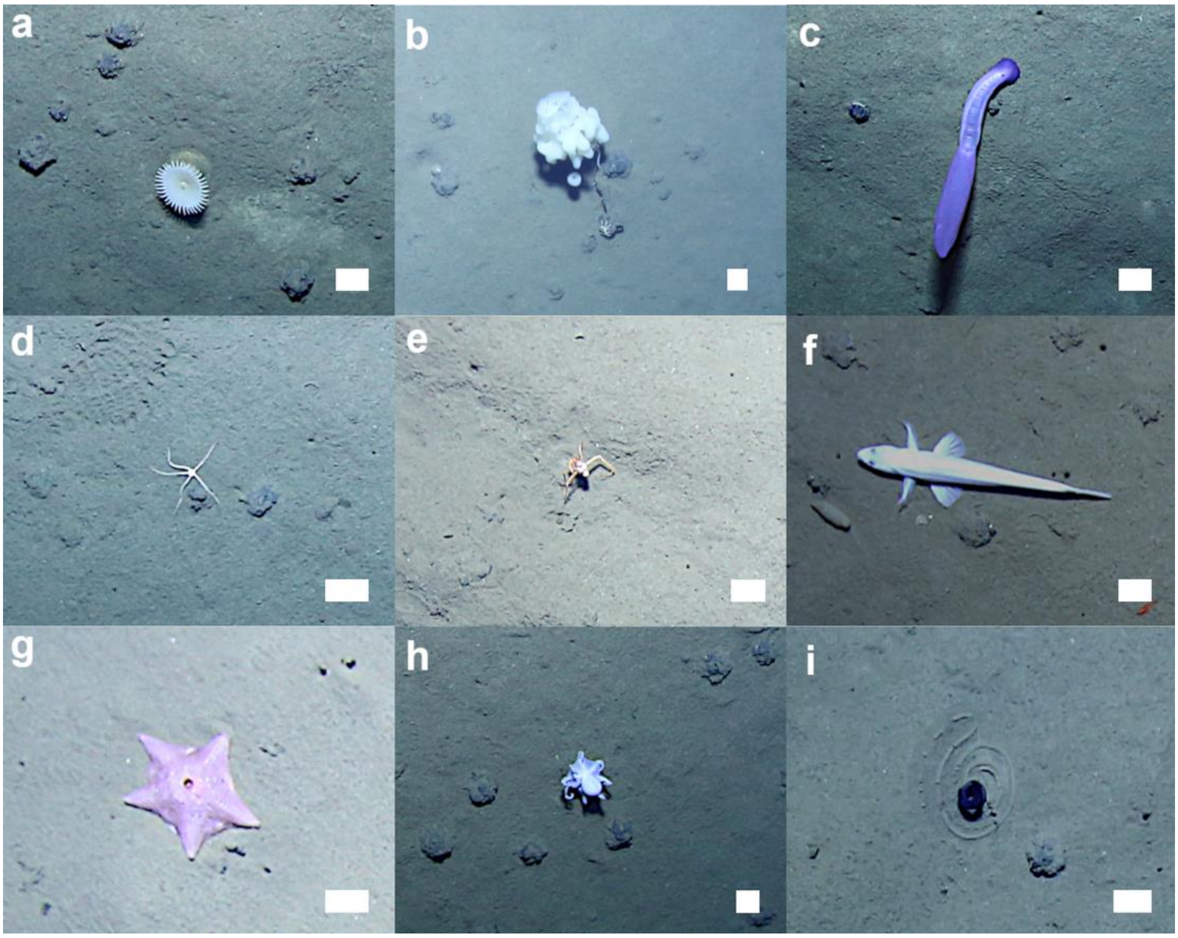

Figure 4.4. Examples of most dominant faunal types surveyed in AUV sampling across the DISCOL site. Scale bars indicate 5 cm. **A)** Anthozoa, Actiniaria msp-2. **B)** Porifera, Aphrocallistidae msp-1. **C)** Holothuroidea, *Psychropotes longicauda* -violet morphotype-. **D)** Ophiuroidea, Ophiuroid msp-1. **E)** Crustacea, *Probeebei mirabilis*. **f)** Actinopterygii, *Bathysaurus mollis.* **G)** Asteroidea, Hymenaster msp-3. **H)** Cephalopoda, 'Casper' msp. **I)** Enteropneusta, *Tergivelum* sp. inc.

A range of ecological parameters were calculated for each replicate sample to explore variations in standing stock and diversity across disturbance levels. These parameters were numerical density (ind ha^{-1}) and Hill's diversity numbers of order 0, 1, and 2 (Jost 2006), respectively morphospecies richness (S), the exponential form of the Shannon index (Exp *H´*), and the inverse form of Simpson's index (1/D). Additional rarefaction-based analyses were performed with varying individual-based sample-unit sizes to explore the potential effect of variable individual counts in our diversity estimations calculated from fixed-area samples (see SM). These analyses were done using the 'vegan' package implemented in R (Oksanen et al. 2018).

Table 4.1. Total abundance of different metazoan taxa surveyed at each study area. Seafloor areal coverage covered by photo-mosaic data: DEA: 58600 m^2; REF: 52500 m^2.

Phylum	Class	Order	Morphospecies (n)	DEA	REF
Porifera					
	Demospongiae		4	49	100
	Hexactinellida		7	215	206
Ctenophora					
	Tentaculata		2	34	28
Cnidaria					
	Anthozoa				
		Actiniaria	7	106	208
		Alcyonacea	3	39	130
		Antipatharia	2	11	7
		Ceriantharia	1	2	0
		Pennatulacea	1	2	2
		Zooantharia	1	10	7
	Hydroidea		2	107	60
Bryozoa					
	Gymnolaemata		1	2	1
Annelida					
	Polychaeta		4	112	88
Arthropoda					
	Malacostraca				
		Decapoda	6	407	305
		Isopoda	1	7	2
		Cirripedia	1	2	2
Echinodermata					
	Asteroidea		7	90	62
	Crinoidea		5	125	94
	Echinoidea		2	9	2
	Holothuroidea		26	992	794
	Ophiuroidea		2	1409	724
Hemichordata					
	Enteropneusta		2	82	77
Mollusca					
	Cephalopoda		3	13	32
Chordata					
	Ascidiacea		1	94	60
	Actinopterigii		6	233	141

Generalized linear models (GLM) (Dobson and Barnett 2008) were built to test whether statistically significant variation in the estimated parameters was apparent between the replicates of different disturbance levels, using the ‘car’ package implemented in R (Fox et al. 2016). Variations in faunal density were tested based on (integer) abundance count data, as all samples covered the same seafloor area. Models were fitted with quasi-Poisson errors in non-negative integer metrics (i.e. S and density) with over-dispersion (Gardner et al. 1995), and with normal errors applied to non-integer variables (i.e. Exp *H´*, 1/D) (Freund and Littell 1981). When statistically significant differences were detected in these global tests, simultaneous tests were applied to make multiple comparisons between individual disturbance levels, using the ‘multcomp’ package in R (Hothorn et al. 2017). Homogeneity of variance and probability-distribution assumptions were verified by visual inspection of model histograms and QQ plots. Statistical significance was reported for $p < 0.05$.

Variations in community composition between disturbance levels were explored following an abundance-based multivariate approach. Dissimilarity in the faunal composition between all pairs of replicate samples was calculated using the Bray-Curtis dissimilarity measure, based on square-root transformed faunal abundance, as calculated using the ‘vegan’ package in R. Non-metric multidimensional scaling (nMDS) ordination was used to visualise variations using ‘vegan’ package in R. A one-way permutational multivariate analysis of variance (PERMANOVA) analysis (Anderson 2001), with follow-up pair-wise tests, was used to test for statistically significant variations in assemblage composition between disturbance levels, using PRIMER v.7 (Clarke and Gorley 2015).

4.4. Results

Dominant taxonomic groups

The 6 most abundant taxonomic groups generally increased (anthozoans, sponges and fishes), decreased (crustaceans), did not change (holothurians) or were variable (ophiuroids) with increased distance from the PTs (Fig. 4.5). Statistically significant differences in density across disturbance levels were exhibited in all groups except for holothurian fauna (Table 4.2). For example, anthozoan and sponge density was substantially and statistically significantly lower in level-A than in the other studied levels (Tukey, $p < 0.05$-0.001). However, while anthozoan density appeared to increase from level A-D, sponge density was almost invariant in the non-directly disturbed levels B-D. Ophiuroid density was substantially and statistically significantly lower in level-D than in all the other levels (Tukey, $p < 0.001$), where these showed comparably little variation. Crustacean density was substantially higher in level-A, showing a statistically significantly higher density than in levels C-D (Tukey, $p < 0.001$). Fish density showed a statistically significant difference between all disturbance levels (Tukey, $p < 0.05$-0.001), increasing from level A-C, yet with a substantially reduced presence in level-D compared to levels B-C.

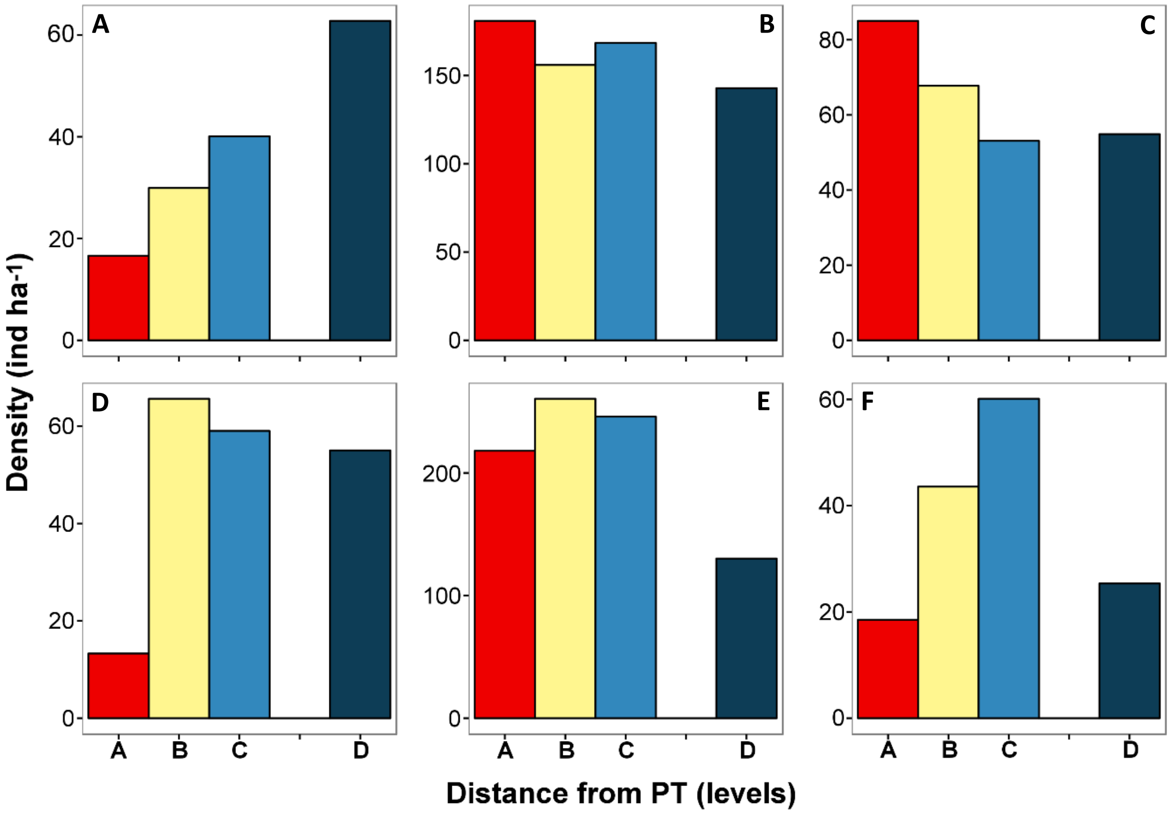

Figure 4.5. Standing stock variations of the most abundant faunal groups across the disturbance levels studied at the DISCOL site. Total density was calculated along the full area of seafloor investigated in each disturbance level. **A)** Anthozoans. **B)** Holothurians. **C)** Crustaceans. **D)** Sponges. **E)** Ophiuroids. **F)** Fishes. Disturbance levels: level-A: PTs + 0-1 m; level-B: 1-10 m; level-C: 10-50 m; and level-D: >3500 m.

Full assemblage

Standing stock and diversity

Total megafaunal density in levels A and D was statistically significantly lower than in levels B-C (Table 4.2) (Tukey, $p < 0.001$). These variations were driven by changes in abundance of different functional groups between disturbance levels (Table 4.2; Fig. 4.6). Suspension feeder faunal density was substantially and statistically significantly reduced in level-A compared to each of the other disturbance levels (Tukey $p < 0.001$), while both deposit feeder and predator & scavenger faunal densities were statistically significantly reduced in level-D compared to each of the other disturbance levels (Tukey, $p < 0.001$). Morphospecies richness in level-A was statistically significantly lower than in level-C (Table 4.2) (Tukey, $p < 0.05$). Richness differences between the other levels were not significant (Tukey, $p > 0.05$). On the other hand, Hill's diversity indices of higher value ($q>0$) were statistically significantly higher in level-D than in all the other disturbance levels at the DEA, where both heterogeneity indices were almost invariant.

Community variations

We found statistically significant variations in faunal composition by abundance between the assemblages of different disturbance levels (PERMANOVA, $R^2 = 0.33$, $p < 0.001$), with statistically significant differences apparent in paired comparisons between all levels (pair-wise PERMANOVA, $R^2 = 0.21\text{-}0.27$, $p < 0.01$), except between levels C and D (pair-wise PERMANOVA, $R^2 = 0.14$, $p > 0.05$), where we found a similar faunal assemblage (Fig. 4.7).

Table 4.2. Biological parameters assessed for each disturbance level investigated at the DISCOL area, with detail on the general linear models (GLM) applied to explore for significance in the variations of these parameters between levels. Values shown as: mean (95% confidence intervals: lower – upper) calculated amongst all replicate samples analysed for each disturbance level.

Standing stock (ind ha^{-1})	**PT + 0-1 m**	**1-10 m**	**10-50 m**	**> 3500 m**	**Error fit**	**F-value** ($F_{3\text{-}24}$)
Megafauna	648 (606-690)	789 (766-813)	797 (726-846)	592 (562-624)	QP	**23.48*****
DF	443 (414-474)	470 (442-507)	470 (434-493)	315 (293-335)	QP	**29.6*****
PSC	141 (127-157)	160 (145-171)	159 (154-154)	114 (105-124)	QP	**14.6*****
SF	63.4 (53.7-73.7)	158 (140-181)	168 (136-194)	161 (150-173)	QP	**28.5*****
Anthozoa	18.9 (13.7-23.4)	32.6 (26.3-40)	42.3 (33.7-53.1)	63.4 (55.1-71.4)	QP	**21.10*****
Sponge	12.6 (11.4-13.7)	69.1 (57.7-80.6)	62.3 (47.4-81.1)	58 (49.7-65.4)	QP	**26.37*****
Holothuroidea	185 (161-209)	165 (148-182)	177 (144-210)	151 (137-163)	QP	1.8
Ophiuroidea	227 (212-242)	273 (254-289)	258 (234-281)	136 (127-145)	QP	**68.96*****
Crustacean	92.6 (84-101.7)	71.4 (58.9-81.1)	55.4 (50.3-60.6)	56.9 (50-64.9)	QP	**9.92*****
Fish	17.7 (9.7-24)	45.7 (42.3-49.1)	63.4 (56.6-70.3)	29.1 (24.3-33.7)	QP	**25.78*****
Diversity						
Richness (S)	43 (41.4 - 45.1)	51 (49.2 - 52.9)	51.8 (48.3-55.1)	47.7 (45.9-49.8)	G	**4.5***
Exp H'	18.4 (16.6-20.4)	21.6 (20.1-23.5)	22.3 (19.1-25.5)	27.5 (26.9-28.2)	G	**17.83*****
1/D	7.1 (6.4-7.9)	7.5 (6.9-8.7)	8.4 (6.7-10.2)	13.4 (12.9-13.9)	G	**35.26*****

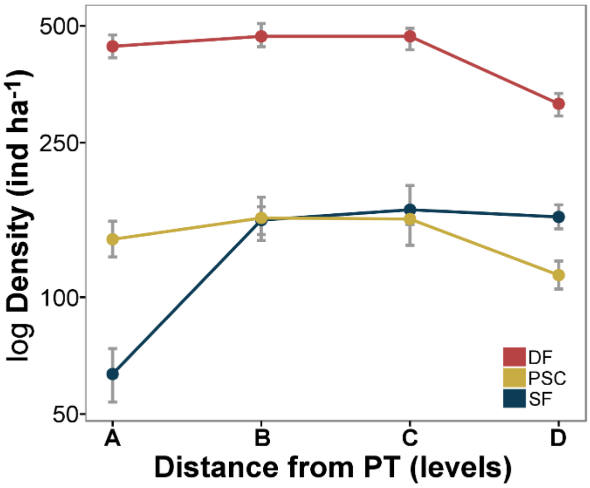

Figure 4.6. Functional group standing stock variations across the disturbance levels studied at the DISCOL site. Points indicate mean faunal density values between all replicate samples analysed for each disturbance level. Error bars represent 95% confidence intervals. Disturbance levels: level-A; PTs + 0-1 m; level-B: 1-10 m; level-C: 10-50 m; and level-D: >3500 m. Functional groups: deposit feeders (DF); predators & scavengers (PSC); and suspension feeders (SF).

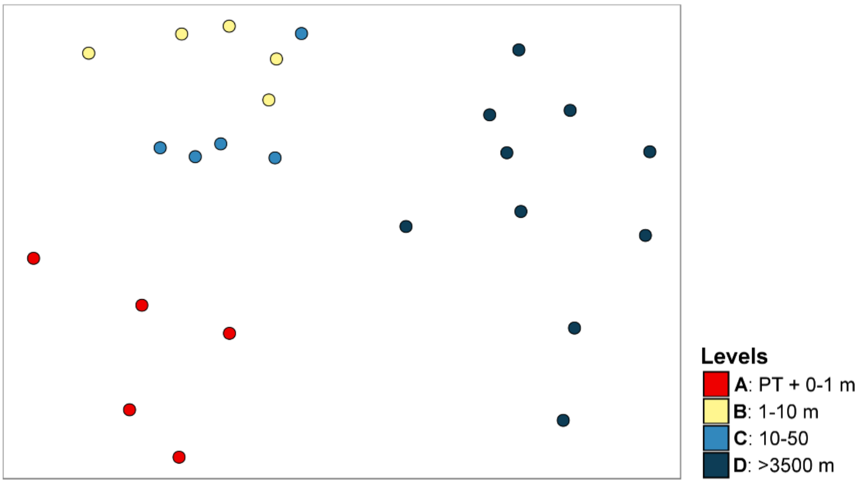

Figure 4.7. Variations in faunal composition between disturbance levels. MDS plot describing 2-dimensional ordination of distance (Bray-Curtis dissimilarity calculated from square-root transformed abundance data) between the assemblages of each generated replicate sample.

4.5. Discussion

The effects of mining impacts are still evident in the megafaunal community of the DISCOL site 26 years after disturbances were induced. Our results show consistently distinct ecological patterns across 3 main seafloor disturbance/distance levels from disturbed PTs; within PT (level-A), outside PT (level-B + level-C), and REF (level-D). Suspension feeder standing stock was clearly reduced within PTs, while density of both deposit feeders and predators & scavengers showed no variations between areas within and outside PTs for the first time since the experiment began, and an overall much larger abundance than at the REF. Nevertheless, these variations generated a significantly lower heterogeneity diversity within the DEA compared to the REF study areas, and markedly distinct faunal compositions between the assemblages found within PTs, outside PTs, and REF. If we assumed that the REF community represents a “true control” to the disturbance experiment, we would conclude that the megabenthos of areas directly impacted by the plough-harrow device and that of areas only affected by sediment re-deposition have, both, not yet recovered after disturbance. Being more conservative, and assuming a potential natural difference in the ecology of the REF area — which given the results obtained in previous REF area surveys (Bluhm 2001) appears likely, see below — our results provide consistent evidence that, at least, areas directly impacted by the plough-harrow are still far from recovery.

Standing stocks

Differences in faunal density across the DEA were predominately driven by variations in suspension feeder abundance, particularly sponge and anthozoan fauna, the abundance of which was substantially reduced within PTs (Fig. 4.8). Suspension feeder abundance is usually highly sensitive to hard substratum availability in deep-sea ecosystems (Baker et al. 2012, Jones et al. 2013, Meyer et al. 2016), markedly so in abyssal Pacific nodule fields (Radziejewska and Stoyanova 2000, Vanreusel et al. 2016), where suspension feeder populations are commonly dominated by nodule-dwelling taxa (Amon et al. 2016, Chapter 3). Burial of nodules during the DISCOL experiment eliminated a basic component of the DEA biotope, limiting the anchoring and subsequent development of most suspension feeder forms within PTs. Consequently, 26 years after the disturbance, the suspension feeder standing stock remains substantially reduced within PTs compared to the other areas, as was observed in each of the previous DISCOL revisits (Bluhm

2001). Thus, their respiration rate within PTs is, to date, 80% lower than outside these (Stratmann et al. 2018a). Mining impacts appeared to have altered the functional structure of the megabenthos, generating a long-lasting reduction of suspension feeder standing stocks within PTs.

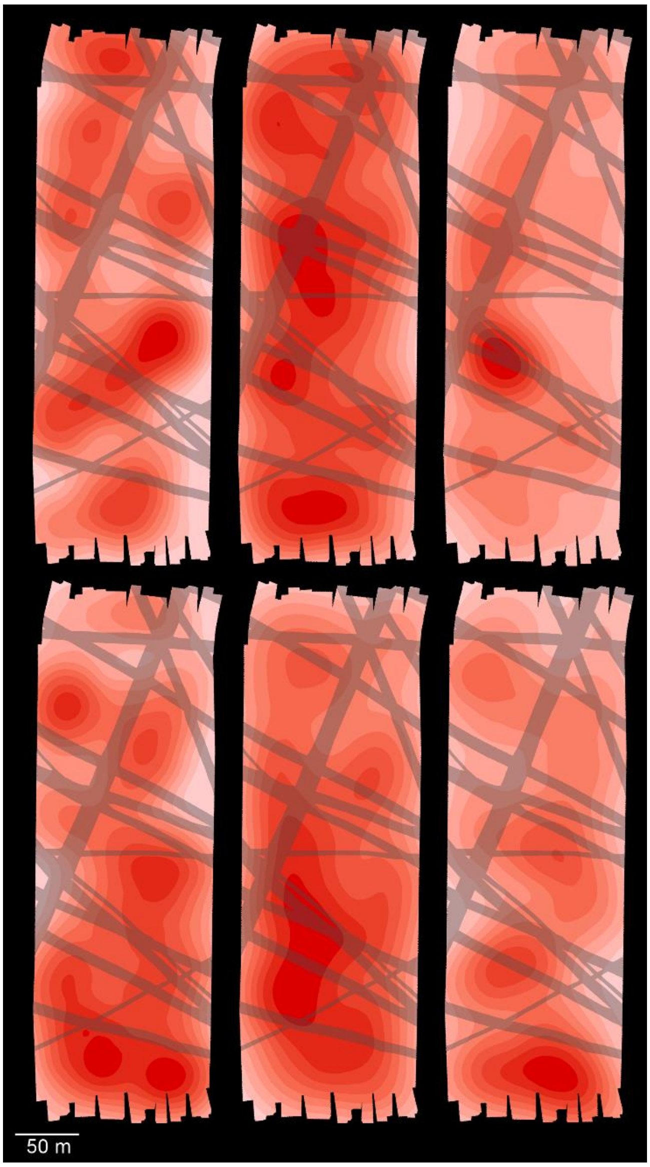

Figure 4.8. Heat maps showing the distribution of density of the six most-dominant megafaunal groups across the DEA. PTs depicted in semi-transparent stripes. Density ranges are classified in 10 equal breaks for each faunal group, from minimum (white) to maximum (red) density. From left to right and top to bottom: anthozoans, holothurians, crustaceans, sponges, ophiuroids, and fishes.

Differences in megafaunal density between areas outside PTs and the REF were predominately driven by variations in deposit feeder and predator & scavenger fauna, the abundance of which was reduced in the REF. This pattern was already observed in previous revisits and was related with an enhanced 'attractiveness' of the areas outside PT of the DEA to the megafauna (Bluhm 2001). This has two main possible interpretations; either there could be indeed an attraction to the ploughed area resulting from the previously buried organic material that was made available (i.e. as occurs when ploughing agricultural soil), or this pattern simply responds to environmental drivers operating at larger scales (DEA to REF: few kilometres), which are not discussed here.

In turn, deposit feeder and predator & scavenger fauna showed no significantly reduced density within PTs for the first time since the experimental disturbance (Fig. 4.6). Bluhm (2001) showed that repopulation of areas within PT by deposit feeders and scavenging animals, except ophiuroids, started shortly after disturbance, almost reaching pre-disturbance levels after 7 years. However, most of these dominant taxonomic groups (i.e. Holothurians, Crustaceans) still showed reduced abundance within PT (Gollner et al, 2017). At present (19 yr later) density of crustaceans, holothurians and ophiuroids shows little variation across the DEA, and ophiuroids are proportionally more abundant than holothurians, as these used to be before disturbance (Bluhm et al. 1995). Consequently, there are no differences in respiratory activity of holothurians across the DEA (Stratmann et al. 2018c), which along with our results suggests that recovery of some functional groups, particularly deposit feeders, may be possible within tens of years after small-scale mining disturbances.

Biological diversity

Reduced taxa richness found within PTs compared to outside PTs needs to be interpreted with caution provided the fixed-area approach we applied during sample generation. Amongst Hill values, richness (q=0) is the most sensitive index to the individuals encompassed within samples (Gotelli and Colwell 2001). This apreciation is particularly important when comparing areas with variable faunal density, as richness estimations derived from samples with lower faunal abundance are more likely to underestimate "true" richness (Chapter 3). For instance, rarefaction analyses (see SM1) also showed a signicantly reduced richness within PTs compared to outside PTs when variations were investigated as a function of the seabed area size surveyed (Fig. 4.9A), yet this difference became non-significant when investigated as a function of the individuals surveyed (Fig. 4.9B), as this analysis diminishes the bias steming from a variable density between samples (Chao et al. 2014). Consequently, richness estimates obtained from our replicate sample design are best interpreted in terms of “taxa density” (Whittaker et al. 2001), rather than as “true” richness. Reduced taxa density within PTs can be indicative of an overall reduction of taxa abundances and/or a reduction of eveness in the proportions between these (Jost 2010). Hence, although taxa richness may show signs of recovery within PT compared to outside these for the first time after disturbance (Bluhm, 2001), impacts of simulated mining are still evident on taxa density within PTs, 26 years later.

Heterogeneity diversity indices (q>0) showed a singificantly higher diversity in the REF compared to each of the disturbed DEA areas, in both the replicate-sample and the rarefaction-based analyses (Table 4.2; Fig. 4.9C-F). These results indicate a higher eveness between the abundance of the different taxa populations inhabiting the REF area compared to the DEA, which was lead by the susbtantially higher dominance of ophiuroids in the DEA (35% of DEA standing stock) compared to the REF (23% of REF standing stock), where holothurians were the most dominant group (25% of REF standing stock). Patterns in heterogeneity diversity have so far only been investigated for particular meio and macrofaunal groups in DISCOL revisits, showing variable results. For instance, 7 years after disturbance, heterogeneity diversity of the nematode community was almost invariant across disturbance levels (Vopel and Thiel 2001), while diversity of the of the polychate community was still significantly reduced within PTs (Borowski 2001). A recent study also shows reduced heterogeneity diversity of the scavenging amphipod community within the DEA compared to undisturbed reference sites nearby (Patel et al. 2018). Combined, these results show that reductions of diversity derived from simulated mining disturbance can be long lasting (>20 years) although the detection of such patterns appears to be highly dependent on the faunal size scale (i.e. meio-, macro-, or megafauna) and the parameters used to investigate biodiversity.

Community composition

The main megafaunal community assessment performed to date between DISCOL study areas (Bluhm 2001) yields rather inconclusive results, possibly owing to the absence of true replicates, and to the inclusion of natural variations as an inherent co-factor by comparing samples collected over multiple time intervals from different locations. In contrast, our analysis of taxa compositions showed three clearly distinct assemblages (Fig. 4.7) matching the observed differences in functional structure between the areas studied (Figs. 4.6). The within PTs assemblage showed a lower abundance of suspension feeder taxa, while both deposit feeder and predator & scavenger taxa abundances were reduced in the REF compared to the assemblages inhabiting the DEA. Previous DISCOL community assessments showed generally a small response to disturbance in smaller faunal size groups. Higher macrofauna taxa, polychaetes, and nematode species showed no major differences in composition between areas within and outside PTs, both 7 years after disturbance (Borowski 2001, Vopel and Thiel 2001), and 26 years after (Stratmann et al. 2018b), while only harpacticoid copepod communities continuously differed between areas (Ahnert and Schriever 2001). Consequently, our results suggest that: i) the megafaunal community may be more sensitive than other size classes to the environmental variations generated by simulated mining impacts, ii) despite the close proximity of source populations (i.e. outside PTs), repopulation of areas within PT by some taxa (i.e. suspension feeders) remains limited by the lack of nodule resource, and iii) changes in the megafaunal habitat resulting from simulated mining appear to be long lasting, and could persist over indefinite timescales within PT areas (Gollner et al. 2017) unless hard-substratum resources can be somehow restored.

Assessment of commercial nodule mining disturbances

Ecological assessments of the effects of simulated nodule mining disturbance on the megabenthos performed at the CCZ (Radziejewska and Stoyanova 2000, Vanreusel et al. 2016) have yielded similar results to those obtained at the Peru Basin (Bluhm et al. 1995, Bluhm 2001, this Chapter). Suspension feeders, particularly anthozoans, consistently showed the highest sensitivity to impacts, exhibiting substantial reductions in standing stock both at the short and long terms after disturbance (Jones et al. 2017), with the subsequent alteration of the functional structure of megafaunal communities. However, all these studies simulate but not mimic the full spectra of disturbances (i.e. sediment compaction, surface sediment layer removal) expected from commercial mining exploitation, nor the actual spatial scales of disturbance, which are expected to be much larger (Gollner et al. 2017, Kuhn et al. 2017). Moreover, different baseline assessments have shown that the relative proportion of suspension feeders in some CCZ areas, where mining may actually occur, is generally much higher than at the Peru Basin (Vanreusel et al. 2016, Tilot et al. 2018), with nodule-dwelling anthozoans often dominating the megabenthic community (Amon et al. 2016, Chapter 1). Impacts derived from commercial mining at the CCZ may hence have the potential to generate much stronger alterations of the megabenthic functional and taxonomic structure within collector-vehicle tracks than observed at the Peru Basin, with the correspondent losses of ecosystem functions and processes (Thurber et al. 2014). Moreover, we still do not understand the precise effect of sediment re-deposition beyond disturbed tracks at the long term, which, as shown in this study, may have a certain influence on the development of dominant anthozoan taxa. Hence, we still lack the information necessary to understand how cumulative mining disturbances may affect nodule-fields at the regional scale.

4.6. Supplementary Material: Chapter 4

4.6.1. SM1: Additional exploration of Hill's diversity rarefaction

Methods

We applied a rarefaction approach based on the range of Hill numbers (Chao et al. 2014) to explore variations in diversity indices as a function of either the individuals or the seabed area encompassed by increasing cell units sampling, within each separate disturbance level. Faunal data (in cells) of each separate disturbance level was randomly resampled 1000 times, with (for Exp H' and 1/D analysis) or without (for S analysis) replacement, into new sampling unit sets of increasing cell number size. The mean and the confidence intervals (95%) of each parameter were calculated at each sample unit size increase, together with the mean number of individuals represented by the cells composing each subset. Rarefaction curves were fitted using the analytical method proposed by Colwell et al. (2012), using Estimate S v.9.1 software (Colwell 2013), while Exp *H´* and 1/D curves were computed using a custom R script implementing multiple functions of the 'vegan' package.

Results

Morphospecies accumulation curves showed no significant variations in taxa richness between disturbance levels in sample sizes up to 1000 individuals (Fig. 4.9B). However, accumulation curves showed significant variations in taxa richness between level-A and level-C (no overlap in confidence intervals, in sample-unit sizes > 6000 m^2 of seafloor).

Exp *H´* diversity was significantly higher in level-D than in the other levels (no overlap in confidence intervals, in sample sizes > 550 individuals), and Exp *H´* ordered as: level-D > levels C-B > level-A (Fig. 4.9D). 1/D diversity in level-D was also significantly higher than in all the other levels (no overlap in confidence intervals, in sample sizes > 350 individuals) and 1/D ordered as: level-D >> level-C > level B-A (Fig. 4.9F).

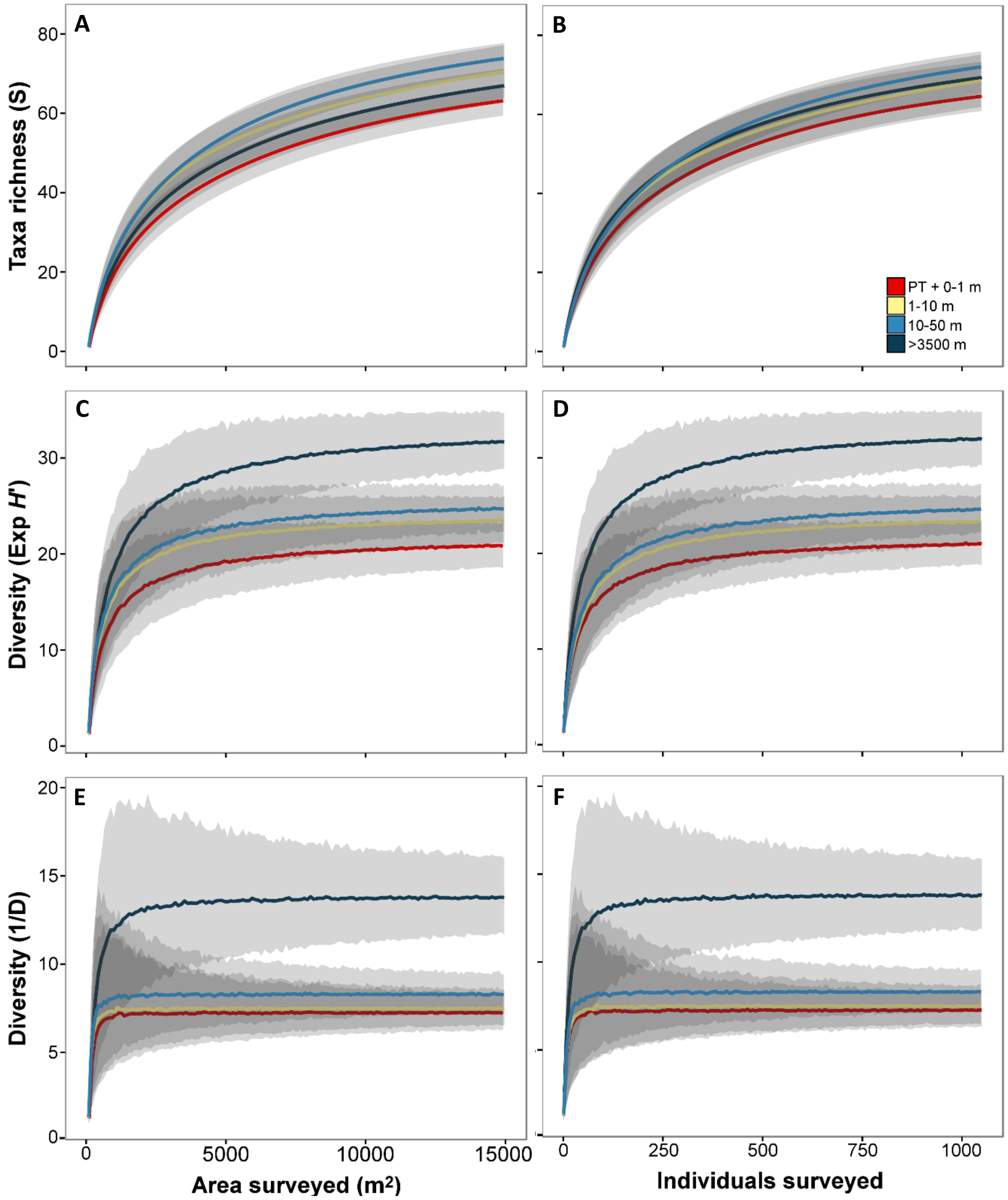

Fig. 4.9. Variation of faunal diversity indices as a function of either the seafloor area or the individuals surveyed in each of the disturbance levels studied. Lines represent mean values along the 1000 randomisations performed at each sample size level, for each disturbance level (see methods). Shadowing represents 95% confidence intervals. **(A-B)** Rarefied morphospecies accumulation curves. **(C-D)** Variation in Exp *H’* diversity. **(E-F)** Variation in 1/D diversity.

5. Chapter 5: Conclusions

5.1. Key ecological findings

The following sections summarise the main research findings presented in Chapters 2 to 4 in the context of the research questions outlined in section 1.2.1.

5.1.1. Q1- Are there differences in the megafaunal ecology between landscape types in polymetallic nodule fields?

Yes. Broad-scale (tens of kilometres) geomorphological variations emerged as a strong driver of megafaunal distribution at the polymetallic nodule fields of the APEI6. Standing stocks were substantially reduced in the Trough, which appeared to generate a reduced heterogeneity diversity and a significantly different assemblage composition in this landscape type. In turn, despite the assemblages of Flat and Ridge were more similar, the Ridge hosted a significantly larger abundance of deposit feeder fauna than the other areas, and also a substantially higher density of xenophyophore tests. Patterns described in Chapter 2 somewhat concur with previously reported differences between abyssal hills and adjacent plains in North Atlantic megafauna (Durden et al. 2015, Stefanoudis et al. 2016), and in fish populations at the CCZ (Leitner et al. 2017). Yet the findings of Chapter 2 add a level of abyssal landscape heterogeneity (troughs), where megafauna showed the clearest variations. These results may significantly alter our perception of global habitat heterogeneity in the high seas, provided that the horst and graben structure studied typically shapes the seafloor of abyssal basins (Harris et al 2014).

5.1.2. Q2- How sensitive are different ecological parameters to the size of the sampling-unit? How large has to be a sample to reliably characterise CCZ megabenthic assemblages?

Narrowing of the precision range and stabilisation of mean values with increasing sample unit size was apparent in all the ecological parameters investigated, as was expected from previous image-based assessments (Durden et al. 2016c), and is commonplace in ecological sampling (Soetaert and Heip 1990, Forcino et al. 2015). However, the estimation of megafaunal density and higher Hill value diversity measures (q>0) were less sensitive to sample size (i.e. mean values and variability levels stabilized at smaller sample-unit sizes), while estimation of taxa richness, biovolume density or community dissimilarity showed higher dependency on the size of the sample-unit. Taxa richness was the parameter that showed a higher sensitivity to sample size, which is also usual in ecological sampling (Chao et al. 2014). As more individuals are sampled, more taxa will be recorded (Bunge and Fitzpatrick 1993), hence stabilisation of richness estimation can be considered to begin at the sampling level where the slope of a taxa rarefaction curve becomes relatively constant (Gotelli and Colwell 2001). Stabilization of richness estimation required sample-unit sizes >500 individuals (seafloor area: 1000-1500 m^2). At this sample-unit size, estimated means of all other parameters investigated were already stable, suggesting that reliable characterisation of the megabenthos required samples containing at least 500 individuals.

Note that the concept of reliability in the characterisation of a community is also relative to the nature and capacity of the sampling approach used, in this case seafloor imagery, and hence Chapter 2 and 4 calculations should not be taken as universal recommendations for megafaunal assessment. The results are dependent on the fauna encountered and the methods used for image acquisition, like the vehicle survey altitude and image resolution. These ultimately determine the minimum organism size that can be included in the analysis, and with this, the number of individuals encompassed in the samples collected. For instance, in this thesis, the higher resolution and closer seabed proximity of the images collected at the APEI6 enabled the reliable detection of smaller sized (> 1 cm) organisms than possible (>5 cm) with the images collected at Peru Basin, yielding total metazoan sample sizes of 7837 (in 18,000 m^2) and 7284 (in 110,000 m^2), respectively. As shown, both datasets enabled the empirical estimation and comparison of biological parameters (Chapter 2, Chapter 4: SM), but a much larger seabed area coverage was required in Chapter 4 to yield the accuracy and precision rates obtained in Chapters 2 and 3. Moreover, the comparison of estimations of taxa density (fixed seabed area samples) and taxa richness (fixed individual size samples) performed in Chapter 3 showed that the use of fixed-area samples can affect the estimation of richness in areas with lower faunal density. These results suggests that individuals rather than areal coverage may be more appropriate sampling targets in in image-based assessments of abyssal communities, particularly given the low density of megafauna at the CCZ, and the possibility of using stratified random designs to maximise the spatial coverage of sampling (i.e. Chapter 2).

5.1.3. Q3- Does the occurrence of nodule resource affect the ecology of megafauna across polymetallic nodule fields?

Yes. Fine-scale (tens of meters) variations in nodule cover emerged as a strong driver of megafaunal distribution at the polymetallic nodule fields of the APEI6. Megafaunal responses were generally graded with nodule cover, although in many aspects the magnitude of change was particularly marked with a very modest initial increase in nodule cover (from 1 to 3%). Along this initial nodule increase, metazoan and xenophyophore standing stocks doubled, heterogeneity diversity increased significantly, and assemblage composition dissimilarity showed the rates of change. These findings concur with Amon et al. (2016) that nodule cover does not need to be high to promote higher megafauna diversity (although not necessarily richness), and with Vanreusel et al. (2016) that changes in the numerical abundance of suspension feeder taxa appears to lead (most) of this variation. However, faunal composition varied between low, mid and high nodule covered areas suggesting a potential diversification of habitats along the nodule gradient beyond the simple presence or absence of a minimum nodule resource. The mosaic habitat generated by the interface between nodules and the sedimentary background may not hence support a single biotope, nor indeed two biotopes, but a progressive habitat change.

5.1.4. Q4- Which aspects of the megabenthos in polymetallic nodule fields show a higher response to geomorphological variations? And in turn, which aspects show a higher response to nodule occurrence variations?

Geomorphology was possibly a stronger control on the overall megabenthic carrying capacity, while nodule occurrence appeared to be more important in the regulation of diversity and community composition. Functional structuring appeared to be mainly regulated by nodule availability, i.e. resource limitation in suspension feeder fauna (i.e. Chapter 3 and 4), yet geomorphology also showed a certain influence on the deposit feeder abundance (i.e. Chapter 2). However, the complex interaction between these two factors and others typically influencing biological diversity in the deep-sea (i.e. bottom water speeds, sedimentary regimes) may be key to understand the local patterns of distribution of megabenthic assemblages at the CCZ, and is hence further addressed in section 5.2.1.

5.1.5. Q5- Is there preliminary numerical evidence to hypothesise about a potential role of xenophyophore test occurrence in the structuring of metazoan megafauna assemblages?

Yes, but further investigations (i.e. see future work) will be required to develop more concise hypothesis in this regard. Xenophyophore test density was positively correlated with deposit feeder abundance (i.e. particularly ophiuroids) across landscape type replicate samples (chapter 2), and with metazoan heterogeneity diversity across the nodule gradient of each split landscape type (Chapter 3; non-included additional partial correlation analysis: $r_s=0.41$, $p < 0.05$, $n=3x9$). Xenophyophore tests can act as refuge or nursery habitat for juvenile or mobile metazoans (Levin et al. 1986), which has shown to increase macro and meiofaunal diversity (Levin 1991, Gooday et al. 2017). Hence, it is possible that xenophyophore tests provide an additional level of structural complexity, promoting taxa coexistence also for the megafauna, which may explain the generally higher heterogeneity diversity observed in the Ridge compared to the Trough in areas with low nodule cover (<3.5%) (Chapter 3: SM). For instance, xenophyophore tests that stand erect above the sediment surface may promote the deposition of organic-rich particles (Levin and Gooday 1992), which explains the common occurrence of ophiuroids near the base of these structures (Levin and Thomas 1988a). However, links between metazoan megafaunal diversity and xenophyophore test occurrence may be best drawn with caution since very little is known about the association between other metazoans (i.e. non ophiuroids) and xenophyophore tests at the megafaunal level. The extremely high xenophyophore density of the CCZ seafloor possibly makes this region one of the best areas of the world to perform such studies.

5.1.6. Q6- Are the effects of simulated mining impacts evident in the spatial distribution of megafauna within the DISCOL site, 26 years after disturbance?

Yes. Differences in the megafaunal ecology between areas with different levels of induced disturbance manifested as changes in standing stock, functional structure, diversity, and community composition. The suspension-feeder abundance in directly disturbed areas (i.e. within disturber tracks) was substantially lower than elsewhere within the DISCOL site. Chapter 2 and 3 provide clear evidence that a large majority of the suspension feeder taxa living in polymetallic nodule fields (~80%) commonly develop attached to nodules, as other studies previously suggested (Amon et al. 2016, Vanreusel et al. 2016). Hence, burial of nodules during the disturbance experiment appears to have generated a loss of habitat for suspension feeder taxa, with the consequent potential loss of any ecosystem functions and processes provided by this group. In turn, abundance of deposit feeder and predator & scavenger fauna was almost invariant within and outside disturbed tracks, suggesting no long-lasting effects of simulated disturbance in the distribution of these groups. These results were supported by an independent analysis of megafaunal carbon stocks within and outside disturbed tracks, also developed with data collected 26 years after disturbance (Stratmann et al. 2018a). Given that nodules reform at rates of mm per million year, it appears that unless restoration actions can be put in place (Cuvelier et al. 2018), impacts derived from simulated mining in directly disturbed areas are likely to persist over geological timescales.

5.1.7. Q7- How do the current megafaunal distribution patterns compare to those observed in previous DISCOL revisits?

A number of factors complicate the comparison of the results obtained in Chapter 4 with those of prior DISCOL studies: limited or no replication, methodological variations, and some variation in the selection or use of 'reference' areas. The closest match is the comprehensive assessment of megafauna provided by Bluhm (2001) that covers the time-period immediately pre-disturbance to 7-years post disturbance.

Bluhm's study showed that megafaunal density was dramatically reduced in directly impacted tracks at the DISCOL site immediately after disturbance, and remained substantially reduced 7 years after. Density recovery within directly disturbed areas after 7 years was only ~ 9% for sessile taxa and ~50% for the mobile compared to pre-disturbance levels. In turn, in areas outside disturbed tracks (i.e. impacted only by sediment re-deposition) the megafaunal standing stock was re-established 7 years after disturbance (Bluhm 2001). However, it remains unclear whether that could be considered a recovery from disturbance, since densities in this area increased above pre-disturbance rates, and clear evidence was found that natural variations had influenced the DISCOL benthos during the 7-year period that the area was monitored, and (Ahnert and Schriever 2001, Bluhm 2001, Borowski 2001).

Direct comparison between Chapter 4 results (i.e. density of particular faunal groups) and those from previous DISCOL revisits is not possible, owing to the different methodology applied for image data collection (i.e. different operating altitude). However, relative comparison of patterns across areas with different levels of induced disturbance showed that: i) anthozoans and sponges remain virtually absent in directly disturbed areas compared to areas outside these, ii) anthozoans are still the only group that shows a lower density in areas affected by sediment re-deposition than in the reference site, iii) ophiuroids, crustaceans, and holothurians showed no diminished presence in disturbed areas, the first time this has been shown since the experiment began, yet iv) the density of ophiuroids in the reference area was substantially lower than in disturbed areas, while these were relatively similar 7 years after disturbance. These results suggest a relatively fast re-establishment of deposit feeder and predator & scavenger standing stocks (i.e. mobile taxa) after simulated mining disturbance, and still no sign of “recovery” in suspension feeder standing stocks (i.e. sessile taxa) since the last time DISCOL was visited.

Figure 5.1 summarises Bluhm’s multivariate analyses with those obtained in Chapter 4. Subjective assessment of the earlier work suggests a clear distinction of plough tracks, but no distinction of resedimented areas from reference conditions (Fig. 5.1A-B). In contrast, the present study suggests a clear distinction of plough tracks, resedimented, and reference areas (Fig. 5.1C). Further investigations (i.e. see future work) will be required to gain insight on the real effects of sediment plume re-deposition.

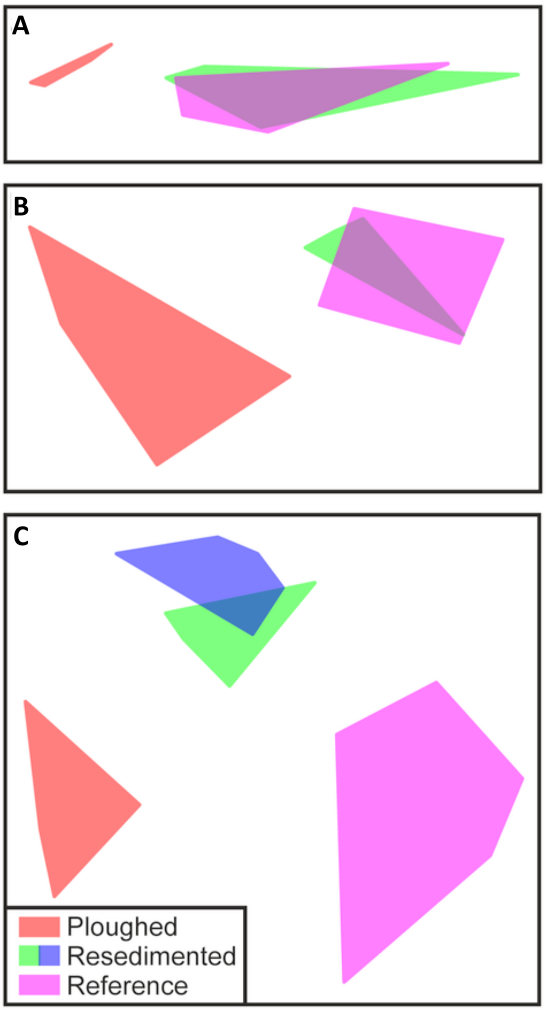

Figure 5.1. Comparison of assessments of variations in megafaunal composition with disturbance type in DISCOL studies. A) Bluhm 24 euclidean dissimilarity, no faunal density transformation. **B)** Bluhm 24 cosine dissimilarity, no faunal density transformation. **C)** Present study (Chapter 4) Bray-Curtis dissimilarity, square-root transformation of faunal density. Note that present study recognises two classes of resedimented area (disturbance levels B and C).

5.2. Implications

This study has provided novel insights about the patterns of distribution and the structuring of megabenthic communities in polymetallic nodule fields, enabling a deeper understanding of the effects of disturbance on these ecosystems, and providing the basis for further exploration of ecological pattern in both pristine and disturbed sites. Together, these findings contribute to the appropriate management of potential mining activities in the CCZ and elsewhere in the deep ocean. This section addresses the implications of the results obtained and draws a series of subsequent recommendations for regulators and other stakeholders in the field of deep-sea nodule mining.

5.2.1. Megabenthic ecological aspects of relevance to deep-sea nodule mining

Environmental drivers of community variation

Benthic carrying capacity at the CCZ has been suggested to be regionally controlled by a gradient of POC-flux to the seafloor (Veillette et al. 2007b, Smith et al. 2008b), increasing towards the more productive surface waters of the north-east (Pennington et al. 2006, Lutz et al. 2007). For instance, with a similar image collection protocol (i.e. same device altitude above seabed), Amon et al. (2016) reported a larger metazoan megafauna density (0.83 ind m^{-2}) within the UK1 site than at the APEI6 (0.46 ind m^{-2}). However, density variations at the local scale, i.e. within the APEI6 (range: 0.22 – 0.56 ind m^{-2}), were of comparable magnitude to those observed at the regional scale (e.g. APEI6 vs UK-1). The results of this thesis suggest that polymetallic nodule field habitats may be much more complex environments than was previously thought. Landscape-scale variations in environmental and ecological characteristics (Chapter 2, Chapter 3) add an additional layer of heterogeneity that can be expected to operate at the physical scale of individual conservation areas (APEI) and potential mining operation areas.

Geomorphological variations at the local scale can modulate bottom water speeds and particle deposition rates at the CCZ (Skornyakova and Murdmaa 1992, Peukert et al. 2018), which are factors that besides possibly controlling nodule occurrence and growth (Mewes et al. 2014), are also known to commonly regulate local community structure in the deep-sea (Thistle et al. 1985, Smith et al. 1986, Jones et al. 2013). Variations in megabenthic standing stock at the APEI6 (i.e. lower density in the Trough) suggest a spatially variable food resource distribution possibly resulting from a different hydrological regime between landscape types, as has commonly been observed in Pacific seamounts (Levin and Thomas 1988b, Lundsten et al. 2009) and in Atlantic abyssal plains (Durden et al. 2015, Morris et al. 2016). Topographically-induced currents can increase the horizontal transport of food favouring suspension feeders, which may explain the higher densities of these fauna at the Ridge and Flat landscapes of the APEI6. In turn, over millions of years, such enhanced currents may have also generated the larger nodule size and abundance observed in these landscape types (Mewes et al. 2014, Peukert et al. 2018). Hence, local populations of suspension feeders may have gradually adapted to develop in areas with higher nodule occurrence, as these provide a suitable anchoring and are commonly found where water flows are stronger. As Vanreusel et al. (2016) point out, factors promoting higher densities of economically viable nodules also enhance the development of suspension feeders, which are the most numerically dominant group in many areas of the CCZ (Amon et al. 2016, Vanreusel et al. 2016, Tilot et al. 2018), and may have hence a paramount value from a conservational perspective.

Functional composition of the megabenthos of polymetallic nodule fields appears to be clearly driven by the occurrence of nodule resource. This study provides two clear examples that where the hard substratum provided by nodules is either naturally absent (Chapter 3) or has been artificially removed (Chapter 4) the suspension feeder population is clearly reduced, as previous research already suggested (Radziejewska and Stoyanova 2000, Bluhm 2001, Amon et al. 2016, Vanreusel et al. 2016). Hard substratum may be initially limiting (i.e. where nodule occurrence is low), but food resource (i.e. advecting organic particles) may become limiting as attached suspension feeder density increases (Jeffreys et al. 2009). On the other hand, changes in deposit feeder density may be related to variations in the food delivery mechanism possibly resulting from geomorphological variations (Chapter 2). For instance, water circulation over the more rugged seafloor of the Ridge (i.e. high BPI and TRI) in the APEi6 may generate patch accumulations of nutrient-rich particles (Lampitt 1985, Smith et al. 1996), which may explain the higher abundance of mobile echinoderms within this landscape type (Chapter 2). These results suggest that both broad-scale geomorphological variations and fine-scale nodule occurrence variations may play a role in the regulation of ecosystem functions and processes at the landscape scale.

The hard substratum provided by nodules combined with the background soft sediment seabed acts to increase habitat complexity for benthic communities in polymetallic nodule fields (Mullineaux 1987, Gooday et al. 2015, Amon et al. 2016). However, different components of megafaunal diversity show a different sensitivity to nodule occurrence variations. Taxa richness appears to be rather insensitive to varying nodule availability, while diversity indices that contemplate evenness between taxa abundances, such as taxa density or Simpson's diversity exhibited an evident response to nodule occurrence variation. The almost invariable taxa richness found across the nodule cover gradient of the APEI6 seafloor was initially surprising: a reduction of richness in nodule-free areas was expected (Amon et al. 2016, Vanreusel et al. 2016) given the high rates of nodule-dwelling taxa observed at the APEI6 (Chapter 2). However, the occurrence of small patches with few small nodules is common even in the most sediment-dominated areas of nodule fields (Gazis et al. 2018, Peukert et al. 2018), and with these, the eventual presence of nodule-dwelling taxa. Although this suggests that small isolated nodule patches in sediment-dominated areas may be important to maintain a relatively homogeneous megafauna species pool at the landscape level (i.e. Chapter 2 and Chapter 3), the small abundance and size of these nodules does not appear to provide a suitable habitat for the generation of dense aggregations of nodule-dwelling populations, leading to the observed reductions in heterogeneity diversity in the least nodule covered areas.

This study shows that megafaunal composition in polymetallic nodule fields varies describing step changes across a nodule occurrence gradient (Chapter 3), which explains the differences in composition observed between different landscape types at the APEI6 (Chapter 2), and those observed between directly and indirectly disturbed areas at the Peru Basin (Chapter 4). The first step on this gradient (from nodule-free to very low nodule cover) appear to be, however, substantially greater than those that follow (Chapter 3). This initial 'jump' is consistent with the change from an overwhelmingly background sedimentary habitat to a mosaic habitat with a varying admixture of nodule hard substrata to that sediment background. Variations in hard-substratum availability typically regulate the changes in faunal composition in the deep-sea (Van Dover et al. 1988, Baker et al. 2012, Jones et al. 2013), while at the CCZ, these had shown to affect meio-, and macrofaunal community composition (Mullineaux 1987, Veillette et al. 2007b). The sharp definition of the first step of change observed in Chapter 3 numerically supports that even subtle increases in nodule occurrence can drive substantial variations in CCZ megafaunal communities (Amon et al. 2016). Yet the following, rather continuous variations, suggest a potential diversification of habitats along the nodule gradient beyond the simple presence or absence of a minimum nodule resource level.

Habitat variation across polymetallic nodule fields is possibly promoted by environmental drivers potentially co-varying along the nodule occurrence gradient. For instance, nodule size was positively correlated with nodule occurrence at the APEI6 (Chapter 3); comparably larger nodule sizes are commonly found in areas with relatively stronger bottom-current speeds (Skornyakova and Murdmaa 1992, Mewes et al. 2014). Beyond the initial environmental filter inherent in the presence-absence of nodule substratum, development of particular deep-sea suspension feeder assemblages can be regulated by the strength of bottom current speeds (Thistle et al. 1985, Smith and Demopoulos 2003), and also by the size of the available anchoring structures (Meyer et al. 2016), especially in soft corals (Watanabe et al. 2009). Areas with larger and hence potentially more physically stable nodules possibly provide a more suitable long-term anchoring point for bamboo coral taxa, enabling their greater final colony height compared to, for example, primnoid soft corals (Lapointe and Watling 2015, Cairns 2016), as observed in Chapter 3. The step changes in taxonomic composition along the nodule occurrence gradient suggest that successful conservation actions at the CCZ will likely require the preservation of areas comprising areas with low, mid, and high nodule cover and not just the lowest covered areas that are least attractive to mining.

Disturbance-mediated variations

Ecological assessments of the effects of simulated nodule mining on the megabenthos of the Clarion-Clipperton Zone (CCZ; (Radziejewska and Stoyanova 2000, Vanreusel et al. 2016) have yielded similar results to those obtained in the Peru Basin (Bluhm et al. 1995, Bluhm 2001, Chapter 4). Suspension feeders, particularly Anthozoa, consistently showed the highest sensitivity to impacts, exhibiting substantial reductions in standing stock, both in the short- and long-term, after disturbance (Jones et al. 2017). These organisms can provide a major contribution to the total faunal carbon in nodule field food webs (Stratmann et al. 2018a), for instance by capturing nutrient resources laterally transported across the benthic boundary layer, making them available for other organisms (Witte et al. 1997). However, different factors may have led to underestimations of the potential impact of nodule mining operations, particularly in suspension feeding communities. First, nodule mining impact simulations performed to date do not mimic the full range or magnitude of disturbances expected from commercial mining (i.e. sediment compaction, nodule resource and sediment layer removal), nor their likely spatial extent (Kuhn et al. 2017). Second, baseline assessments have shown that the relative proportion of suspension feeders at the CCZ is generally much higher than encountered in the Peru Basin (Vanreusel et al. 2016, Chapter 2). In the CCZ, nodule-attached Anthozoa and Porifera often dominate the megabenthic community (Amon et al. 2016, Chapter 2, Simon-Lledo et al. in prep). Consequently, commercial-scale mining in the CCZ may exert a greater impact on the structure and function of megabenthic assemblages than observed in the DISCOL plough tracks.

It seems clear that we still do not have a good understanding of the impact of sediment redeposition beyond plough tracks. Chapter 4 suggests that even 26-years post-disturbance, the area of redeposition remains ecologically distinct – in standing stock, biological diversity, and faunal composition – from the reference area. Without such knowledge, it will be difficult to gauge the true extent or recovery timescale for the cumulative mining disturbances that may affect nodule-fields at the regional scale. Obtaining that knowledge depends upon selecting and monitoring appropriate control (reference) sites. Indeed that is a weakness of Chapter 4, in that we cannot be entirely certain that the Southern reference area is an entirely appropriate control for the DEA. This lack of representivity of control sites may also be an issue for management and monitoring of commercial mining, which can be addressed, in part, by careful baseline assessment (Jones et al. 2018). Nevertheless, the need for control sites is clear and must form a key criterion for the selection of “Areas of Particular Environmental Importance” (APEIs) in the CCZ (Smith et al. 2008b) and ocean observatory sites more generally (see e.g. the Deep Ocean Observing Strategy, deepoceanobserving.org). Given that, it may ultimately be impossible to establish ‘perfect’ controls of the necessary physical scale, a gradient approach to the assessment of the diffused effects of mining, i.e. similar to what was attempted in Chapter 4, may also be valuable in assessing the impact of sediment plume redeposition.

Previous studies exploring the effect of simulated mining impacts on the megabenthos typically included data collected in multiple periods after and typically one pre-disturbance “baseline” sampling (Bluhm et al. 1995, Radziejewska and Stoyanova 2000). In such analyses, ecological parameters inferred from pre-disturbance data are commonly used as threshold, often as the sole basis, for determining whether a particular aspect has or has not recovered. However, both of these studies were affected by natural variations. For instance, Radziejewska and Stoyanova (2000) found a significant increase in the overall megafaunal standing stock between sampling events resulting from a pulse of freshly deposited phyto-detritus, and Bluhm et al. (1995) found a substantially increased density across all study areas in surveys performed after 3 years of disturbance, which had “vanished” 4 years after (Bluhm 2001). Temporal, even abrupt, changes in organic matter fluxes regulating biotic variables are more common in abyssal environments than was previously thought (Ruhl and Smith 2004, Smith et al. 2008a). Hence, characterisation of pre-disturbance patterns in these areas may increase in reliability if based on data collected over multiple years before disturbance. This would enable a clearer distinction between underlying natural and disturbance-mediated variations during post-disturbance monitoring, and ultimately aid the definition of what represents a severe harm to the ecosystem in each particular target area, which is crucial for the protection of these environments (Levin et al. 2016, Niner et al. 2018).

5.2.2. Recommendations for deep-sea nodule mining research and conservation

This section provides a series of recommendations and best practices for the study and conservation of polymetallic nodule fields, based on the outcomes of the present thesis. As such, these are aimed to improve the robustness of the research and the efficiency of future conservation strategies at the CCZ and other abyssal environments. Recommendations were drawn from, and grouped into, three main areas of interest or value: theoretical (Table 5.1), methodological (Table 5.2), or conservational (Table 5.3).

Table 5.1. Theoretical recommendations for deep-sea nodule mining ecological research.

Recommendation	**Rationale**
Suspension feeding fauna should be primary monitoring targets	Suspension feeders numerically dominate the megabenthos of CCZ polymetallic nodule fields and show a higher sensitivity to environmental variations, either naturally occurring or derived from simulated mining disturbance (Chapters 2 and 3, Chapter 4), than other commonly studied faunal groups (e.g. deposit feeders). These taxa, predominantly sessile cnidarians and sponges, have hence a high ecological value for the exploration of baseline patterns (i.e. pre-mining conditions) and for the future monitoring of disturbed areas (i.e. post-mining conditions).
Explore different components of biological diversity	Abyssal nodule field communities are highly diverse but most taxa show extremely low abundances, while a few numerically dominate. The use of Hill's values provides a robust framework to explore these patterns, as these incorporate a

Table 5.1. (*Continued*)

	variable appreciation of the relative abundances of different taxa in the assessment of diversity. The results of this thesis suggest that taxa richness variations are relatively minor within polymetallic nodule fields (Chapter 2, 3, and 4) when sufficiently large sampling sizes are used. In turn, indices that incorporate the evenness component of diversity varied at fine-scales, particularly across areas with different levels of simulated mining disturbance (Chapter 4). This apparently higher sensitivity to disturbance makes heterogeneity diversity indices more suited, i.e. more informative, for monitoring purposes than simple analysis of taxa richness.
Accurately quantify the true nature, extent, and effects of nodule mining impacts	Understanding the nature of physical and geochemical impacts (e.g. nodule resource removal, resedimentation, solubilisation of metals) is key for interpreting the effects on biological systems. Experimental studies should mimic the full range and magnitude of nodule mining impacts to improve the reliability and usefulness of the results obtained. On the same basis, experimental tests should be conducted in representative areas (e.g. across the CCZ), instead of nearby locations where mining is not prospected (e.g. Peru Basin), since the potentially different baseline ecological conditions in these areas may constrain the interpretability and generalisation of the results obtained.
Integrate natural variability in baseline ecological assessments, disturbance experiments, and EIAs	Naturally occurring temporal variability is frequent in abyssal benthic communities (e.g. Bett et al. 2001, Billett et al. 2010), although very little if anything is known about such processes at the CCZ. Pre-disturbance scenarios derived from a single pre-impact survey should not be used as 'control' in recolonization investigations across time, as such approaches neglect the potential effect of natural variations. Natural variations in such studies have so far only been discussed *a posteriori*, usually when the results of the experiment do not follow the expected patterns (e.g. Bluhm et al. 1995, Radziejewska and Stoyanova 2000). Instead, natural variations should be considered *a priori*, in the early survey planning. Assessments aimed to characterise pre-mining biological and ecological features should be based on multiple surveys collected across time (i.e. periods of 1-2 years, during 5-10 years). This would enable the quantification of natural variation ranges (i.e. generate error margins), leading to the possibility to robustly detect impact-driven variations.

Table 5.2. Methodological recommendations for deep-sea nodule mining data collection.

Large volumes of data are required for fine-scale detection of variations	The results of this thesis show that precise detection of biological variations in abyssal nodule field areas requires the analysis of large volumes of data. Autonomous sampling approaches can collect such volumes of data, using reduced ship-time. For instance, all the biological investigations performed in this thesis resulted from a total of 5 AUV deployments, e.g. Chapters 2 and 3: three AUV surveys; Chapter 4: two AUV surveys. However, image analysis are extremely time-consuming, particularly the detection and taxonomical classification of fauna from images (e.g. in order: generation of taxa catalogues, 3-5 min per picture analysed, quality-control of identification consistency, etc.). Careful consideration of the study aims, the subsequent survey design, and the minimum sampling effort needed for robust assessment are essential to optimise AUV sampling approaches.
Image sampling should be conducted upon hypothesis-driven predefined survey designs	Statistically robust designs, such as stratified random sampling, should be used when possible to ensure that truly independent samples are collected for analysis. These also maximise the areal coverage of the survey, optimising sampling effort. Precise detection of biological variations using environmentally stratified sampling designs can be achieved using a minimum of four replicates per category or treatment (e.g. Chapter 2). In these, operator bias should be minimised by conducting objective standardization protocols throughout the collection and analysis of image data (e.g. see following recommendations).
Sufficiently large sample unit sizes should be obtained, and empirically supported	Faunal densities are low in abyssal nodule fields. Therefore, it is important that sufficiently large areas of seafloor are surveyed, to encounter enough organisms, to enable a precise estimation of biological parameters and associated error margins. For instance, the sampling unit size used in Chapter 2 (c. 1320 m^2 of seafloor) appeared to be sufficiently large for reliable estimation of faunal density, heterogeneity diversity measures, and community dissimilarity, but was potentially below ideal for the assessment of taxon richness and biovolume. Evaluation of sample unit size performed in both Chapters 2 and 4, despite using datasets with different faunal density (e.g. APEI6: fauna > 1 cm; DISCOL: fauna > 5 cm, respectively), suggested a similar minimum sample size > 500 individuals to be necessary to cover the full range of biological parameters considered, up to taxa richness. The effect of sample unit size in such analyses is hence best considered in

Table 5.2. (*Continued*)

	terms of the individuals encompassed in samples (see below), rather than by the area surveyed. Studies that demonstrate adequate levels of sampling to support their conclusions are key in ecology, not least those concerned with the regulation of mining activities. Analysis of sampling effort power can aid the generation of appropriate monitoring protocols, urgent in the deep-sea mining context.
Image data should be collected at fixed altitudes < 5m above the seabed	Although also dependant on image quality, altitude of collection ultimately determines our capacity to detect and reliably classify (i.e. taxonomically) the fauna encountered in image samples. There are no organisms living in abyssal nodule fields that are large enough to justify the collection of images at altitudes > 5 m. For instance, 85% of the organisms identified at the APEI6 were smaller than 5 cm (Chapters 2, 3), which is a size fraction that was deemed inconsistently sampled (i.e. low taxonomical resolution) in the image data collected at the Peru Basin (Chapter 4), owing to the higher altitude of collection. Lower survey altitudes, optimally 2-4 m, capture smaller and hence more fauna per unit of area sampled (e.g. see below), which ultimately increases the precision of the subsequent parameter estimation.
The smallest organism size for homogenous detection should be considered, in any image-based assessment	Logistical constrains usually difficult the acquisition of imagery at low and/or constant altitudes above to the seabed. Thus, objective photogrammetric analysis of the minimum organism size for reliable detection, and taxonomical identification, should be conducted prior to the start of quantitative analyses, to standardize the data obtained from different image samplings. Fauna detectability assessments (e.g. section 1.1.5) provide an objective basis to minimise operator bias. Such standardizations can be implemented either by limiting the use of certain images (i.e. exclude images taken above a certain altitude) or limiting the use of the smallest organism sizes (i.e. exclude faunal sizes that cannot be detected throughout all the images collected).
Applicability of resampling techniques should be considered in image assessments	The nature of image datasets, i.e. can be subdivided in image-data units, makes these particularly well suited for the implementation of data resampling and randomisation techniques. These can be useful to test statistical hypotheses, and/or create confidence intervals, for instance in the evaluation of minimum sample unit size (Chapter 2), or to explore variations using sampling designs in which true replication is constrained (e.g. Chapter 3). These

Table 5.2. (*Continued*)

	methodologies can be readily implemented nowadays using open source statistical programing software (i.e. R, Python).
Seabed photo-mosaics enable fine-scale mapping of physical disturbance	The photo-mosaic approach used in Chapter 4 allowed a graded assessment of disturbance, not readily possible from prior towed-camera efforts which typically follow long and relatively narrow (i.e. few meter wide) nodule-collector tracks. The methodology and workflow used in Chapter 4 allowed a rapid mapping of disturbance and minimised the potential issues in the spatial alignment of the fauna encountered, since disturbance levels and faunal distributions were obtained from the same georeferenced data source, i.e. full coverage photo-mosaics. Thus the presented photo-mosaic approach may be an effective tool for evaluating megabenthic distribution patterns in disturbed and reference sites prior and after impact in similar investigations to come.

Table 5.3. Recommendations for deep-sea mining regulation and conservation.

Local-scale variations should be considered in conservation management plans	Environmental management plans at the CCZ have so far only contemplated the restriction of mining activities within APEI areas. The rationale that led to the design the APEI network was based on a pre-assumed homogeneity at the local scale within the CCZ, and hence considered only potential biological variations occurring at a regional scales (Smith et al. 2008b). However, the results of this thesis show that abyssal nodule fields exhibit a much higher habitat heterogeneity at the local scale than was previously thought. In other words, habitat complexity operating within-claim scales may have been underappreciated in the environmental management plans drafted so far developed by the ISA. Therefore, thorough review of the functionality of these plans is highly recommended to make these sensitive to the real complexity of nodule fields. This will necessarily require the assessment of ecological variations within-claim scales.
Creation of claim-scale reference zones needs fine-scale environmental mapping	International regulation stipulates the creation of objectively defined impact reference zones (IRZ) and preservation reference zones (PRZ) within claims, to robustly monitor of the effects of deep-sea mining activities (see e.g. Jones et al. 2018). Provided the habitat complexity that may operate within the scale of claim areas (i.e. suggested by the results of this thesis), IRZs and PRZ will need to be designated upon fine-

Table 5.3. (*Continued*)

	scale environmental mapping, not just at random within claims, to ensure that the areas selected exhibit comparable environmental and biological features (see more below). This will necessarily require the previous exploration and sampling of large areas of seabed and the use of statistically robust analytical approaches, as showed in this thesis.
Reference zones need to cover a range of potential habitats	The results of this thesis show that fine-scale variations in nodule cover and broad-scale variations in geomorphology generate local variations nodule field communities. While further work is needed to investigate other potential environmental drivers (i.e. bottom current variations, local POC flux and lateral transport of nutrients, etc.), it seems clear that IRZs and PRZs will need to include, at least, appreciable areas of with variable ranges of nodule cover (i.e. low, mid, and high) and a range of landscape types if they are to effectively by used to address conservational aspects. Given the usual spatial dimensions of flats, ridges and troughs across the CCZ (i.e. tens of km: Olive et al. 2015), reference zones will need to cover large extensions of seabed, e.g. possibly similar to those considered in Chapter 2 (i.e. > 250 km^2, Fig 2.1), to include at least one landscape of each type, and a broad spectrum of nodule occurrence levels.
Preservation actions are to date the most reliable conservation measures	While the effects of sediment redeposition are still to be fully addressed (see future work), it seems clear that the removal of nodules will generate, at least, a permanent loss of habitat for nodule-dwelling fauna (i.e. sessile suspension feeders; Chapter 4), with subsequent loss of the ecosystem functions provided by these. Mitigation actions in this regard are extremely limited, as nodule removal is essential to nodule mining. Since restoration actions proposed to date seem rather unfeasible, i.e. deployment of artificial substrates to enhance faunal colonisation (Cuvelier et al. 2018), the designation of set-aside areas (refuges) is of utmost importance as it appears to be the most comprehensive approach, both for well-known and lesser studied areas. Only the combination of claim-scale and regional-scale research can determine if APEIs are sufficient protection measures, or protection needs to also be granted within claims. While that information is lacking, the precautionary principle, i.e. lack of full scientific certainty should not postpone measures to avoid probable environmental threats (Ardron et al. 2008), will remain the most objective approach to guide regulation.

5.3. Future work

This thesis addresses many aspects of the ecology of polymetallic nodule field habitats, but many other questions were raised during the conduction of this work. These last are summarised in the following section, along with other key ongoing aspects (i.e. raised in other studies) that need further consideration in investigations to come.

Environmental drivers of benthic change at the CCZ

Further research is required to fully understand the role of both geomorphological and nodule occurrence variations in the structuring of megabenthic communities. The generalisation of the results obtained in Chapters 2 and 3 to other CCZ areas has clear limitations. For instance, the analysis performed in Chapter 2 lacks replicates of the landscape types studied. Thus, further sampling in other hills, plains, and troughs will be needed to determine if the patterns observed within the APEI6 are consistent at larger scales. Such studies would provide key information for management, since these horst and graben seafloor features shape most areas of the CCZ seafloor (Macdonald et al. 1996), especially in the centre of this basin (Klitgord and Mammerickx, 1982) where most mining claims are located. On the other hand, the range of nodule cover found in the APEI6 (0–38%) possibly misrepresents those found in central CCZ areas, where a usually higher diagenetic growth appears to have generated larger nodules, leading to higher seabed coverage levels (e.g. up to 70-80%; International Seabed Authority 2010). Further analyses of benthic variations along nodule occurrence gradients need to be conducted in other locations across the CCZ to complement and expand the results obtained at the APEI6, particularly in areas where a wider coverage spectrum can be investigated. Last, consideration should be given to the possible role of bottom current speeds in the structuring of benthic CCZ communities. Recent investigations have shown that even mild topographical variations can influence bottom current speeds in the abyssal Pacific (van Haren 2018), which have been suggested to modulate nodule formation and growth (Mewes et al. 2014). It is hence possible that a substantial part of the ecological patterns described in Chapters 2 and 3 may be partially derived from slight changes in current velocity modulated at broad-scale by the terrain, and generating variations in nodule occurrence at the fine-scale. All of these hypothesis need to be fully investigated to generate useful information to efficiently manage abyssal nodule field areas.

The study and characterisation of CCZ suspension feeders

Sessile suspension feeding megafauna were key throughout most of the investigations conducted in this thesis. These taxa, mostly anemones and soft corals, dominated the CCZ megabenthos (Chapter 2) and showed the clearest responses to naturally occurring environmental variations (Chapter 3,) and anthropogenic disturbance (Chapter 4). However, little if anything is known about their life-habits, reproductive cycles, or their taxonomy in the CCZ (Lapointe and Watling 2015, Dahlgren et al. 2016, Molodtsova and Opresko 2017). Moreover, given the small body sizes of these organisms (i.e. Chapter 3), previous image-based assessments may have consistently underestimated their importance at the CCZ, as many studies performed to date have used minimum organism sizes > 5 cm in diameter (Vanreusel et al. 2016, Tilot et al. 2018). If appropriately investigated, many of the sessile cnidarians surveyed during this work may have the potential to be used as indicator species, i.e. serve as a measure of the environmental conditions that exist in a given location (Hilty and Merenlender 2000), as has been proposed with the small encrusting sponge *Plenaster craigi* (Lim et al. 2017).

Taxonomical/methodological standardization for regional assessments

It is not yet clear if the environmental conditions and faunas in the currently designated APEIs are similar to those of the mining claims and therefore it is not “safe” to assume their functionality. Besides the taxonomic connections stablished with the areas surveyed in Amon et al. (2016) (APEI6-UK1; Jones et al. in prep), comparisons of APEI6 megabenthic features with those in other previously explored CCZ areas are not possible owing to the use of different sampling devices and methodological standards (i.e. definition of megafauna size, camera altitude, sample size applied). This is an ongoing issue in image-based analyses (Durden et al. 2016c). The application of improved imaging systems over time tends to increase fauna detectability, leading to higher reported megafauna densities. Also, the lack of sampling power analyses in most image-based studies may constrain the reliability of their conclusions. This stresses the need for a standardization of megafaunal sampling methodologies, especially across the CCZ, to enable the study of ecological patterns at the regional scale, which are in urgent need to re-assess the functionality of the current APEI system (ISA 2012).

The possible role of xenophyophores in the structuring of the CCZ megabenthos

Xenophyophore tests clearly dominated the megabenthos of the APEI6, as these usually do across the CCZ (Kamenskaya et al. 2013, Amon et al. 2016). Standing stocks of the larger sized fauna decrease dramatically with water depth (Rex et al. 2006) as diminishing food supply appears to prevent growth to larger body sizes (McClain et al. 2005). This hypothesis sustains the large dominance of xenophyophores in abyssal megabenthos. The protoplasm volume (i.e. “true size”) of xenophyophores represents 1–0.01% of their visible test size (Levin and Gooday 1992). Thus, despite we can sample them along with the megafauna (i.e. > 1 cm) in images, these are best considered as a smaller size faunal group. Yet, this still does not explain why these organisms are more abundant and diverse at the CCZ (Gooday et al. 2017) than in other abyssal areas. This exceptionally high density in the abyssal Pacific allows them to play role in the structuring of CCZ macrofaunal communities (Kamenskaya et al. 2015, Gooday et al. 2017), for instance by providing a stable substratum that can function as refuge from predators and or nursey habitat for juvenile mobile metazoans (Levin 1991). This thesis shows that the density distribution of deposit feeder, and predator & scavenger fauna at the APEI6 correlated with that of xenophyophore tests (Chapter 2). Further analysis on the nature of the relationship between metazoan megafauna and xenophyophores at the CCZ should be considered in studies to come, for instance to assess the prospective use of xenophyophore test density data, readily inferred from minor image sampling effort (Chapter 2), as a factor in the study of metazoan distributions, both locally and regionally.

The full impacts of nodule mining

After more than 30 years of research, sufficient information is still lacking to generalise the biological effects to the longer terms, larger scales, and greater disturbance intensities expected to result from full-scale nodule mining activities (Smith et al. 2008c, Jones et al. 2017). Experimental tests performed to date have generally failed to mimic or appropriately assess potentially important impacts derived from real nodule mining, such as soil compaction or sediment redeposition. Recolonization of seafloor communities is usually scale dependent (Smith and Brumsickle 1989). Consequently, recolonization of vast areas of seafloor repeatedly impacted, i.e. by sediment redeposition, may require potentially larger time scales to “recover” than suggested by the small-scale experiments conducted so far (Jones et al. 2017), like the DISCOL experiment (Chapter 4). However, the reluctance of part of the mining industry to provide final prototypes of nodule-collector vehicles has also hampered scientific research. The involvement of industry will be key in future investigations to come. Real nodule mining tests need to be conducted by mining contractors, and these need to be transparently monitored using multi-disciplinary research plans designed upon objectively defined scientific terms. Nodule mining research will remain missing “the big picture” until such investigations can be conducted.

5.4. Concluding remark

Simplistically, a nodule field could be considered as two habitats: (a) the background sedimentary habitat, and (b) the hard substratum environment of the nodules. More realistically, and certainly at the physical scales inhabited by megafauna, the nodule field is likely better considered as a mosaic habitat comprising those two components. The results of this study make clear that the mosaic habitat does not support a single biotope, nor indeed two biotopes; within the limits of the nodule occurrence gradient of a polymetallic nodule field, faunal composition exhibits step-shaped variation. Removal of the hard substratum provided by nodules during mining operations will almost certainly generate a loss of habitat for many taxa, leading to biodiversity losses in these environments. Yet we are still far from being able to numerically evaluate the cumulative impacts of potential mining operations in the CCZ megabenthos, since the full range of impacts derived from seafloor mining are still largely unclear, untested or barely investigated (i.e. soil compaction, sediment plumes). Equally, it is also clear that we do not yet fully understand the drivers of ecological variation within polymetallic nodule fields. Consequently, sustainable management and conservation plans (Levin et al. 2016, Durden et al. 2017), together with the monitoring programmes that support them, must recognise this complexity and uncertainty if they are to be effective.

References

Ahnert, A., and G. Schriever. 2001. Response of abyssal Copepoda Harpacticoida (Crustacea) and other meiobenthos to an artificial disturbance and its bearing on future mining for polymetallic nodules. Deep Sea Research Part II: Topical Studies in Oceanography **48**:3779-3794.

Aleynik, D., M. E. Inall, A. Dale, and A. Vink. 2017. Impact of remotely generated eddies on plume dispersion at abyssal mining sites in the Pacific. Scientific Reports **7**:16959.

Amon, D., A. Ziegler, J. Drazen, A. Grischenko, A. Leitner, D. Lindsay, J. Voight, M. Wicksten, C. Young, and C. Smith. 2017. Megafauna of the UKSRL exploration contract area and eastern Clarion-Clipperton Zone in the Pacific Ocean: Annelida, Arthropoda, Bryozoa, Chordata, Ctenophora, Mollusca. Biodiversity Data Journal **5**:e14598.

Amon, D. J., A. F. Ziegler, T. G. Dahlgren, A. G. Glover, A. Goineau, A. J. Gooday, H. Wiklund, and C. R. Smith. 2016. Insights into the abundance and diversity of abyssal megafauna in a polymetallic-nodule region in the eastern Clarion-Clipperton Zone. Sci Rep **6**:30492.

Amos, A., C. Garside, R. Gerard, S. Levitus, S. Malone, A. Paul, G. Rice, and O. Roels. 1973. Physical, chemical and biological oceanography of a manganese nodule province in the eastern equatorial Pacific Ocean and the impact upon it of deep-sea mining operations. EOS **54**:339.

Amos, A. F. 1975. Deep ocean mining and its effect on the environment. Lamont-Doherty Geological Observatory of Columbia University Yearbook **1975-76**:31-36.

Anderson, M. J. 2001. A new method for non-parametric multivariate analysis of variance. Austral ecology **26**:32-46.

Andrew, N. L., and B. D. Mapstone. 1987. Sampling and the description of spatial pattern in marine ecology. Oceanography and Marine Biology: Annual Review **25**:39-90.

Ardron, J., K. Gjerde, S. Pullen, and V. Tilot. 2008. Marine spatial planning in the high seas. Marine Policy **32**:832-839.

Ayma, A., J. Aguzzi, M. Canals, G. Lastras, N. Bahamon, A. Mecho, and J. B. Company. 2016. Comparison between ROV video and Agassiz trawl methods for sampling deep water fauna of submarine canyons in the Northwestern Mediterranean Sea with observations on behavioural reactions of target species. Deep Sea Research Part I: Oceanographic Research Papers **114**:149-159.

Baddeley, A., P. J. Diggle, A. Hardegen, T. Lawrence, R. K. Milne, and G. Nair. 2014. On tests of spatial pattern based on simulation envelopes. Ecological monographs **84**:477-489.

Baker, K. D., V. E. Wareham, P. V. R. Snelgrove, R. L. Haedrich, D. A. Fifield, E. N. Edinger, and K. D. Gilkinson. 2012. Distributional patterns of deep-sea coral assemblages in three submarine canyons off Newfoundland, Canada. Marine Ecology Progress Series **445**:235-249.

Barckhausen, U., M. Bagge, and D. S. Wilson. 2013. Seafloor spreading anomalies and crustal ages of the Clarion-Clipperton Zone. Marine Geophysical Research **34**:79-88.

Beaulieu, S. E. 2001. Life on glass houses: sponge stalk communities in the deep sea. Marine Biology **138**:803-817.

Bell, J. B., C. H. S. Alt, and D. O. B. Jones. 2016. Benthic megafauna on steep slopes at the Northern Mid-Atlantic Ridge. Marine Ecology **37**:1290-1302.

Bell, T. H. 1975. Topographically generated internal waves in the open ocean. Journal of Geophysical Research **80**:320-327.

Benoist, N. M., B. J. Bett, K. J. Morris, and H. A. Ruhl. submitted. A generalised method to estimate the biomass of photographically surveyed benthic megafauna. Limnology & Oceanography: Methods.

Benoist, N. M. A., K. J. Morris, B. J. Bett, J. M. Durden, V. A. I. Huvenne, T. P. Le Bas, R. B. Wynn, S. J. Ware, and H. A. Ruhl. in press. Monitoring mosaic biotopes in a marine conservation zone by autonomous underwater vehicle. Conservation biology **0**.

Bett, B. J., M. G. Malzone, B. E. Narayanaswamy, and B. D. Wigham. 2001. Temporal variability in phytodetritus and megabenthic activity at the seabed in the deep Northeast Atlantic. Progress in Oceanography **50**:349-368.

Bett, B. J., A. L. Rice, and M. H. Thurston. 1995. A Quantitative Photographic Survey of ‘Spoke-Burrow’ Type Lebensspuren on the Cape Verde Abyssal Plain. Internationale Revue der gesamten Hydrobiologie und Hydrographie **80**:153-170.

Billett, D. S. M., B. J. Bett, W. D. K. Reid, B. Boorman, and I. G. Priede. 2010. Long-term change in the abyssal NE Atlantic: The ‘Amperima Event’ revisited. Deep Sea Research Part II: Topical Studies in Oceanography **57**:1406-1417.

Billett, D. S. M., B. J. Bett, A. L. Rice, M. H. Thurston, J. Galéron, M. Sibuet, and G. A. Wolff. 2001. Long-term change in the megabenthos of the Porcupine Abyssal Plain (NE Atlantic). Progress in Oceanography **50**:325-348.

Billett, D. S. M., R. S. Lampitt, A. L. Rice, and R. F. C. Mantoura. 1983. Seasonal sedimentation of phytoplankton to the deep-sea benthos. Nature **302**:520.

Blott, S. J., and K. Pye. 2001. GRADISTAT: a grain size distribution and statistics package for the analysis of unconsolidated sediments. Earth Surface Processes and Landforms **26**:1237-1248.

Bluhm, H. 2001. Re-establishment of an abyssal megabenthic community after experimental physical disturbance of the seafloor. Deep Sea Research Part II: Topical Studies in Oceanography **48**:3841-3868.

Bluhm, H., and A. Gebruk. 1999. Holothuroidea (Echinodermata) of the Peru Basin - Ecological and Taxonomic Remarks Based on Underwater Images. Marine Ecology **20**:167-195.

Bluhm, H., G. Schriever, and H. Thiel. 1995. Megabenthic recolonization in an experimentally disturbed abyssal manganese nodule area. Marine Georesources & Geotechnology **13**:393-416.

Bo, M., S. Bava, S. Canese, M. Angiolillo, R. Cattaneo-Vietti, and G. Bavestrello. 2014. Fishing impact on deep Mediterranean rocky habitats as revealed by ROV investigation. Biological Conservation **171**:167-176.

Bodenmann, A., B. Thornton, and T. Ura. 2013. Development of long range color imaging for wide area 3D reconstructions of the seafloor. Pages 1-5 *in* 2013 IEEE International Underwater Technology Symposium (UT).

Borg, I., and P. Groenen. 2003. Modern Multidimensional Scaling: Theory and Applications. Journal of Educational Measurement **40**:277-280.

Borowski, C. 2001. Physically disturbed deep-sea macrofauna in the Peru Basin, southeast Pacific, revisited 7 years after the experimental impact. Deep Sea Research Part II: Topical Studies in Oceanography **48**:3809-3839.

Boschen, R. E., A. A. Rowden, M. R. Clark, S. J. Barton, A. Pallentin, and J. P. A. Gardner. 2015. Megabenthic assemblage structure on three New Zealand seamounts: implications for seafloor massive sulfide mining. Marine Ecology Progress Series **523**:1-14.

Brown, C. J., S. J. Smith, P. Lawton, and J. T. Anderson. 2011. Benthic habitat mapping: A review of progress towards improved understanding of the spatial ecology of the seafloor using acoustic techniques. Estuarine, Coastal and Shelf Science **92**:502-520.

Buckland, S. T., D. R. Anderson, K. P. Burnham, J. L. Laake, D. L. Borchers, and L. Thomas. 2001. Introduction to Distance Sampling: Estimating Abundance of Biological Populations. Oxford University Press, Oxford.

Buckland, S. T., E. A. Rexstad, T. A. Marques, and C. S. Oedekoven. 2015. Designing Surveys. Pages 15-28 Distance Sampling: Methods and Applications. Springer International Publishing, Cham.

Buesseler, K. O., C. H. Lamborg, P. W. Boyd, P. J. Lam, T. W. Trull, R. R. Bidigare, J. K. B. Bishop, K. L. Casciotti, F. Dehairs, M. Elskens, M. Honda, D. M. Karl, D. A. Siegel, M. W. Silver, D. K. Steinberg, J. Valdes, B. Van Mooy, and S. Wilson. 2007. Revisiting Carbon Flux Through the Ocean's Twilight Zone. science **316**:567-570.

Buhl-Mortensen, L., A. Vanreusel, A. J. Gooday, L. A. Levin, I. G. Priede, P. Buhl-Mortensen, H. Gheerardyn, N. J. King, and M. Raes. 2010. Biological structures as a source of habitat heterogeneity and biodiversity on the deep ocean margins. Marine Ecology **31**:21-50.

Bunge, J., and M. Fitzpatrick. 1993. Estimating the Number of Species: A Review. Journal of the American Statistical Association **88**:364-373.

Cairns, S. D. 2016. New abyssal Primnoidae (Anthozoa: Octocorallia) from the Clarion-Clipperton Fracture Zone, equatorial northeastern Pacific. Marine Biodiversity **46**:141-150.

Chao, A., R. K. Colwell, C.-W. Lin, and N. J. Gotelli. 2009. Sufficient sampling for asymptotic minimum species richness estimators. Ecology **90**:1125-1133.

Chao, A., N. J. Gotelli, T. C. Hsieh, E. L. Sander, K. H. Ma, R. K. Colwell, and A. M. Ellison. 2014. Rarefaction and extrapolation with Hill numbers: a framework for sampling and estimation in species diversity studies. Ecological monographs **84**:45-67.

Chung, J. S. 1985. Advances in Manganese Nodule Mining Technology. Journal of the Marine Technology Society **19**:39-44.

Clague, D. A., B. M. Dreyer, J. B. Paduan, J. F. Martin, D. W. Caress, J. B. Gill, D. S. Kelley, H. Thomas, R. A. Portner, J. R. Delaney, T. P. Guilderson, and M. L. McGann. 2014. Eruptive and tectonic history of the Endeavour Segment, Juan de Fuca Ridge, based on AUV mapping data and lava flow ages. Geochemistry, Geophysics, Geosystems **15**:3364-3391.

Clark, J. P., and M. R. Neutra. 1983. Mining manganese nodules: Potential economic and environmental effects. Resources Policy **9**:99-109.

Clark, M. R., A. A. Rowden, T. Schlacher, A. Williams, M. Consalvey, K. I. Stocks, A. D. Rogers, T. D. O'Hara, M. White, T. M. Shank, and J. M. Hall-Spencer. 2010a. The Ecology of Seamounts: Structure, Function, and Human Impacts. Annual Review of Marine Science **2**:253-278.

Clark, M. R., A. A. Rowden, T. Schlacher, A. Williams, M. Consalvey, K. I. Stocks, A. D. Rogers, T. D. O'Hara, M. White, T. M. Shank, and J. M. Hall-Spencer. 2010b. The ecology of seamounts: structure, function, and human impacts. Ann Rev Mar Sci **2**:253-278.

Clarke, K. R. 1990. Comparisons of dominance curves. Journal of Experimental Marine Biology and Ecology **138**:143-157.

Clarke, K. R. 1993. Non-parametric multivariate analyses of changes in community structure. Australian Journal of Ecology **18**:117-143.

Clarke, K. R., and R. N. Gorley. 2015. PRIMER v7: User Manual/Tutorial, PRIMER-E. Plymouth.

Clarke, K. R., P. J. Somerfield, and M. G. Chapman. 2006. On resemblance measures for ecological studies, including taxonomic dissimilarities and a zero-adjusted Bray–Curtis coefficient for denuded assemblages. Journal of Experimental Marine Biology and Ecology **330**:55-80.

Cochran, W. G. 1977. Sampling techniques. John Wiley & Sons.

Colwell, R. 2013. EstimateS: Statistical estimation of species richness and shared species from samples. Version 9. User's Guide and Application published at: http://purloclcorg/estimates.

Colwell, R. K., A. Chao, N. J. Gotelli, S. Y. Lin, C. X. Mao, R. L. Chazdon, and J. T. Longino. 2012. Models and estimators linking individual-based and sample-based rarefaction, extrapolation and comparison of assemblages. Journal of Plant Ecology **5**:3-21.

Conrad, O., B. Bechtel, M. Bock, H. Dietrich, E. Fischer, L. Gerlitz, J. Wehberg, V. Wichmann, and J. Böhner. 2015. System for Automated Geoscientific Analyses (SAGA) v. 2.1.4. Geosci. Model Dev. **8**:1991-2007.

Conti, L. A., A. Lim, and A. J. Wheeler. 2019. High resolution mapping of a cold water coral mound. Scientific Reports **9**:1016.

Cribari-Neto, F., and A. Zeileis. 2010. Beta Regression in R. 2010 **34**:24.

Crowley, P. H. 1992. Resampling Methods for Computation-Intensive Data Analysis in Ecology and Evolution. Annual Review of Ecology and Systematics **23**:405-447.

Cuvelier, D., S. Gollner, D. O. B. Jones, S. Kaiser, P. M. Arbizu, L. Menzel, N. C. Mestre, T. Morato, C. Pham, F. Pradillon, A. Purser, U. Raschka, J. Sarrazin, E. Simon-Lledó, I. M. Stewart, H. Stuckas, A. K. Sweetman, and A. Colaço. 2018. Potential Mitigation and Restoration Actions in Ecosystems Impacted by Seabed Mining. Frontiers in Marine Science **5**.

Dahlgren, T. G., H. Wiklund, M. Rabone, D. J. Amon, C. Ikebe, L. Watling, C. R. Smith, and A. G. Glover. 2016. Abyssal fauna of the UK-1 polymetallic nodule exploration area, Clarion-Clipperton Zone, central Pacific Ocean: Cnidaria. Biodivers Data J:e9277.

Danovaro, R., P. V. Snelgrove, and P. Tyler. 2014. Challenging the paradigms of deep-sea ecology. Trends Ecol Evol **29**:465-475.

Davison, A. C., and D. V. Hinkley. 1997. Bootstrap Methods and their Application. Cambridge University Press, Cambridge.

De Leo, F. C., C. R. Smith, A. A. Rowden, D. A. Bowden, and M. R. Clark. 2010. Submarine canyons: hotspots of benthic biomass and productivity in the deep sea. Proc Biol Sci **277**:2783-2792.

De Smet, B., E. Pape, T. Riehl, P. Bonifácio, L. Colson, and A. Vanreusel. 2017. The Community Structure of Deep-Sea Macrofauna Associated with Polymetallic Nodules in the Eastern Part of the Clarion-Clipperton Fracture Zone. Frontiers in Marine Science **4**.

Deuser, W. G., and E. H. Ross. 1980. Seasonal change in the flux of organic carbon to the deep Sargasso Sea. Nature **283**:364.

Dobson, A. J., and A. G. Barnett. 2008. An Introduction to Generalized Linear Models, Third Edition. Chapman & Hall/CRC Press, Boca Raton, FL.

Dormann, C. F. 2007. Effects of incorporating spatial autocorrelation into the analysis of species distribution data. Global Ecology and Biogeography **16**:129-138.

Dorschel, B., J. Gutt, D. Piepenburg, M. Schröder, and J. E. Arndt. 2014. The influence of the geomorphological and sedimentological settings on the distribution of epibenthic assemblages on a flat topped hill on the over-deepened shelf of the western Weddell Sea (Southern Ocean). Biogeosciences **11**:3797-3817.

Durden, J. M., B. J. Bett, T. Horton, A. Serpell-Stephens, K. J. Morris, and D. S. Billett. 2016a. Improving the estimation of deep-sea megabenthos biomass: dimension to wet weight conversions for abyssal invertebrates. Marine Ecology Progress Series.

Durden, J. M., B. J. Bett, D. O. B. Jones, V. A. I. Huvenne, and H. A. Ruhl. 2015. Abyssal hills – hidden source of increased habitat heterogeneity, benthic megafaunal biomass and diversity in the deep sea. Progress in Oceanography **137**:209-218.

Durden, J. M., B. J. Bett, T. Schoening, K. J. Morris, T. W. Nattkemper, and H. A. Ruhl. 2016b. Comparison of image annotation data generated by multiple investigators for benthic ecology. Marine Ecology Progress Series **552**:61-70.

Durden, J. M., K. Murphy, A. Jaeckel, C. L. Van Dover, S. Christiansen, K. Gjerde, A. Ortega, and D. O. B. Jones. 2017a. A procedural framework for robust environmental management of deep-sea mining projects using a conceptual model. Marine Policy **84**:193-201.

Durden, J. M., T. Schoening, F. Althaus, A. Friedman, R. Garcia, A. G. Glover, J. Greinert, N. Jacobsen Stout, D. O. B. Jones, A. Jordt, J. Kaeli, K. Köser, L. A. Kuhnz, D. Lindsay, K. J. Morris, T. W. Nattkemper, J. Osterloff, H. A. Ruhl, H. Singh, M. Tran, and B. J. Bett. 2016c. Perspectives in visual imaging for marine biology and ecology: from acquisition to understanding. Pages 1-72 *in* R. N. Hughes, D. J. Hughes, I. P. Smith, and A. C. Dale, editors. Oceanography and Marine Biology: An Annual Review, Vol. 54. CRC Press, Boca Raton, FL.

Durden, J. M., E. Simon-Lledo, A. J. Gooday, and D. O. B. Jones. 2017b. Abundance and morphology of Paleodictyon nodosum, observed at the Clarion-Clipperton Zone. Marine Biodiversity **47**:265-269.

Dutilleul, P. 1993. Spatial Heterogeneity and the Design of Ecological Field Experiments. Ecology **74**:1646-1658.

Ebbe, B., D. S. Billett, A. Brandt, K. Ellingsen, A. Glover, S. Keller, M. Malyutina, P. Martínez Arbizu, T. Molodtsova, M. Rex, C. R. Smith, and A. Tselepides. 2010. Diversity of Abyssal Marine Life.*in* A. D. McIntyre, editor. Life in the World's Oceans. Wiley-Blackwell, doi:10.1002/9781444325508.ch8.

Etter, R., and L. Mullineaux. 2001. Deep-sea communities. Marine Community Ecology. Sinauer Associates, Inc., Sunderland:367-393.

Fabri, M. C., A. Bargain, I. Pairaud, L. Pedel, and I. Taupier-Letage. 2017. Cold-water coral ecosystems in Cassidaigne Canyon: An assessment of their environmental living conditions. Deep Sea Research Part II: Topical Studies in Oceanography **137**:436-453.

Ferrari, S., and F. Cribari-Neto. 2004. Beta Regression for Modelling Rates and Proportions. Journal of Applied Statistics **31**:799-815.

Flach, E., and L. Thomsen. 1998. Do physical and chemical factors structure the macrobenthic community at a continental slope in the NE Atlantic? Pages 265-285. Springer Netherlands, Dordrecht.

Foell, E. J., and D. L. Pawson. 1986. Photographs of invertebrate megafauna from abyssal depths of the northeastern equatorial Pacific Ocean. The Ohio Journal of Science **86**:61-68.

Forcino, F. L., L. R. Leighton, P. Twerdy, and J. F. Cahill. 2015. Reexamining Sample Size Requirements for Multivariate, Abundance-Based Community Research: When Resources are Limited, the Research Does Not Have to Be. PLoS One **10**:e0128379.

Fortin, M.-J., and M. R. Dale. 2005. Spatial analysis: a guide for ecologists. Cambridge University Press.

Foster, S. D., G. R. Hosack, N. A. Hill, N. S. Barrett, V. L. Lucieer, and M. Spencer. 2014. Choosing between strategies for designing surveys: autonomous underwater vehicles. Methods in Ecology and Evolution **5**:287-297.

Fox, J., S. Weisberg, D. Adler, D. Bates, G. Baud-Bovy, S. Ellison, D. Firth, M. Friendly, G. Gorjanc, and S. Graves. 2016. car: An R Companion to Applied Regression. R package version 3.2-0. https://CRAN.R-project.org/package=car.

Frazer, J. Z., and M. B. Fisk. 1981. Geological factors related to characteristics of sea-floor manganese nodule deposits. Deep Sea Research Part A. Oceanographic Research Papers **28**:1533-1551.

Freund, R. J., and R. C. Littell. 1981. SAS for linear models: a guide to the ANOVA and GLM procedures. Sas Institute Cary, North Carolina.

Furlong, M. E., D. Paxton, P. Stevenson, M. Pebody, S. D. McPhail, and J. Perrett. 2012. Autosub long range: A long range deep diving AUV for ocean monitoring. Pages 1-7 *in* 2012 IEEE/OES Autonomous Underwater Vehicles (AUV). IEEE.

Gage, J. D., and B. J. Bett. 2005. Deep-sea benthic sampling. Pages 273-325 *in* A. Eleftheriou and A. McIntyre, editors. Methods for the study of marine benthos, 3rd ed. Blackwell Science.

Gage, J. D., and P. A. Tyler. 1992. Deep-sea biology: a natural history of organisms at the deep-sea floor. Cambridge University Press.

Gardner, W., E. P. Mulvey, and E. C. Shaw. 1995. Regression analyses of counts and rates: Poisson, overdispersed Poisson, and negative binomial models. Psychological bulletin **118**:392.

Gazis, I. Z., T. Schoening, E. Alevizos, and J. Greinert. 2018. Quantitative mapping and predictive modelling of Mn-nodules' distribution from hydroacoustic and optical AUV data linked by Random Forests machine learning. Biogeosciences Discuss. **2018**:1-44.

Genin, A., P. K. Dayton, P. F. Lonsdale, and F. N. Spiess. 1986. Corals on seamount peaks provide evidence of current acceleration over deep-sea topography. Nature **322**:59.

Gerdes, K., P. Martínez Arbizu, U. Schwarz-Schampera, M. Schwentner, and T. C. Kihara. 2019. Detailed Mapping of Hydrothermal Vent Fauna: A 3D Reconstruction Approach Based on Video Imagery. Frontiers in Marine Science **6**.

Getis, A. 2008. A History of the Concept of Spatial Autocorrelation: A Geographer's Perspective. Geographical Analysis **40**:297-309.

Gille, S. T., E. J. Metzger, and R. Tokmakian. 2004. Seafloor topography and ocean circulation. Oceanography **17**:https://doi.org/10.5670/oceanog.2004.5666.

Ginger, M. L., D. S. M. Billett, K. L. Mackenzie, K. Konstandinos, R. R. Neto, D. K. Boardman, V. L. C. S. Santos, I. M. Horsfall, and G. A. Wolff. 2001. Organic matter assimilation and selective feeding by holothurians in the deep sea: some observations and comments. Progress in Oceanography **50**:407-421.

Glasby, G., P. Stoffers, A. Sioulas, T. Thijssen, and G. Friedrich. 1982. Manganese nodule formation in the Pacific Ocean: a general theory. Geo-marine letters **2**:47-53.

Glover, A., T. Dahlgren, S. Taboada, G. Paterson, H. Wiklund, A. Waeschenbach, A. Cobley, P. Martínez, S. Kaiser, S. Schnurr, S. Khodami, U. Raschka, D. Kersken, H. Stuckas, L. Menot, P. Bonifacio, A. Vanreusel, L. Macheriotou, M. Cunha, A. Hilário, C. Rodrigues, A. Colaço, P. Ribeiro, M. Błażewicz, A. Gooday, D. Jones, D. Billett, A. Goineau, D. Amon, C. Smith, T. Patel, K. McQuaid, R. Spickermann, and S. Brager. 2016a. The London Workshop on the Biogeography and Connectivity of the Clarion-Clipperton Zone. Research Ideas and Outcomes **2**:e10528.

Glover, A., T. Dahlgren, H. Wiklund, I. Mohrbeck, and C. Smith. 2015. An End-to-End DNA Taxonomy Methodology for Benthic Biodiversity Survey in the Clarion-Clipperton Zone, Central Pacific Abyss. Journal of Marine Science and Engineering **4**:2.

Glover, A. G., C.R.Smith, G. L. J. Paterson, G.D.F.Wilson, L. Hawkins, and M.Sheader. 2002. Polychaete species diversity in the central Pacific abyss: local and regional patterns, and relationships with productivity. Marine Ecology Progress Series **240**:157-170.

Glover, A. G., and C. R. Smith. 2003. The deep-sea floor ecosystem: current status and prospects of anthropogenic change by the year 2025. Environmental Conservation **30**:219-241.

Glover, A. G., H. Wiklund, M. Rabone, D. J. Amon, C. R. Smith, T. O'Hara, C. L. Mah, and T. G. Dahlgren. 2016b. Abyssal fauna of the UK-1 polymetallic nodule exploration claim, Clarion-Clipperton Zone, central Pacific Ocean: Echinodermata. Biodiversity Data Journal:e7251.

Gollner, S., S. Kaiser, L. Menzel, D. O. B. Jones, A. Brown, N. C. Mestre, D. van Oevelen, L. Menot, A. Colaco, M. Canals, D. Cuvelier, J. M. Durden, A. Gebruk, G. A. Egho, M. Haeckel, Y. Marcon, L. Mevenkamp, T. Morato, C. K. Pham, A. Purser, A. Sanchez-Vidal, A. Vanreusel, A. Vink, and P. Martinez Arbizu. 2017. Resilience of benthic deep-sea fauna to mining activities. Marine Environmental Research **129**:76-101.

Gooday, A. J., B. J. Bett, and D. N. Pratt. 1993. Direct observation of episodic growth in an abyssal xenophyophore (Protista). Deep Sea Research Part I: Oceanographic Research Papers **40**:2131-2143.

Gooday, A. J., A. Goineau, and I. Voltski. 2015. Abyssal foraminifera attached to polymetallic nodules from the eastern Clarion Clipperton Fracture Zone: a preliminary description and comparison with North Atlantic dropstone assemblages. Marine Biodiversity **45**:391-412.

Gooday, A. J., M. Holzmann, C. Caulle, A. Goineau, D. O. B. Jones, O. Kamenskaya, E. Simon-Lledó, A. A. T. Weber, and J. Pawlowski. 2018. New species of the xenophyophore genus Aschemonella (Rhizaria: Foraminifera) from areas of the abyssal eastern Pacific licensed for polymetallic nodule exploration. Zoological Journal of the Linnean Society **182**:479-499.

Gooday, A. J., M. Holzmann, C. Caulle, A. Goineau, O. Kamenskaya, A. A. T. Weber, and J. Pawlowski. 2017. Giant protists (xenophyophores, Foraminifera) are exceptionally diverse in parts of the abyssal eastern Pacific licensed for polymetallic nodule exploration. Biological Conservation **207**:106-116.

Gotelli, N. J., and R. K. Colwell. 2001. Quantifying biodiversity: procedures and pitfalls in the measurement and comparison of species richness. Ecology Letters **4**:379-391.

Grasmueck, M., G. P. Eberli, D. A. Viggiano, T. Correa, G. Rathwell, and J. Luo. 2006. Autonomous underwater vehicle (AUV) mapping reveals coral mound distribution, morphology, and oceanography in deep water of the Straits of Florida. Geophysical Research Letters **33**.

Grassle, J. F., and N. J. Maciolek. 1992. Deep-Sea Species Richness: Regional and Local Diversity Estimates from Quantitative Bottom Samples. The American Naturalist **139**:313-341.

Grassle, J. F., H. L. Sanders, R. R. Hessler, G. T. Rowe, and T. McLellan. 1975. Pattern and zonation: a study of the bathyal megafauna using the research submersible Alvin. Deep Sea Research and Oceanographic Abstracts **22**:457-481.

Greinert, J. 2015. RV SONNE Fahrtbericht/cruise report SO242-1 [SO242/1]: JPI OCEANS ecological aspects of deep-sea mining, DISCOL revisited, Guayaquil-Guayaquil (Equador), 28.07.-25.08. 2015. Cruise Report 2193-8113, Kiel, German.

Griffith, D. A., and Y. Chun. 2016. Spatial Autocorrelation and Uncertainty Associated with Remotely-Sensed Data. Remote Sensing **8**:535.

Grupe, B., H. J. Becker, and H. U. Oebius. 2001. Geotechnical and sedimentological investigations of deep-sea sediments from a manganese nodule field of the Peru Basin. Deep Sea Research Part II: Topical Studies in Oceanography **48**:3593-3608.

Hanberry, B. B., S. Fraver, H. S. He, J. Yang, D. C. Dey, and B. J. Palik. 2011. Spatial pattern corrections and sample sizes for forest density estimates of historical tree surveys. Landscape Ecology **26**:59-68.

Hannides, A., and C. Smith. 2003. The northeast abyssal Pacific plain. Pages 208-237 *in* K. D. Black and G. B. Shimmield, editors. Biogeochemistry of Marine Systems. Blackwell, Boca Raton, Florida.

Harada, K., and T. Fukushima. 1997. Results of seabed disturbance experiment and bottom sediment investigation. Pages 133-141 Proceedings of International Symposium on Environmental Studies for Deep-Sea Mining, Tokyo, Japan, November 20-21, 1997.

Harris, P. T., and E. K. Baker. 2012. Seafloor Geomorphology as Benthic Habitat: GeoHab Atlas of seafloor geomorphic features and benthic habitats. Elsevier, London.

Harris, P. T., M. Macmillan-Lawler, J. Rupp, and E. K. Baker. 2014. Geomorphology of the oceans. Marine Geology **352**:4-24.

Heck Jr, K. L., G. van Belle, and D. Simberloff. 1975. Explicit calculation of the rarefaction diversity measurement and the determination of sufficient sample size. Ecology:1459-1461.

Heezen, B. C., and A. Laughton. 1963. Abyssal plains. Pages 312-364 *in* N. M. Hill, editor. The Earth Beneath the Sea History. Interscience Publishers, New York.

Henry, L.-A., J. Vad, H. S. Findlay, J. Murillo, R. Milligan, and J. M. Roberts. 2014. Environmental variability and biodiversity of megabenthos on the Hebrides Terrace Seamount (Northeast Atlantic). Scientific Reports **4**:5589.

Hill, M. O. 1973. Diversity and Evenness: A Unifying Notation and Its Consequences. Ecology **54**:427-432.

Hilty, J., and A. Merenlender. 2000. Faunal indicator taxa selection for monitoring ecosystem health. Biological Conservation **92**:185-197.

Hollister, C. D., and I. N. McCave. 1984. Sedimentation under deep-sea storms. Nature **309**:220.

Hothorn, T., F. Bretz, and P. Westfall. 2008. Simultaneous Inference in General Parametric Models. Biometrical Journal **50**:346-363.

Hothorn, T., F. Bretz, P. Westfall, R. M. Heiberger, A. Schuetzenmeister, S. Scheibe, and M. T. Hothorn. 2017. multcomp: Simultaneous Inference in General Parametric Models. R package version 1.4-8. https://CRAN.R-project.org/package=multcomp.

Howell, K. L., J. S. Davies, and B. E. Narayanaswamy. 2010. Identifying deep-sea megafaunal epibenthic assemblages for use in habitat mapping and marine protected area network design. Journal of the Marine Biological Association of the United Kingdom **90**:33-68.

Hughes, D. J., and J. D. Gage. 2004. Benthic metazoan biomass, community structure and bioturbation at three contrasting deep-water sites on the northwest European continental margin. Progress in Oceanography **63**:29-55.

Hughes, J. A., and A. J. Gooday. 2004. Associations between living benthic foraminifera and dead tests of Syringammina fragilissima (Xenophyophorea) in the Darwin Mounds region (NE Atlantic). Deep Sea Research Part I: Oceanographic Research Papers **51**:1741-1758.

Hurlbert, S. H. 1971. The Nonconcept of Species Diversity: A Critique and Alternative Parameters. Ecology **52**:577-586.

Hurlbert, S. H. 1984. Pseudoreplication and the Design of Ecological Field Experiments. Ecological monographs **54**:187-211.

Huvenne, V. A., P. A. Tyler, D. G. Masson, E. H. Fisher, C. Hauton, V. Huhnerbach, T. P. Le Bas, and G. A. Wolff. 2011. A picture on the wall: innovative mapping reveals cold-water coral refuge in submarine canyon. PLoS One **6**:e28755.

Huvenne, V. A. I., K. Robert, L. Marsh, C. Lo Iacono, T. Le Bas, and R. B. Wynn. 2018. ROVs and AUVs. Pages 93-108 *in* A. Micallef, S. Krastel, and A. Savini, editors. Submarine Geomorphology. Springer International Publishing, Cham.

Iken, K., T. Brey, U. Wand, J. Voigt, and P. Junghans. 2001. Food web structure of the benthic community at the Porcupine Abyssal Plain (NE Atlantic): a stable isotope analysis. Progress in Oceanography **50**:383-405.

Ingole, B. S., Z. A. Ansari, V. Rathod, and N. Rodrigues. 2001. Response of deep-sea macrobenthos to a small-scale environmental disturbance. Deep Sea Research Part II: Topical Studies in Oceanography **48**:3401-3410.

International Seabed Authority. 2010. Development of geological models for the Clarion Clipperton Zone polymetallic nodule deposits. ISA technical studies **6**.

ISA. 2010. A geological model of polymetallic nodule deposits in the Clarion Clipperton Fracture Zone. International Seabed Authority, Kingston, Jamaica.

ISA, I. S. A. 2012. Decision of the Council relating to an environmental management plan for the Clarion-Clipperton Zone. ISBA/18/C/22. Kingston, Jamaica.

Jeffreys, R. M., G. A. Wolff, and G. L. Cowie. 2009. Influence of oxygen on heterotrophic reworking of sedimentary lipids at the Pakistan margin. Deep Sea Research Part II: Topical Studies in Oceanography **56**:358-375.

Jones, D. O., S. Kaiser, A. K. Sweetman, C. R. Smith, L. Menot, A. Vink, D. Trueblood, J. Greinert, D. S. Billett, P. M. Arbizu, T. Radziejewska, R. Singh, B. Ingole, T. Stratmann, E. Simon-Lledo, J. M. Durden, and M. R. Clark. 2017. Biological responses to disturbance from simulated deep-sea polymetallic nodule mining. PLoS One **12**:e0171750.

Jones, D. O. B. 2015. RRS James Cook Cruise JC120 15 Apr - 19 May 2015. Manzanillo to Manzanillo, Mexico. Managing Impacts of Deep-seA resource exploitation (MIDAS): Clarion-Clipperton Zone North Eastern Area of Particular Environmental Interest. Southampton, National Oceanography Centre, 117pp.

Jones, D. O. B., J. A. Ardron, A. Colaço, and J. M. Durden. 2018. Environmental considerations for impact and preservation reference zones for deep-sea polymetallic nodule mining. Marine Policy.

Jones, D. O. B., B. J. Bett, and P. A. Tyler. 2007. Megabenthic ecology of the deep Faroe–Shetland channel: A photographic study. Deep Sea Research Part I: Oceanographic Research Papers **54**:1111-1128.

Jones, D. O. B., B. J. Bett, R. B. Wynn, and D. G. Masson. 2009. The use of towed camera platforms in deep-water science. Underwater Technology **28**:41-50.

Jones, D. O. B., and M. E. Brewer. 2012. Response of megabenthic assemblages to different scales of habitat heterogeneity on the Mauritanian slope. Deep Sea Research Part I: Oceanographic Research Papers **67**:98-110.

Jones, D. O. B., A. R. Gates, and B. Lausen. 2012. Recovery of deep-water megafaunal assemblages from hydrocarbon drilling disturbance in the Faroe–Shetland Channel. Marine Ecology Progress Series **461**:71-82.

Jones, D. O. B., C. O. Mrabure, and A. R. Gates. 2013. Changes in deep-water epibenthic megafaunal assemblages in relation to seabed slope on the Nigerian margin. Deep Sea Research Part I: Oceanographic Research Papers **78**:49-57.

Jones, D. O. B., A. Walls, M. Clare, M. S. Fiske, R. J. Weiland, R. O'Brien, and D. F. Touzel. 2014. Asphalt mounds and associated biota on the Angolan margin. Deep Sea Research Part I: Oceanographic Research Papers **94**:124-136.

Jost, L. 2006. Entropy and diversity. Oikos **113**:363-375.

Jost, L. 2010. The Relation between Evenness and Diversity. Diversity **2**:207-232.

Juan, C., D. Van Rooij, and W. De Bruycker. 2018. An assessment of bottom current controlled sedimentation in Pacific Ocean abyssal environments. Marine Geology **403**:20-33.

Jumars, P. A., L. M. Mayer, J. W. Deming, J. A. Baross, and R. A. Wheatcroft. 1990. Deep-Sea Deposit-Feeding Strategies Suggested by Environmental and Feeding Constraints. Philosophical Transactions of the Royal Society of London. Series A, Mathematical and Physical Sciences **331**:85-101.

Jung, H.-S., Y.-T. Ko, S.-B. Chi, and J.-W. Moon. 2001. Characteristics of Seafloor Morphology and Ferromanganese Nodule Occurrence in the Korea Deep-sea Environmental Study (KODES) Area, NE Equatorial Pacific. Marine Georesources & Geotechnology **19**:167-180.

Kamenskaya, O. E., A. J. Gooday, O. S. Tendal, and V. F. Melnik. 2015. Xenophyophores (Protista, Foraminifera) from the Clarion-Clipperton Fracture Zone with description of three new species. Marine Biodiversity **45**:581-593.

Kamenskaya, O. E., V. F. Melnik, and A. J. Gooday. 2013. Giant protists (xenophyophores and komokiaceans) from the Clarion-Clipperton ferromanganese nodule field (eastern Pacific). Biology Bulletin Reviews **3**:388-398.

Kempenaers, B., and M. Valcu. 2010. Spatial autocorrelation: an overlooked concept in behavioral ecology. Behavioral Ecology **21**:902-905.

Kenkel, N. C., P. Juhász-Nagy, and J. Podani. 1989. On sampling procedures in population and community ecology. Vegetatio **83**:195-207.

Kersken, D., D. Janussen, and P. Martínez Arbizu. 2018. Deep-sea glass sponges (Hexactinellida) from polymetallic nodule fields in the Clarion-Clipperton Fracture Zone (CCFZ), northeastern Pacific: Part I – Amphidiscophora. Marine Biodiversity **48**:545-573.

Khripounoff, A., J.-C. Caprais, P. Crassous, and J. Etoubleau. 2006. Geochemical and biological recovery of the disturbed seafloor in polymetallic nodule fields of the Clipperton-Clarion Fracture Zone (CCFZ) at 5,000-m depth. Limnology and Oceanography **51**:2033-2041.

Klein, H. 1993. Near-bottom currents in the deep Peru Basin, DISCOL experimental area. Deutsche Hydrografische Zeitschrift **45**:31-42.

Klitgord, K. D., and J. Mammerickx. 1982. Northern East Pacific Rise: magnetic anomaly and bathymetric framework. Journal of Geophysical Research: Solid Earth **87**:6725-6750.

Krebs, C. J. 1999. Ecological Methodology. Benjamin Cummings, Menlo Park, CA.

Krumbein, W. C. 1936. Application of logarithmic moments to size frequency distributions of sediments. Journal of Sedimentary Research **6**:35-47.

Kuhn, T., A. Wegorzewski, C. Rühlemann, and A. Vink. 2017. Composition, Formation, and Occurrence of Polymetallic Nodules. Pages 23-63 *in* R. Sharma, editor. Deep-Sea Mining: Resource Potential, Technical and Environmental Considerations. Springer International Publishing, Cham.

Kwasnitschka, T., K. Köser, J. Sticklus, M. Rothenbeck, T. Weiß, E. Wenzlaff, T. Schoening, L. Triebe, A. Steinführer, C. Devey, and J. Greinert. 2016. DeepSurveyCam—A Deep Ocean Optical Mapping System. Sensors **16**:164.

Lampitt, R. S. 1985. Evidence for the seasonal deposition of detritus to the deep-sea floor and its subsequent resuspension. Deep Sea Research Part A. Oceanographic Research Papers **32**:885-897.

Lampitt, R. S., and A. N. Antia. 1997. Particle flux in deep seas: regional characteristics and temporal variability. Deep Sea Research Part I: Oceanographic Research Papers **44**:1377-1403.

Langenkämper, D., M. Zurowietz, T. Schoening, and T. W. Nattkemper. 2017. BIIGLE 2.0 - Browsing and Annotating Large Marine Image Collections. Frontiers in Marine Science **4**:10.

Lapointe, A., and L. Watling. 2015. Bamboo corals from the abyssal Pacific: Bathygorgia. Proceedings of the Biological Society of Washington **128**:125-136.

Lauerman, L. M. L., J. M. Smoak, T. J. Shaw, W. S. Moore, and K. Smith, L. 1997. 234Th and 21Pb evidence for rapid ingestion of settling particles by mobile epibenthic megafauna in the abyssal NE Pacific. Limnology and Oceanography **42**:589-595.

Laureillard, J., L. Méjanelle, and M. Sibuet. 2004. Use of lipids to study the trophic ecology of deep-sea xenophyophores. Marine Ecology Progress Series **270**:129-140.

Le Bas, T. P., and V. A. I. Huvenne. 2009. Acquisition and processing of backscatter data for habitat mapping – Comparison of multibeam and sidescan systems. Applied Acoustics **70**:1248-1257.

Legendre, P. 1993. Spatial Autocorrelation: Trouble or New Paradigm? Ecology **74**:1659-1673.

Legendre, P., and M. J. Fortin. 1989. Spatial Pattern and Ecological Analysis. Vegetatio **80**:107-138.

Legendre, P., and L. Legendre. 1998. Numerical ecology. 2nd English Edition. Elsevier, Amsterdam.

Leitner, A. B., A. B. Neuheimer, E. Donlon, C. R. Smith, and J. C. Drazen. 2017. Environmental and bathymetric influences on abyssal bait-attending communities of the Clarion Clipperton Zone. Deep Sea Research Part I: Oceanographic Research Papers **125**:65-80.

Levin, L. A. 1991. Interactions Between Metazoans and Large, Agglutinating Protozoans: Implications for the Community Structure of Deep-Sea Benthos1. American Zoologist **31**:886-900.

Levin, L. A., D. J. Demaster, L. D. McCann, and C. L. Thomas. 1986. Effects of giant protozoans (Class Xenophyophorea) on deep-seamount benthos. Marine Ecology-Progress Series **29**:99-104.

Levin, L. A., R. J. Etter, M. A. Rex, A. J. Gooday, C. R. Smith, J. Pineda, C. T. Stuart, R. R. Hessler, and D. Pawson. 2001. Environmental Influences on Regional Deep-Sea Species Diversity. Annual Review of Ecology and Systematics **32**:51-93.

Levin, L. A., and A. J. Gooday. 1992. Possible Roles for Xenophyophores in Deep-Sea Carbon Cycling. Pages 93-104 *in* G. T. Rowe and V. Pariente, editors. Deep-Sea Food Chains and the Global Carbon Cycle. Springer Netherlands, Dordrecht.

Levin, L. A., K. Mengerink, K. M. Gjerde, A. A. Rowden, C. L. Van Dover, M. R. Clark, E. Ramirez-Llodra, B. Currie, C. R. Smith, K. N. Sato, N. Gallo, A. K. Sweetman, H. Lily, C. W. Armstrong, and J. Brider. 2016. Defining “serious harm” to the marine environment in the context of deep-seabed mining. Marine Policy **74**:245-259.

Levin, L. A., and C. L. Thomas. 1988a. The ecology of xenophyophores (Protista) on eastern Pacific seamounts. Deep Sea Research Part A. Oceanographic Research Papers **35**:2003-2027.

Levin, L. A., and C. L. Thomas. 1988b. The influence of hydrodynamic regime on infaunal assemblages inhabiting carbonate sediments on central Pacific seamounts. Deep Sea Research Part A. Oceanographic Research Papers **36**:1897-1915.

Lim, S.-C., H. Wiklund, A. G. Glover, T. G. Dahlgren, and K.-S. Tan. 2017. A new genus and species of abyssal sponge commonly encrusting polymetallic nodules in the Clarion-Clipperton Zone, East Pacific Ocean. Systematics and Biodiversity **15**:507-519.

Lodge, M., D. Johnson, G. Le Gurun, M. Wengler, P. Weaver, and V. Gunn. 2014. Seabed mining: International Seabed Authority environmental management plan for the Clarion–Clipperton Zone. A partnership approach. Marine Policy **49**:66-72.

Ludvigsen, M., B. Sortland, G. Johnsen, and H. Singh. 2007. Applications of Geo-Referenced Underwater Photo Mosaics in Marine Biology and Archaeology. Oceanography **20**:140-149.

Lundsten, L., J. P. Barry, G. M. Cailliet, D. A. Clague, A. P. DeVogelaere, and J. B. Geller. 2009. Benthic invertebrate communities on three seamounts off southern and central California, USA. Marine Ecology Progress Series **374**:23-32.

Lutz, M. J., K. Caldeira, R. B. Dunbar, and M. J. Behrenfeld. 2007. Seasonal rhythms of net primary production and particulate organic carbon flux to depth describe the efficiency of biological pump in the global ocean. Journal of Geophysical Research **112**:doi:10.1029/2006JC003706.

Macdonald, K. C., P. J. Fox, R. T. Alexander, R. Pockalny, and P. Gente. 1996. Volcanic growth faults and the origin of Pacific abyssal hills. Nature **380**:125.

Magurran, A. E. 2004. Measuring biological diversity. Blackwell Science Ltd., Blackwell Publishing (2004).

Marchig, V., U. von Stackelberg, H. Hufnagel, and G. Durn. 2001. Compositional changes of surface sediments and variability of manganese nodules in the Peru Basin. Deep Sea Research Part II: Topical Studies in Oceanography **48**:3523-3547.

Marcon, Y., H. Sahling, and G. Bohrmann. 2013. LAPM: a tool for underwater large-area photo-mosaicking. Geosci. Instrum. Method. Data Syst. **2**:189-198.

Margolis, S. V., and R. G. Burns. 1976. Pacific Deep-Sea Manganese Nodules: Their Distribution, Composition, and Origin. Annual Review of Earth and Planetary Sciences **4**:229-263.

Marouchos, A., M. Sherlock, and J. Cordell. 2018. Challenges in underwater image capture. Pages 1-5 *in* OCEANS 2018 MTS/IEEE Charleston.

Marsh, L., J. T. Copley, V. A. I. Huvenne, P. A. Tyler, and R. O. V. F. the Isis. 2013. Getting the bigger picture: Using precision Remotely Operated Vehicle (ROV) videography to acquire high-definition mosaic images of newly discovered hydrothermal vents in the Southern Ocean. Deep Sea Research Part II: Topical Studies in Oceanography **92**:124-135.

Martinez, C., and P. Keener-Chavis. 2006. NOAA Ship Okeanos Explorer: Telepresence in the Service of Science, Education and Outreach. Pages 1-5 *in* OCEANS 2006.

McClain, C. R. 2007. Seamounts: identity crisis or split personality? Journal of Biogeography **34**:2001-2008.

McClain, C. R., A. P. Allen, D. P. Tittensor, and M. A. Rex. 2012. Energetics of life on the deep seafloor. Proc Natl Acad Sci U S A **109**:15366-15371.

McClain, C. R., and J. P. Barry. 2010. Habitat heterogeneity, disturbance, and productivity work in concert to regulate biodiversity in deep submarine canyons. Ecology **91**:964-976.

McClain, C. R., and S. M. Hardy. 2010. The dynamics of biogeographic ranges in the deep sea. Proceedings of the Royal Society B: Biological Sciences.

McClain, C. R., M. A. Rex, and R. Jabbour. 2005. Deconstructing bathymetric body size patterns in deep-sea gastropods. Marine Ecology Progress Series **297**:181-187.

McPhail, S. 2009. Autosub6000: A Deep Diving Long Range AUV. Journal of Bionic Engineering **6**:55-62.

Menzies, R. J. 1965. Conditions for the existence of life on the abyssal sea floor. Oceanography and Marine Biology: An Annual Review **3**:195-210.

Mero, J. L. 1968. Mineral Deposits in the Sea. Natural Resources Lawyer **1**:130-137.

Mewes, K., J. M. Mogollón, A. Picard, C. Rühlemann, T. Kuhn, K. Nöthen, and S. Kasten. 2014. Impact of depositional and biogeochemical processes on small scale variations in nodule abundance in the Clarion-Clipperton Fracture Zone. Deep Sea Research Part I: Oceanographic Research Papers **91**:125-141.

Meyer, K. S., C. M. Young, A. K. Sweetman, J. Taylor, T. Soltwedel, and M. Bergmann. 2016. Rocky islands in a sea of mud: biotic and abiotic factors structuring deep-sea dropstone communities. Marine Ecology Progress Series **556**:45-57.

Miljutin, D. M., M. A. Miljutina, P. M. Arbizu, and J. Galéron. 2011. Deep-sea nematode assemblage has not recovered 26 years after experimental mining of polymetallic nodules (Clarion-Clipperton Fracture Zone, Tropical Eastern Pacific). Deep Sea Research Part I: Oceanographic Research Papers **58**:885-897.

Miljutina, M. A., D. M. Miljutin, R. Mahatma, and J. Galéron. 2010. Deep-sea nematode assemblages of the Clarion-Clipperton Nodule Province (Tropical North-Eastern Pacific). Marine Biodiversity **40**:1-15.

Molodtsova, T. N., and D. M. Opresko. 2017. Black corals (Anthozoa: Antipatharia) of the Clarion-Clipperton Fracture Zone. Marine Biodiversity **47**:349-365.

Morgan, C. L., N. Allotey Odunton, and A. T. Jones. 1999. Synthesis of Environmental Impacts of Deep Seabed Mining. Marine Georesources & Geotechnology **17**:307-356.

Morris, K., P. A. Tyler, B. Murton, and A. D. Rogers. 2012. Lower bathyal and abyssal distribution of coral in the axial volcanic ridge of the Mid-Atlantic Ridge at 45°N. Deep Sea Research Part I: Oceanographic Research Papers **62**:32-39.

Morris, K. J., B. J. Bett, J. M. Durden, N. M. Benoist, V. A. Huvenne, D. O. Jones, K. Robert, M. C. Ichino, G. A. Wolff, and H. A. Ruhl. 2016. Landscape-scale spatial heterogeneity in phytodetrital cover and megafauna biomass in the abyss links to modest topographic variation. Sci Rep **6**:34080.

Morris, K. J., B. J. Bett, J. M. Durden, V. A. I. Huvenne, R. Milligan, D. O. B. Jones, S. McPhail, K. Robert, D. M. Bailey, and H. A. Ruhl. 2014. A new method for ecological surveying of the abyss using autonomous underwater vehicle photography. Limnology and Oceanography: Methods **12**:795-809.

Mullineaux, L. S. 1987. Organisms living on manganese nodules and crusts: distribution and abundance at three North Pacific sites. Deep Sea Research Part A. Oceanographic Research Papers **34**:165-184.

Mullineaux, L. S. 1988. The role of settlement in structuring a hard-substratum community in the deep sea. Journal of Experimental Marine Biology and Ecology **120**:247-261.

Nasr-Azadani, M., and E. Meiburg. 2014. Turbidity currents interacting with three-dimensional seafloor topography. Journal of Fluid Mechanics **745**:409-443.

Niner, H. J., J. A. Ardron, E. G. Escobar, M. Gianni, A. Jaeckel, D. O. B. Jones, L. A. Levin, C. R. Smith, T. Thiele, P. J. Turner, C. L. Van Dover, L. Watling, and K. M. Gjerde. 2018. Deep-Sea Mining With No Net Loss of Biodiversity—An Impossible Aim. Frontiers in Marine Science **5**.

O'Hara, T. D., S. Stöhr, A. F. Hugall, B. Thuy, and A. Martynov. 2018. Morphological diagnoses of higher taxa in Ophiuroidea (Echinodermata) in support of a new classification. 2018.

Oksanen, J., F. Guillaume Blanchet, M. Friendly, R. Kindt, P. Legendre, D. McGlinn, P. R. Minchin, R. B. O'Hara, G. L. Simpson, P. Solymos, M. H. H. Stevens, E. Szoecs, and H. Wagner. 2018. vegan: Community Ecology Package. R package version 2.4-6. https://CRAN.R-project.org/package=vegan.

Olive, J. A., M. D. Behn, G. Ito, W. R. Buck, J. Escartín, and S. Howell. 2015. Sensitivity of seafloor bathymetry to climate-driven fluctuations in mid-ocean ridge magma supply. science **350**:310-313.

Orejas, C., A. Gori, C. Lo Iacono, P. Puig, J. M. Gili, and M. R. Dale. 2009. Cold-water corals in the Cap de Creus canyon, northwestern Mediterranean: spatial distribution, density and anthropogenic impact. Marine Ecology Progress Series **397**:37-51.

Ozturgut, E., G. C. Anderson, R. E. Burns, J. W. Lavelle, and S. A. Swift. 1978. Deep ocean mining of manganese nodules in the North Pacific: pre-mining environmental conditions and anticipated mining effects. Marine Ecosystems Analysis Program, Environmental Research Laboratories, National Oceanic and Atmospheric Administration. NOAA technical memorandum, ERL MESA-33. Rep. No. PB/293545/OST, Boulder, CO.

Ozturgut, E., J. W. Lavelle, and R. E. Burns. 1981. Impacts of manganese nodule mining on the environment: results from pilot-scale mining tests in the North Equatorial Pacific. Pages 437-474 *in* R. A. Geyer, editor. Marine Environmental Pollution, 2: Dumping and mining. Elsevier Scientific Publishing, Amsterdam.

Pape, E., T. N. Bezerra, F. Hauquier, and A. Vanreusel. 2017. Limited Spatial and Temporal Variability in Meiofauna and Nematode Communities at Distant but Environmentally Similar Sites in an Area of Interest for Deep-Sea Mining. Frontiers in Marine Science **4**.

Patel, T., H. Robert, C. D'Udekem D'Acoz, K. Martens, I. De Mesel, S. Degraer, and I. Schön. 2018. Biogeography and community structure of abyssal scavenging Amphipoda (Crustacea) in the Pacific Ocean. Biogeosciences Discuss. **2018**:1-36.

Paul, S. A. L., B. Gaye, M. Haeckel, S. Kasten, and A. Koschinsky. 2018. Biogeochemical Regeneration of a Nodule Mining Disturbance Site: Trace Metals, DOC and Amino Acids in Deep-Sea Sediments and Pore Waters. Frontiers in Marine Science **5**.

Pennington, J. T., K. L. Mahoney, V. S. Kuwahara, D. D. Kolber, R. Calienes, and F. P. Chavez. 2006. Primary production in the eastern tropical Pacific: A review. Progress in Oceanography **69**:285-317.

Peukert, A., T. Schoening, E. Alevizos, K. Köser, T. Kwasnitschka, and J. Greinert. 2018. Understanding Mn-nodule distribution and evaluation of related deep-sea mining impacts using AUV-based hydroacoustic and optical data. Biogeosciences **15**:2525-2549.

Podowski, E. L., S. Ma, I. G. Luther, D. Wardrop, and C. R. Fisher. 2010. Biotic and abiotic factors affecting distributions of megafauna in diffuse flow on andesite and basalt along the Eastern Lau Spreading Center, Tonga. Marine Ecology Progress Series **418**:25-45.

Polzin, K. L., J. M. Toole, J. R. Ledwell, and R. W. Schmitt. 1997. Spatial Variability of Turbulent Mixing in the Abyssal Ocean. science **276**:93-96.

Prados, R., R. Garcia, N. Gracias, J. Escartin, and L. Neumann. 2012. A Novel Blending Technique for Underwater Gigamosaicing. IEEE Journal of Oceanic Engineering **37**:626-644.

Purser, A., Y. Marcon, H. T. Hoving, M. Vecchione, U. Piatkowski, D. Eason, H. Bluhm, and A. Boetius. 2016. Association of deep-sea incirrate octopods with manganese crusts and nodule fields in the Pacific Ocean. Curr Biol **26**:R1268-R1269.

Pushcharovsky, Y. M. 2006. Tectonic types of the Pacific abyssal basins. Geotectonics **40**:345-356.

R Core Team. 2017. R: A language and environment for statistical computing. R Foundation for Statistical Computing, Vienna, Austria.

Radziejewska, T. 2002. Responses of deep-sea meiobenthic communities to sediment disturbance simulating effects of polymetallic nodule mining. International review of hydrobiology **87**:457-477.

Radziejewska, T. 2014a. Characteristics of the Sub-equatorial North-Eastern Pacific Ocean’s Abyss, with a Particular Reference to the Clarion-Clipperton Fracture Zone. Pages 13-28 Meiobenthos in the Sub-equatorial Pacific Abyss: A Proxy in Anthropogenic Impact Evaluation. Springer, Berlin, Heidelberg.

Radziejewska, T. 2014b. Meiobenthos of the Sub-equatorial North-Eastern Pacific Abyssal Seafloor: A Synopsis. Pages 29-65 Meiobenthos in the Sub-equatorial Pacific Abyss: A Proxy in Anthropogenic Impact Evaluation. Springer Berlin Heidelberg, Berlin, Heidelberg.

Radziejewska, T., and V. Stoyanova. 2000. Abyssal epibenthic megafauna of the Clarion-Clipperton area (NE Pacific): changes in time and space versus anthropogenic environmental disturbance. Oceanological Studies **29**:83-101.

Ramirez-Llodra, E., A. Brandt, R. Danovaro, B. De Mol, E. Escobar, C. R. German, L. A. Levin, P. Martinez Arbizu, L. Menot, P. Buhl-Mortensen, B. E. Narayanaswamy, C. R. Smith, D. P. Tittensor, P. A. Tyler, A. Vanreusel, and M. Vecchione. 2010. Deep, diverse and definitely different: unique attributes of the world's largest ecosystem. Biogeosciences **7**:2851-2899.

Ramirez-Llodra, E., P. A. Tyler, M. C. Baker, O. A. Bergstad, M. R. Clark, E. Escobar, L. A. Levin, L. Menot, A. A. Rowden, C. R. Smith, and C. L. Van Dover. 2011. Man and the last great wilderness: human impact on the deep sea. PLoS One **6**:e22588.

Rao, P. S. 2000. Sampling methodologies with applications. Chapman and Hall/CRC, New York.

Rex, M. A., R. Etter, J. , J. S. Morris, J. Crouse, C. R. McClain, N. A. Johnson, C. T. Stuart, J. W. Deming, R. Thies, and R. Avery. 2006. Global bathymetric patterns of standing stock and body size in the deep-sea benthos. Marine Ecology Progress Series **317**:1-8.

Rex, Michael A., Craig R. McClain, Nicholas A. Johnson, Ron J. Etter, John A. Allen, P. Bouchet, and A. Warén. 2005. A Source-Sink Hypothesis for Abyssal Biodiversity. The American Naturalist **165**:163-178.

Ripley, B. D. 1979. Tests of `Randomness' for Spatial Point Patterns. Journal of the Royal Statistical Society. Series B (Methodological) **41**:368-374.

Ripley, B. D. 1981. Spatial statistics. J. Wiley & Sons.

Robert, K., V. A. I. Huvenne, A. Georgiopoulou, D. O. B. Jones, L. Marsh, G. D. O. Carter, and L. Chaumillon. 2017. New approaches to high-resolution mapping of marine vertical structures. Scientific Reports **7**:9005.

Robert, K., D. O. B. Jones, and V. A. I. Huvenne. 2014. Megafaunal distribution and biodiversity in a heterogeneous landscape: the iceberg-scoured Rockall Bank, NE Atlantic. Marine Ecology Progress Series **501**:67-88.

Robert, K., D. O. B. Jones, P. A. Tyler, D. Van Rooij, and V. A. I. Huvenne. 2015. Finding the hotspots within a biodiversity hotspot: fine-scale biological predictions within a submarine canyon using high-resolution acoustic mapping techniques. Marine Ecology **36**:1256-1276.

Roberts, J. M., A. J. Wheeler, and A. Freiwald. 2006. Reefs of the deep: the biology and geology of cold-water coral ecosystems. science **312**:543-547.

Rodgers, J. L. 1999. The Bootstrap, the Jackknife, and the Randomization Test: A Sampling Taxonomy. Multivariate Behavioral Research **34**:441-456.

Roels, O. A. 1974. Will nodule mining disturb the marine environment? Marine Technology Society Journal **8**:17-20.

Rowe, G., M. Sibuet, J. Deming, A. Khripounoff, J. Tietjen, S. Macko, and R. Theroux. 1991. 'Total' sediment biomass and preliminary estimates of organic carbon residence time in deep-sea benthos. Marine Ecology Progress Series **79**:99-114.

Ruhl, H. A. 2007. ABUNDANCE AND SIZE DISTRIBUTION DYNAMICS OF ABYSSAL EPIBENTHIC MEGAFAUNA IN THE NORTHEAST PACIFIC. Ecology **88**:1250-1262.

Ruhl, H. A. 2008. COMMUNITY CHANGE IN THE VARIABLE RESOURCE HABITAT OF THE ABYSSAL NORTHEAST PACIFIC. Ecology **89**:991-1000.

Ruhl, H. A., J. A. Ellena, and K. L. Smith, Jr. 2008. Connections between climate, food limitation, and carbon cycling in abyssal sediment communities. Proc Natl Acad Sci U S A **105**:17006-17011.

Ruhl, H. A., and K. L. Smith. 2004. Shifts in Deep-Sea Community Structure Linked to Climate and Food Supply. science **305**:513-515.

Sanders, H. L. 1968. Marine Benthic Diversity: A Comparative Study. The American Naturalist **102**:243-282.

Sanders, H. L., and R. R. Hessler. 1969. Ecology of the deep-sea benthos. science **163**:1419-1424.

Sautya, S., B. Ingole, D. O. B. Jones, D. Ray, and K. A. Kameshraju. 2016. First quantitative exploration of benthic megafaunal assemblages on the mid-oceanic ridge system of the Carlsberg Ridge, Indian Ocean. Journal of the Marine Biological Association of the United Kingdom:1-9.

Schneck, F., and A. S. Melo. 2010. Reliable sample sizes for estimating similarity among macroinvertebrate assemblages in tropical streams. Annales de Limnologie - International Journal of Limnology **46**:93-100.

Schoening, T., D. O. B. Jones, and J. Greinert. 2017. Compact-Morphology-based poly-metallic Nodule Delineation. Scientific Reports **7**:13338.

Schoening, T., T. Kuhn, D. O. B. Jones, E. Simon-Lledo, and T. W. Nattkemper. 2016. Fully automated image segmentation for benthic resource assessment of poly-metallic nodules. Methods in Oceanography **15-16**:78-89.

Schriever, G. 1992. Cruise report DISCOL 3, SONNE cruise 77 : January 26 - February 27, 1992, Balboa/Panama-Balboa/Panama. Cruise Report, Hamburg.

Sharma, R. 2011. Deep-sea mining: economic, technical, technological and environmental considerations for sustainable development Mar. Technol. Soc. J. **45**:28-41.

Simon-Lledo, E., S. Thompson, A. Flynt, T. Pomme, J. Parianos, and D. O. Jones. in prep. The abyssal megafauna of Kiribati. Frontiers in Ecology and the Environment.

Skornyakova, N. S., and I. O. Murdmaa. 1992. Local variations in distribution and composition of ferromanganese nodules in the Clarion-Clipperton Nodule Province. Marine Geology **103**:381-405.

Smith, A. N. H., M. J. Anderson, and M. D. M. Pawley. 2017. Could ecologists be more random? Straightforward alternatives to haphazard spatial sampling. Ecography **40**:1251-1255.

Smith, C. R., and S. J. Brumsickle. 1989. The effects of patch size and substrate isolation on colonization modes and rates in an intertidal sediment. Limnology and Oceanography **34**:1263-1277.

Smith, C. R., F. C. De Leo, A. F. Bernardino, A. K. Sweetman, and P. M. Arbizu. 2008a. Abyssal food limitation, ecosystem structure and climate change. Trends in Ecology and Evolution **23**:518-528.

Smith, C. R., and A. W. J. Demopoulos. 2003. Ecology of the deep Pacific Ocean floor. Pages 179-218 *in* P. A. Tyler, editor. Ecosystems of the World: Ecosystems of the Deep Ocean. Elsevier, Amsterdam, the Netherlands.

Smith, C. R., J. Drazen, and S. L. Mincks. 2006. Deep-sea biodiversity and biogeography: Perspectives from the abyss.*in* International Seabed Authority Seamount Biodiversity Symposium.

Smith, C. R., S. Gaines, A. Friedlander, C. Morgan, A. Thurnherr, S. Mincks, L. Watling, A. Rogers, M. Clark, and A. Baco-Taylor. 2008b. Preservation reference areas for nodule mining in the clarion-clipperton zone: rationale and recommendations to the International Seabed Authority. Manoa.

Smith, C. R., D. J. Hoover, S. E. Doan, R. H. Pope, D. J. Demaster, F. C. Dobbs, and M. A. Altabet. 1996. Phytodetritus at the abyssal seafloor across 10° of latitude in the central equatorial Pacific. Deep Sea Research Part II: Topical Studies in Oceanography **43**:1309-1338.

Smith, C. R., P. A. Jumars, and D. J. DeMaster. 1986. In situ studies of megafaunal mounds indicate rapid sediment turnover and community response at the deep-sea floor. Nature **323**:251.

Smith, C. R., L. A. Levin, A. Koslow, P. A. Tyler, and A. G. Glover. 2008c. The near future of the deep seafloor ecosystems. Pages 334-352 Aquatic ecosystems: trends and global prospects. Cambridge University Press.

Smith, K. L., Jr., H. A. Ruhl, B. J. Bett, D. S. Billett, R. S. Lampitt, and R. S. Kaufmann. 2009. Climate, carbon cycling, and deep-ocean ecosystems. Proc Natl Acad Sci U S A **106**:19211-19218.

Snelgrove, P. V. 1999. Getting to the bottom of marine biodiversity: Sedimentary habitats: Ocean bottoms are the most widespread habitat on earth and support high biodiversity and key ecosystem services. BioScience **49**:129-138.

Snelgrove, P. V. R., and C. A. Butman. 1995. Animal-sediment relationships revisited: cause versus effect. Oceanography and Marine Biology: An Annual Review **32**:111-117.

Soetaert, K., and C. Heip. 1990. Sample-size dependence of diversity indices and the determination of sufficient sample size in a high-diversity deep-sea environment. Marine Ecology Progress Series **59**:305-307.

Sokal, R. R., and F. J. Rohlf. 1995. Biometry: the principles and practice of statistics in biological research. 3rd edition. WH Freemand and Company, New York.

Stefanoudis, P. V., B. J. Bett, and A. J. Gooday. 2016. Abyssal hills: Influence of topography on benthic foraminiferal assemblages. Progress in Oceanography **148**:44-55.

Stoyanova, V. 2012. Megafaunal Diversity Associated with Deep-sea Nodule-bearing Habitats in the Eastern Part of the Clarion-Clipperton Zone, NE Pacific. International Multidisciplinary Scientific GeoConference: SGEM: Surveying Geology & mining Ecology Management; Sofia. **1**:645-651.

Stratmann, T., L. Lins, A. Purser, Y. Marcon, C. F. Rodrigues, A. Ravara, M. R. Cunha, E. Simon-Lledó, D. O. B. Jones, A. K. Sweetman, K. Köser, and D. van Oevelen. 2018a. Abyssal plain faunal carbon flows remain depressed 26 years after a simulated deep-sea mining disturbance. Biogeosciences **15**:4131-4145.

Stratmann, T., L. Mevenkamp, A. K. Sweetman, A. Vanreusel, and D. van Oevelen. 2018b. Has Phytodetritus Processing by an Abyssal Soft-Sediment Community Recovered 26 Years after an Experimental Disturbance? Frontiers in Marine Science **5**.

Stratmann, T., I. Voorsmit, A. Gebruk, A. Brown, A. Purser, Y. Marcon, A. K. Sweetman, D. O. B. Jones, and D. van Oevelen. 2018c. Recovery of Holothuroidea population density, community composition, and respiration activity after a deep-sea disturbance experiment. Limnology and Oceanography.

Strindberg, S., and S. T. Buckland. 2004. Zigzag survey designs in line transect sampling. Journal of Agricultural, Biological, and Environmental Statistics **9**:443-461.

Sun, Z., J.-F. Hamel, and A. Mercier. 2011. Planulation, larval biology, and early growth of the deep-sea soft corals Gersemia fruticosa and Duva florida (Octocorallia: Alcyonacea). Invertebrate Biology **130**:91-99.

Tempera, F., E. Giacomello, N. C. Mitchell, A. S. Campos, A. Braga Henriques, I. Bashmachnikov, A. Martins, A. Mendonça, T. Morato, A. Colaço, F. M. Porteiro, D. Catarino, J. Gonçalves, M. R. Pinho, E. J. Isidro, R. S. Santos, and G. Menezes. 2012. Mapping Condor Seamount Seafloor Environment and Associated Biological Assemblages (Azores, NE Atlantic).807-818.

Tews, J., U. Brose, V. Grimm, K. Tielbörger, M. C. Wichmann, M. Schwager, and F. Jeltsch. 2004. Animal species diversity driven by habitat heterogeneity/diversity: the importance of keystone structures. Journal of Biogeography **31**:79-92.

Thiel, H. 1975. The size structure of the deep-sea benthos. Internationale Revue der gesamten Hydrobiologie **60**:575-606.

Thiel, H., and G. Schriever. 1989. Cruise report DISCOL 1, Sonne cruise 61, Balboa/Panama - Callao/Peru 02.02. - 05.03.1989, Callao/Peru - Callao/Peru 07.03. - 03.04.1989. Cruise Report, Hamburg.

Thiel, H., and G. Schriever. 1990. Deep-sea mining, environmental impact and the DISCOL project. AMBIO **19**:245-250.

Thiel, H., G. Schriever, A. Ahnert, H. Bluhm, C. Borowski, and K. Vopel. 2001. The large-scale environmental impact experiment DISCOL—reflection and foresight. Deep Sea Research Part II: Topical Studies in Oceanography **48**:3869-3882.

Thiel, H., G. Schriever, C. Bussau, and C. Borowski. 1993. Manganese nodule crevice fauna. Deep Sea Research Part I: Oceanographic Research Papers **40**:419-423.

Thistle, D., S. C. Ertman, and K. Fauchald. 1991. The fauna of the HEBBLE site: patterns in standing stock and sediment-dynamic effects. Marine Geology **99**:413-422.

Thistle, D., J. Y. Yingst, and K. Fauchald. 1985. A deep-sea benthic community exposed to strong near-bottom currents on the Scotian Rise (western Atlantic). Marine Geology **66**:91-112.

Thurber, A. R., A. K. Sweetman, B. E. Narayanaswamy, D. O. B. Jones, J. Ingels, and R. L. Hansman. 2014. Ecosystem function and services provided by the deep sea. Biogeosciences **11**:3941-3963.

Tilman, D. 1982. Resource competition and community structure. Monogr Popul Biol **17**:1-296.

Tilot, V., R. Ormond, J. Moreno Navas, and T. S. Catalá. 2018. The Benthic Megafaunal Assemblages of the CCZ (Eastern Pacific) and an Approach to their Management in the Face of Threatened Anthropogenic Impacts. Frontiers in Marine Science **5**.

Trueblood, D. D., and E. Ozturgut. 1997. The Benthic Impact Experiment: A Study of the Ecological Impacts of Deep Seabed Mining on Abyssal Benthic Communities. Seventh (1997) International Offshore and Polar Engineering Conference. International Society of Offshore and Polar Engineers, Honolulu, USA, May 25-30 1997.

Van Dover, C. L. 2014. Impacts of anthropogenic disturbances at deep-sea hydrothermal vent ecosystems: a review. Mar Environ Res **102**:59-72.

Van Dover, C. L., J. A. Ardron, E. Escobar, M. Gianni, K. M. Gjerde, A. Jaeckel, D. O. B. Jones, L. A. Levin, H. J. Niner, L. Pendleton, C. R. Smith, T. Thiele, P. J. Turner, L. Watling, and P. P. E. Weaver. 2017. Biodiversity loss from deep-sea mining. Nature Geoscience **10**:464.

Van Dover, C. L., C. J. Berg, and R. D. Turner. 1988. Recruitment of marine invertebrates to hard substrates at deep-sea hydrothermal vents on the East Pacific Rise and Galapagos spreading center. Deep Sea Research Part A. Oceanographic Research Papers **35**:1833-1849.

van Haren, H. 2018. Abyssal plain hills and internal wave turbulence. Biogeosciences **15**:4387-4403.

Vangriesheim, A., B. Springer, and P. Crassous. 2001. Temporal variability of near-bottom particle resuspension and dynamics at the Porcupine Abyssal Plain, Northeast Atlantic. Progress in Oceanography **50**:123-145.

Vanreusel, A., G. Fonseca, R. Danovaro, M. C. Da Silva, A. M. Esteves, T. Ferrero, G. Gad, V. Galtsova, C. Gambi, V. Da Fonsêca Genevois, J. Ingels, B. Ingole, N. Lampadariou, B. Merckx, D. Miljutin, M. Miljutina, A. Muthumbi, S. Netto, D. Portnova, T. Radziejewska, M. Raes, A. Tchesunov, J. Vanaverbeke, S. Van Gaever, V. Venekey, T. N. Bezerra, H. Flint, J. Copley, E. Pape, D. Zeppilli, P. A. Martinez, and J. Galeron. 2010. The contribution of deep-sea macrohabitat heterogeneity to global nematode diversity. Marine Ecology **31**:6-20.

Vanreusel, A., A. Hilario, P. A. Ribeiro, L. Menot, and P. M. Arbizu. 2016. Threatened by mining, polymetallic nodules are required to preserve abyssal epifauna. Sci Rep **6**:26808.

Veillette, J., S. K. Juniper, A. J. Gooday, and J. Sarrazin. 2007a. Influence of surface texture and microhabitat heterogeneity in structuring nodule faunal communities. Deep Sea Research Part I: Oceanographic Research Papers **54**:1936-1943.

Veillette, J., J. Sarrazin, A. J. Gooday, J. Galéron, J.-C. Caprais, A. Vangriesheim, J. Étoubleau, J. R. Christian, and S. Kim Juniper. 2007b. Ferromanganese nodule fauna in the Tropical North Pacific Ocean: Species richness, faunal cover and spatial distribution. Deep Sea Research Part I: Oceanographic Research Papers **54**:1912-1935.

Victorero, L., K. Robert, L. F. Robinson, M. L. Taylor, and V. A. I. Huvenne. 2018a. Species replacement dominates megabenthos beta diversity in a remote seamount setting. Scientific Reports **8**:4152.

Victorero, L., L. Watling, M. L. Deng Palomares, and C. Nouvian. 2018b. Out of Sight, But Within Reach: A Global History of Bottom-Trawled Deep-Sea Fisheries From >400 m Depth. Frontiers in Marine Science **5**.

von Stackelberg, U., and H. Beiersdorf. 1991. The formation of manganese nodules between the Clarion and Clipperton fracture zones southeast of Hawaii. Marine Geology **98**:411-423.

Vopel, K., and H. Thiel. 2001. Abyssal nematode assemblages in physically disturbed and adjacent sites of the eastern equatorial Pacific. Deep Sea Research Part II: Topical Studies in Oceanography **48**:3795-3808.

Wang, C., and D. Lu. 2002. Application of deep ocean photo and video tow system in deep-sea megafaunal studies. China Ocean Press **14**:74-81.

Weaver, P., and J. Thomson. 1987. Geology and geochemistry of abyssal plains. Blackwell Scientific Publications Ltd, United Kingdom.

Wedding, L., S. Reiter, C. Smith, K. Gjerde, J. Kittinger, A. Friedlander, S. Gaines, M. Clark, A. Thurnherr, and S. Hardy. 2015. Managing mining of the deep seabed. science **349**:144-145.

Weiss, A. 2001. Topographic position and landforms analysis.*in* 21st Annual ESRI User Conference, San Diego, CA.

Whittaker, R. J., K. J. Willis, and R. Field. 2001. Scale and species richness: towards a general, hierarchical theory of species diversity. Journal of Biogeography **28**:453-470.

Wiegand, T., and K. A. Moloney. 2013. Handbook of spatial point-pattern analysis in ecology. Chapman and Hall/CRC, New York.

Wildish, D., and D. Kristmanson. 2005. Benthic suspension feeders and flow. Cambridge University Press, Cambridge.

Wilson, M. F., B. O'Connell, C. Brown, J. C. Guinan, and A. J. Grehan. 2007. Multiscale terrain analysis of multibeam bathymetry data for habitat mapping on the continental slope. Marine Geodesy **30**:3-35.

Wishner, K., L. Levin, M. Gowing, and L. Mullineaux. 1990. Involvement of the oxygen minimum in benthic zonation on a deep seamount. Nature **346**:57.

Witte, U., T. Brattegard, G. Graf, and B. Springer. 1997. Particle capture and deposition by deep-sea sponges from the Norwegian-Greenland Sea. Marine Ecology Progress Series **154**:241-252.

Wynn, R. B., V. A. I. Huvenne, T. P. Le Bas, B. J. Murton, D. P. Connelly, B. J. Bett, H. A. Ruhl, K. J. Morris, J. Peakall, D. R. Parsons, E. J. Sumner, S. E. Darby, R. M. Dorrell, and J. E. Hunt. 2014. Autonomous Underwater Vehicles (AUVs): Their past, present and future contributions to the advancement of marine geoscience. Marine Geology **352**:451-468.

Yamamuro, M., and H. Kayanne. 1995. Rapid direct determination of organic carbon and nitrogen in carbonate-bearing sediments with a Yanaco MT-5 CHN analyzer. Limnology and Oceanography **40**:1001-1005.

Yoerger, D. R., D. S. Kelley, and J. R. Delaney. 2000. Fine-Scale Three-Dimensional Mapping of a Deep-Sea Hydrothermal Vent Site Using the Jason ROV System. The International Journal of Robotics Research **19**:1000-1014.

Yool, A., A. P. Martin, C. Fernández, and D. R. Clark. 2007. The significance of nitrification for oceanic new production. Nature **447**:999.